



ACTA

MINERALOGICA-PETROGRAPHICA

FIELD GUIDE SERIES

Volume 31

Szeged, 2013

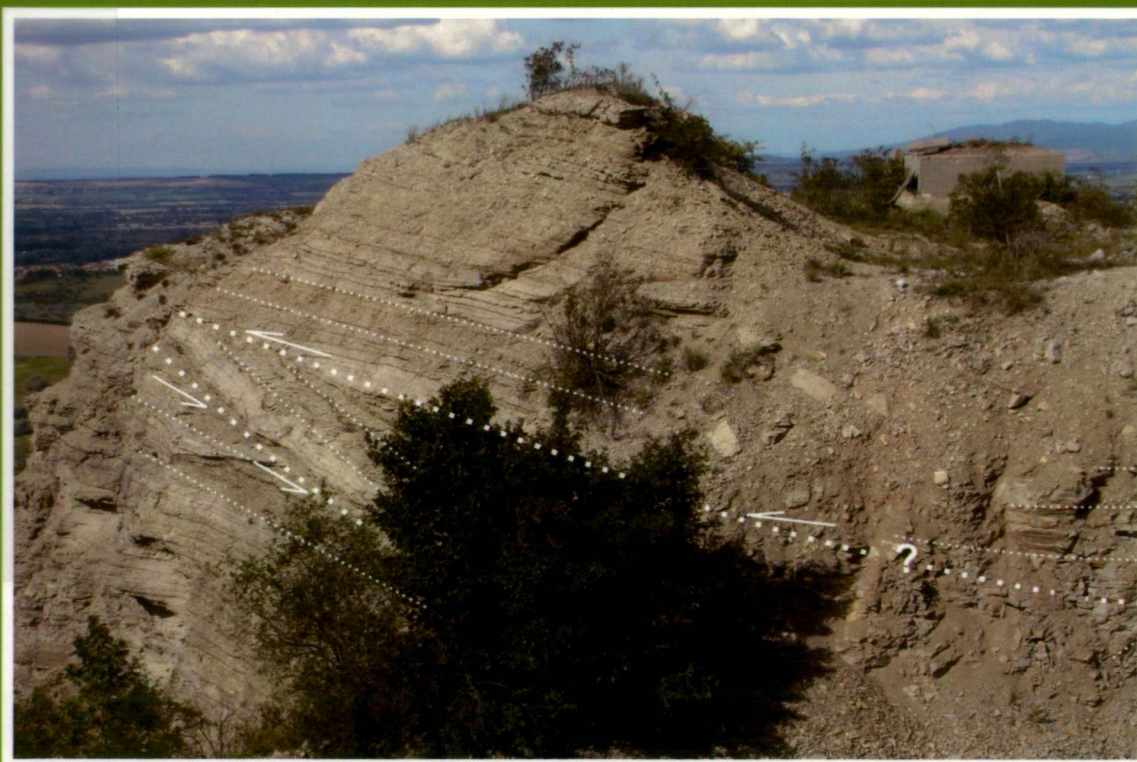
LÁSZLÓ FODOR, ORSOLYA SZTANÓ, SZILVIA KÖVÉR:
Mesozoic deformation of the northern Transdanubian Range (Gerecse and Vértes Hills)

LÁSZLÓ FODOR, SZILVIA KÖVÉR:
Cenozoic deformation of the northern Transdanubian Range (Vértes Hills)

CETEG 2013 PRE- AND POST-CONFERENCE FIELD TRIP GUIDE



XC 63014



ACTA MINERALOGICA-PETROGRAPHICA

established in 1923

FIELD GUIDE SERIES

HU ISSN 0324-6523

HU ISSN 2061-9766

Editor-In-Chief

Elemér Pál-Molnár

University of Szeged, Szeged, Hungary

E-mail: palm@geo.u-szeged.hu

Guest Editor

László Fodor, Szilvia Kövér

Geological, Geophysical and Space Science Research Group

of the Hungarian Academy of Sciences

at Eötvös University, Budapest, Hungary

E-mail: lasz.fodor@yahoo.com, koversz@yahoo.com

Editorial Board

Balázs Koroknai György Buda

Csaba Szabó István Viczián

István Dódony János Földessy

Magdolna Hetényi Péter Árkai

Mihály Pósfai Péter Sipos

Péter Rózsa Sándor Szakáll

Szabolcs Harangi Tamás Fancsik

Tibor Zelenka Tibor Szederkényi

Gábor Papp Tivadar M. Tóth

CETEG 2013 Field Trip Subcommittee

Chairman: László Fodor, Budapest, Hungary

Members: Orsolya Sztanó, Eötvös University, Budapest;
Szilvia Kövér, Hungarian Academy of Sciences

Editorial Office Manager

Anikó Batki

University of Szeged, Szeged, Hungary

E-mail: batki@geo.u-szeged.hu

Editorial Address

H-6701 Szeged, Hungary

P.O. Box 651

E-mail: asviroda@geo.u-szeged.hu

The Acta Mineralogica-Petrographica Field Guide Series is published by the Department of Mineralogy, Geochemistry and Petrology, University of Szeged, Szeged, Hungary

© Department of Mineralogy, Geochemistry and Petrology, University of Szeged

On the cover: Panoramic view on gravity slided Cretaceous clastic sediments of the Bersek Hill quarry (Stop 1.4).

X 175794

Pre-conference field trip: Mesozoic deformation of the northern Transdanubian Range (Gerecse and Vértes Hills)

SZTE Klebelsberg Könyvtár
Egyetemi Gyűjtemény
2.

SZTE Klebelsberg Könyvtár



J001030201



László Fodor^{1,2}, Orsolya Sztanó³, Szilvia Kövér¹

HELYBEN
OLVASHATÓ

1 Geological, Geophysical and Space Science Research Group of the Hungarian Academy of Sciences at Eötvös University, 1/c Pázmány Péter sétány, H-1117, Budapest, Hungary

2 Department of Regional Geology, Eötvös University, 1/c Pázmány Péter sétány, H-1117, Budapest, Hungary

3. Department of Physical and Applied Geology, Eötvös University, 1/c Pázmány Péter sétány, H-1117, Budapest, Hungary
lasz.fodor@yahoo.com, sztano@caesar.elte.hu, kovorsz@yahoo.com

Table of contents

1. Introduction..... 2

2. Geological setting and brief Mesozoic evolution..... 2

3. Mesozoic structural phases of the Gerecse and Vértes Hills..... 6

4. Introduction to geodynamic interpretations..... 8

5. Excursion stops..... 9

 Stop 1. Tardos, Nyerges Hill..... 9

 Stop 2. Lábatlan, Tölgyhát Quarry. Bathonian(?) to Callovian normal faults, dykes 11

 Stop 3. Lábatlan, Ördögát quarry. Early Valanginian slides..... 15

 Stop 4. Lábatlan, Bersek Hill quarry. Valanginian–Barremian slides, syn-sedimentary and syn-lithification faults, Eocene and post-Eocene reactivation 18

 Stop 5. Környe, roadside panoramic view to the east. Albian?–Coniacian? fold..... 22

 Introduction to the Vértesomló Line and the structure of the northern Vértes Hills (Stops 6 and 7)..... 22

 Stop 6, Véressomló, church hill. Albian to Coniacian fold, the Vértesomló thrust. 24

 Stop 7. Tatabánya, Szarvas-kút, Terv road. Albian to Coniacian folds, the Vértesomló thrust. 25

6. Discussion – Geodynamic evolution..... 29

References..... 32

X 175794

1. Introduction

The pre-conference field trip will present the main structural phases of the Mesozoic deformation of the northern Transdanubian Range (TR) (Fig. 1, 2), starting from the Early Jurassic rifting through different Cretaceous deformation phases. The Mesozoic evolution of the TR was equally linked to the opening and closure of the Meliata-Vardar branch of the Neotethys Ocean, but also to the events in Alpine Tethys (Ligurian-Piemont Ocean) (Fig. 4). Excursion will present outcrops showing the structures and sediments connected to minor extension, which is related to the Early Jurassic rifting and Late Jurassic bending of the lithosphere, respectively. During the early Cretaceous, the northern part of the TR was the location of a flexural basin with clastic infill, which is in contrast with the carbonate sedimentation of the remaining part of the TR. New sedimentological and structural observations reposition the present-day outcrops within the basin. Finally, the excursion visit sites where the mid-Cretaceous deformation is well pronounced in the structure of the Range.

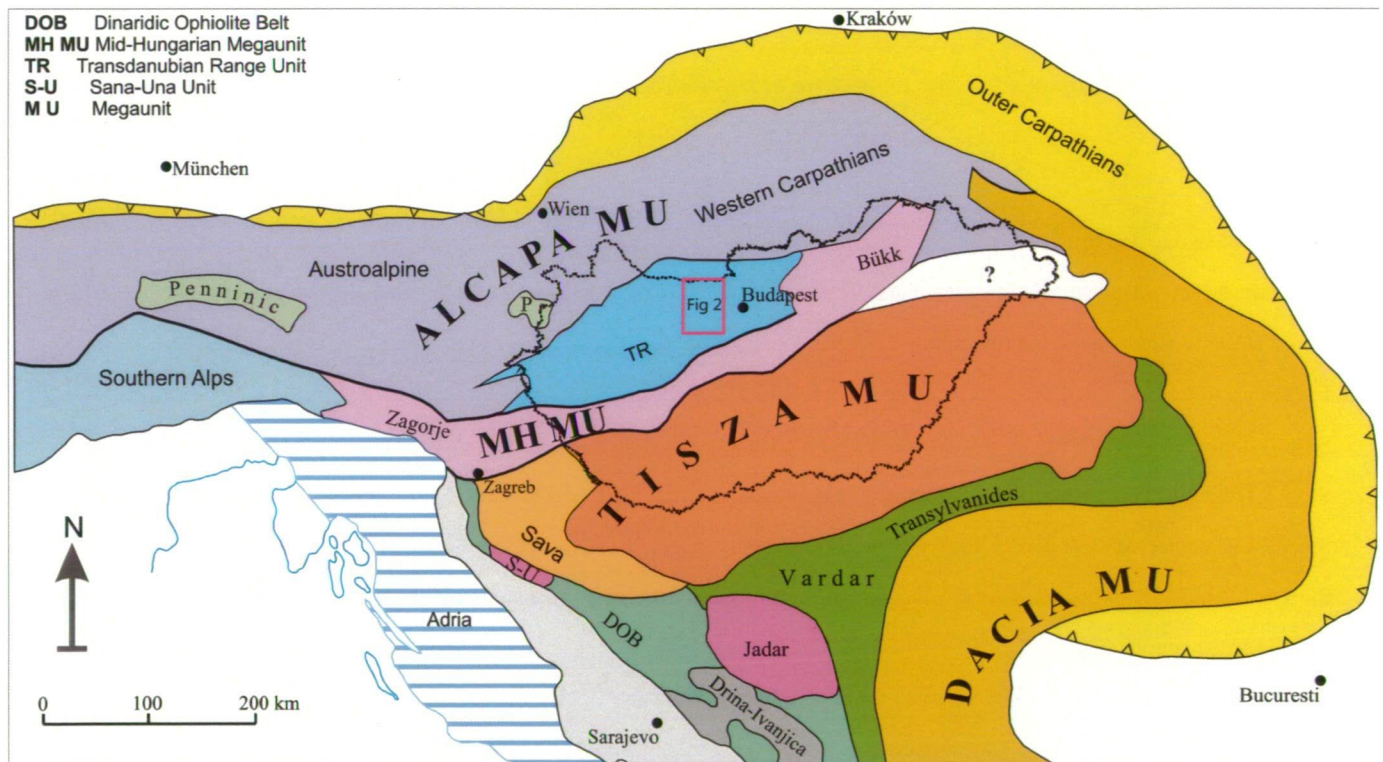


Fig. 1. Tectonic position of the excursion locations within the tectonic frame of the Alps, Carpathians, Dinarides. (Haas et al. 2010).

2. Geological setting and brief Mesozoic evolution

Late Triassic uniform platform stage (~220–200Ma)

In the Triassic the TR was located at the passive margin of the Vardar-Meliata Ocean (Fig. 3) (Kovács, 1982; Dercourt et al., 1986; Haas et al., 1995). As a consequence, the north-eastern part of the TR, the

Vértes, Gerecse and Pilis Hills were probably involved in the characteristic Mid-Triassic rifting of the Vardar-Meliata branch of the Neotethys (Kovács et al., 2010), although this is merely a projection of observations from the Balaton Highland located ca. 100 km to the SW (Budai and Vörös, 1992). The subsequent passive margin subsidence resulted in the deposition of ca. 2.5–3 km thick shallow marine carbonate rocks (e.g. Hauptdolomit, Dachstein Limestone) (Fig. 5) which represented the solid, quite uniform base of the subsequent Jurassic deposits (Oravec and Végh-Neubrandt, 1961; Haas, 1988).

Early Jurassic extension: sedimentary dykes, syn-sedimentary faulting (~200–190Ma)

After a relatively long and uniform period of subsidence (Late Triassic), fault-controlled differential motions renewed in the Early Jurassic in the whole of the TR (Galácz and Vörös, 1972; Galácz, 1988; Vörös and Galácz, 1998) including the Gerecse Hills. Their intense fracturing is demonstrated by Sinemurian sedimentary dykes (Stop 1.1) of various, often coarse-grained infill (Hierlatz Limestone) (Fig.

5) (Vörös, 1991; Lantos, 1997) whose age was precisely documented by brachiopods, ammonites and gastropods (Dulai, 1998; Szabó, 1998). Thickness variations, facies changes from fine- to coarse grained limestones, signify redeposition by gravity mass flows and have led to the postulation of the presence of syn-depositional faults or fault zones which limited shallower highs and somewhat deeper basins (Vigh, 1961; Fözy, 1993; Lantos, 1997; Császár et al., 1998). The largest high was named as Gorba High (Császár et al., 1998) which was marked by a very thin Jurassic sequence (ca. 5–10m) with large hiatus. Although the strike of facies belts were delineated already by the first works on Jurassic rocks (Vigh, 1961), and specified in sev-

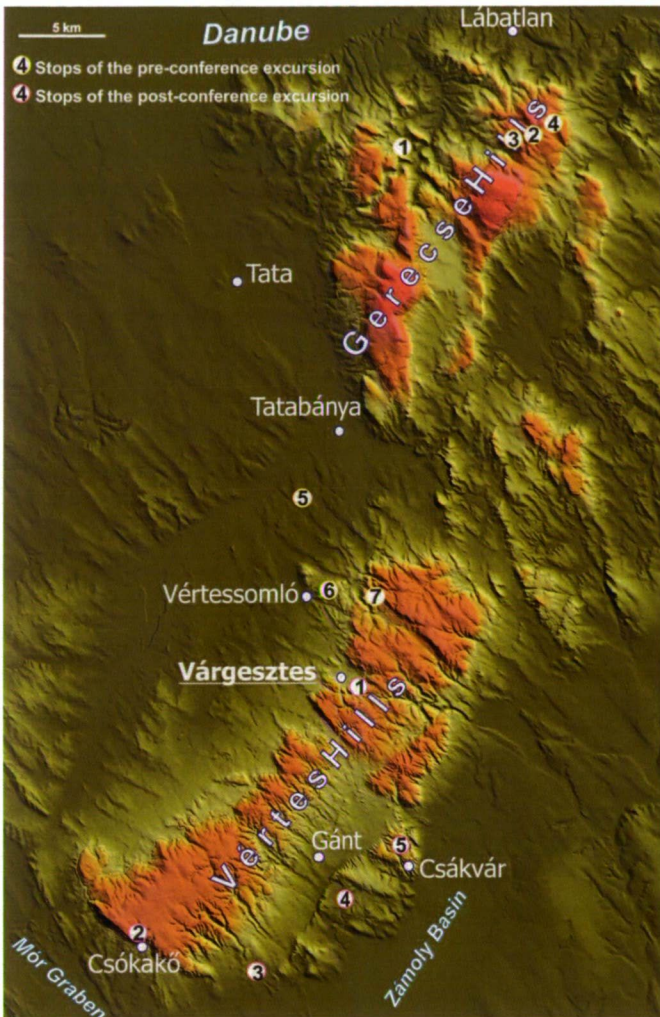


Fig. 2. Excursion stops for the pre- and post-conference excursion placed on a digital elevation model of the Gerecse and Vértes Hills. Note steep morphological slopes which mainly correspond to Cenozoic faults.

eral later works (Főzy, 1993; Császár et al. 1998) outcrop-scale faults were only very occasionally demonstrated (Fodor and Lantos, 1998). Without doubt, this faulting and platform disintegration can be connected to the early rifting stages of the Alpine Tethys further to the west (Fig. 4) (Stampfli and Borel, 2002; Schmid et al., 2004).

Middle Jurassic sedimentation (~180–165Ma)

Continuation of faulting probably went on during the Toarcian-Bajocian, the time of deposition of “Ammonitico rosso”, (Fig. 5) the characteristic ammonite-bearing, red pelagic limestone of the TR (Tölgyhát Fm., Vörös and Galász, 1988), although small-scale structural elements are missing. This relative tectonic quiescence is indicative for the relatively distal position of the Gerecse in the Alpine Tethys framework, while this is the major time of ocean drifting (Schmid et al., 2004; Schettino and Turco, 2011).

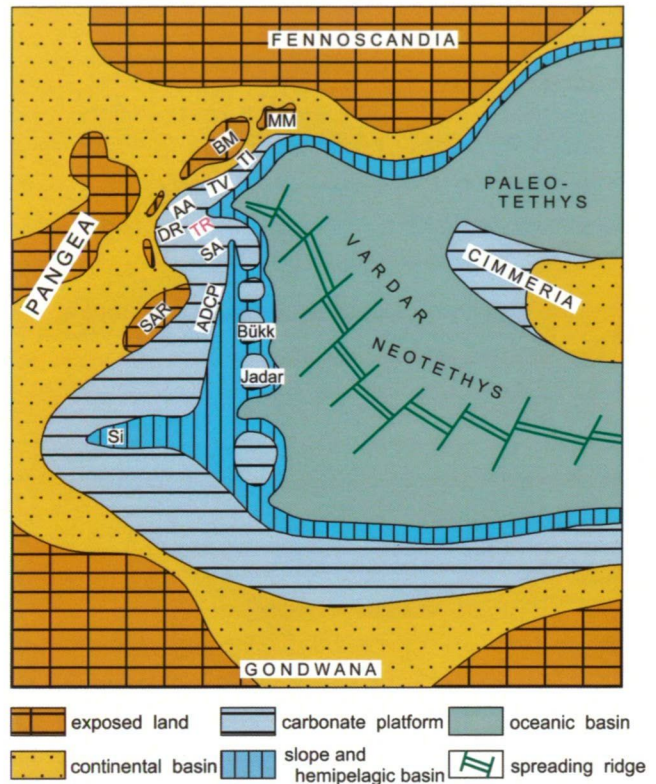


Fig. 3. Paleogeographic reconstruction for the Late Triassic showing paleo-position of the basement structural unit of the Pannonian Basin and the surrounding regions (After Haas et al. 2013). TR: Transdanubian Range, AA: Auszroalpine, DR: Drauzug, ADCP: Adriatic-Dinaridic Carbonate Platform, SA: Southern-Alps, BM: Bohemian Massif

Late Middle Jurassic to Berriasian sedimentation (165–140Ma)

The next step in sedimentary evolution was the deposition of radiolarite (Lókút Fm.). The age of this formation is Callovian to mid-Oxfordian, but in the most complete succession it went on up to the Early Kimmeridgian (Dosztály, 1998). It was originally radiolarian-rich carbonate sediment with sedimentary structures (Stop 1.2) but silicification during the diagenesis changed the rock to chert. The thickness and presence of siliceous sediments is variable, from 0 to 18m (Konda, 1988). This variation may reflect paleogeographic position within the late Jurassic basin (Fodor and Főzy, 2013). Two of the Gerecse sites show active faulting during chert formation, one of them is stop 1.2. The radiolarite is kept or dissected by a peculiar bed, the so-called Oxfordian breccia. Its age is well-constrained as Middle Oxfordian (Főzy and Meléndez, 2013). This is a redeposited bed (Bárány, 2004) consisted of limestone and chert clasts with limestone and chert cement. All these components form chaotic structure.

The upper Jurassic to early Berriasian is marked by pelagic limestone layers of generally 3-5m in thickness. Slight thickness variations, change in completeness of the succession, and fauna preservation are those characteristics which point to paleotopographical variations, and the survival of Liassic topographic highs.

Redeposited layers are present occasionally (Bárány, 2004), but they are limited in extent. Fault-related breccia bodies have restricted occurrences along active faults (Fodor, 2013). They have micritic matrix and angular clasts of Triassic and Liassic rocks derived from local

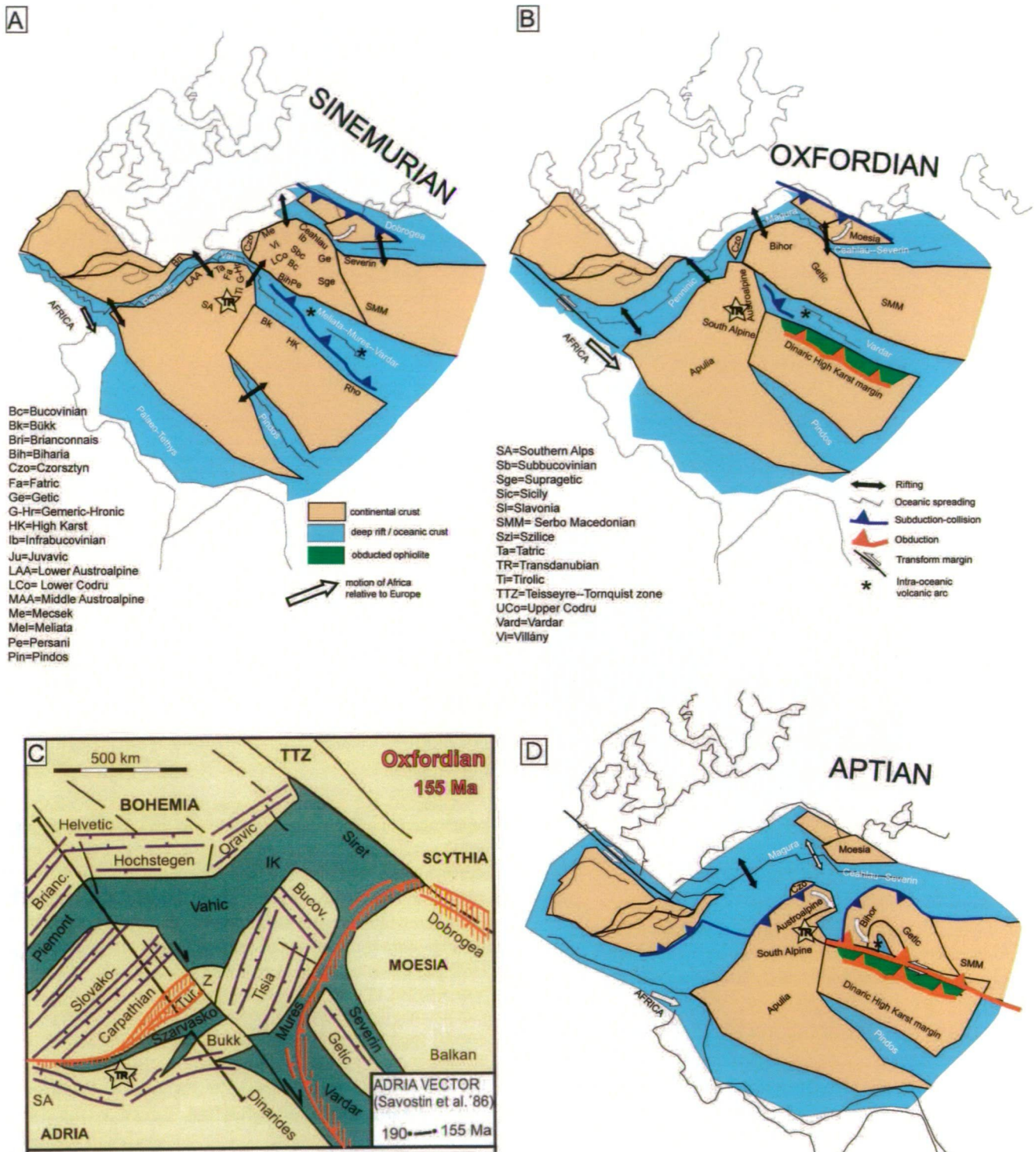


Fig. 4. Plate tectonic evolution of the Tethys for Sinemurian, Oxfordian and Aptian. A,B,D after Csontos and Vörös, 2004, while C is after Plašienka (2000). Note location of the Transdanubian Range with respect to opening and closing oceanic domains.

footwall block. The induced paleotopography, small highs and slopes could favour the settlements of different organism like crinoids, brachiopods, molluscs; their bodies were incorporated in coarse-grained bioclastic limestones (including so-called “Tithonian Hierlatz”, Vigh, 1945; Fözy et al., 1994; Császár et al., 1998).

Late Berriasian to Aptian sedimentation (140–110 Ma)

The Late Jurassic to Berriasian carbonate sedimentation terminated and changed to mixed siliciclastic-carbonate sedimentation in the Gerecse Hills. The pelagic ammonite-bearing limestones were replaced in almost all cases by the latest Berriasian to Hautrivian marl-

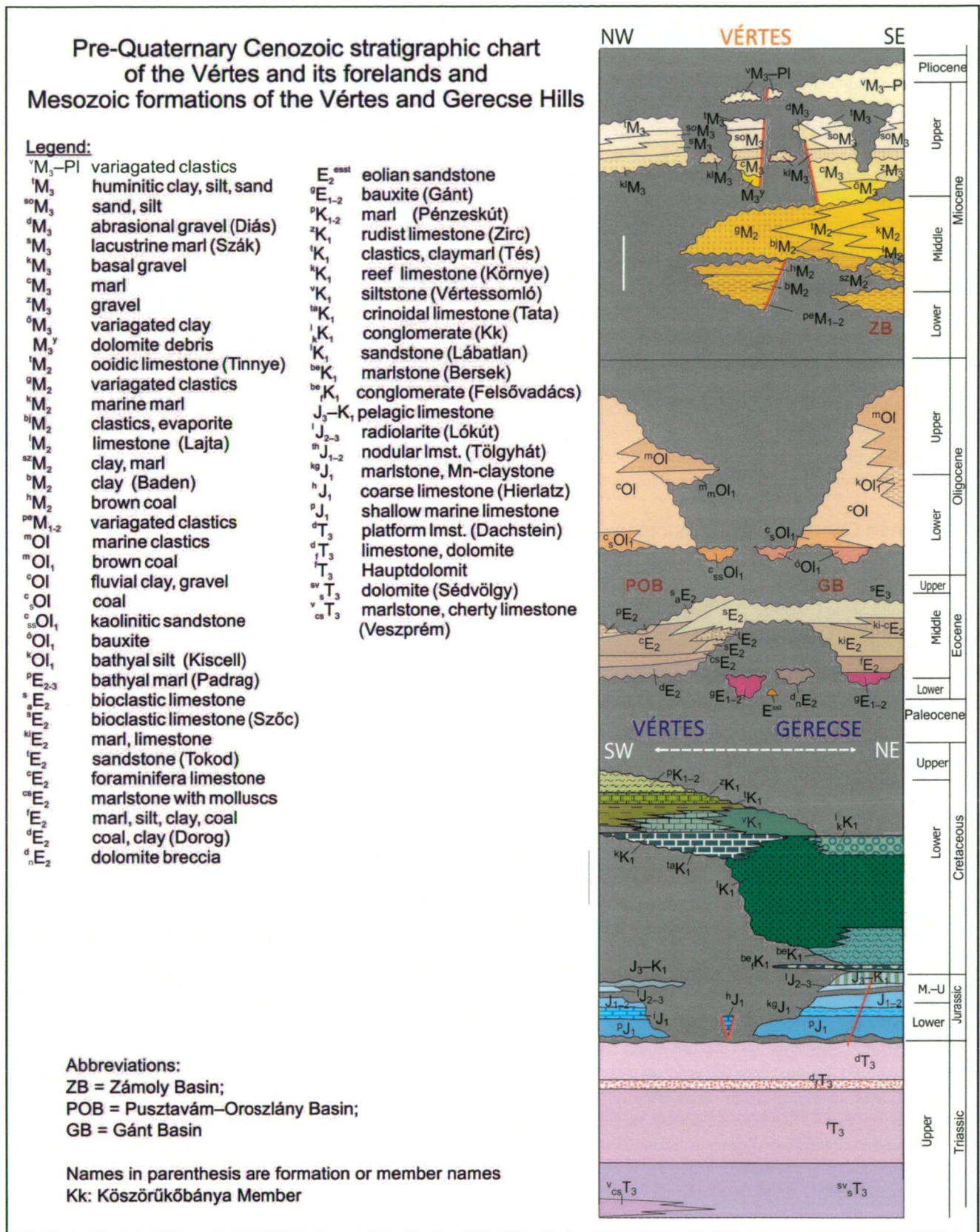


Fig. 5. Simplified stratigraphical chart of the Vértes and Gerecse Hills for the Mesozoic and of the Vértes Hills for the Cenozoic after Budai and Fodor (2008) and Császár (1995), modified. The chart tries to indicate variations across the ranges in thickness, completeness of the sequences and partly structural control.

stone, the Bersek Fm. (Fig. 5) (Fülöp, 1958; Császár, 1995) (Stop 1.3, 1.4). The first layers of this new sedimentary unit, the late Berriasian Felsővadács Conglomerate, are already the result of sediment density flows of long transport distance. Clast composition and heavy mineral assemblage indicate a complex source, which contained, among others, ophiolite sequence, radiolarite, neutral volcanic and intrusive rocks (Császár and Árgyelán 1994; B. Árgyelán, 1996; Árgyelán and Császár, 1998). Recently, shallow-water Jurassic limestone clasts were also identified (Császár *et al.*, 2008).

In the Barremian input of coarse clastics increased, the marlstone was replaced by sandstone (Lábatlan Fm) (Stop 1.4). Its deposition was mostly governed by gravity mass movements, turbidity currents and debris flows. Paleocurrent directions are from E to W, based on sole marks. These beds were deposited on a deep sea fan, probably at mid-fan (Fogarasi, 1995b; Császár *et al.* 2012).

Finally, the youngest known unit is a conglomerate, sandstone, siltstone (Köszörükőbánya Member), which contains mainly chert clasts but also shallow marine reef or lagunal limestone of Aptian to early Albian age. It represents deposits of high-density gravelly turbidity current and debris flows, which were formed in channels or terminal splays of mid-fan environment (Sztanó 1990; Császár *et al.* 2012).

Late Aptian to Cenomanian sedimentation (~115–90 Ma)

West and south of the Gerecse clastic basin, the sedimentation history was different (Kázmér 1987). After the Berriasian, there is a general hiatus. Shallow marine sedimentation started only in the late Aptian or earliest Albian with a crinoideal limestone (Tata Fm). The remaining part of the Early Albian is marked by the formation of a shallow bathyal sediment (Császár, 1995, Vértessomló Siltstone). It shows transition both to the crinoideal limestone (Tata Limestone) and to a reef (Császár, 2002, Környe Limestone). The Middle Albian is marked by a fluvial to lagunal formation (Császár, 1986, Tés clastics). It passes upward into the shallow marine limestone (Császár, 2002, Zirc Fm.). With notable subsidence or sea level drop, the limestone was replaced by marlstone of Late Albian to Cenomanian in age (Pénzeskút Fm) (Fig. 5).

The Senonian is missing in the central and northern TR, but one may speculate their presence and complete erosion. In fact, the TR was subject to several, very strong denudation phases during the Cretaceous, namely in the early Albian (ca. ~113–108 Ma), Turonian-Cenomanian (~94–86 Ma) and finally and for longest in the Paleocene to early mid-Eocene (~66–48 Ma). These denudation events occurred during subtropical climate with very low uplift rate, and resulted in the formation of sub-horizontal very low relief surfaces, (etchplains) with combination of subtropical karstification (Stop 2.4) (Mindszenty *et al.*, 1989; 2001). The early Albian denudation surface was buried and re-exhumed and slightly modified up to the mid-Eocene sedimentation. This surface can be used as reference for Cenozoic and late Cretaceous deformation. Although the traditional view considered the major Cretaceous stratigraphic gaps as the time spans for deformation phases (Császár *et al.*, 1982), we will try to convince participants that deformation was active during the sedimentation, too.

3. Mesozoic structural phases of the Gerecse and Vértes Hills

D1 phase: Early, Middle and Late Jurassic extension (200–142 Ma)

Visited outcrops connected to D1 phase: Nyerges Hill (1.1), Tölgyhát Quarry (1.2)

The detectable Jurassic structural elements are mainly sedimentary dykes, syn-sedimentary or covered faults. Several map-scale faults are suggested on the basis of different Jurassic successions in the two fault blocks. The orientation of the fractures is quite changeable, WNW-ESE, N-S (NNW-SSW), NW-SE and E-W directions are equally present (Fig. 6). Tilt-test of several locations proved that the fractures developed in horizontal bedding position. The infilling material of the Neptunian dykes is variable in lithology and in age, referring to numerous distinct deformation events throughout the Jurassic. Due to the similar style of deformation, all of these Jurassic extensional features were classified into the D1 deformation phase (Fodor, 2008).

On the basis of the field measurements the stress field can only be estimated. The extensional style of the deformation is proved in all cases, however, the direction of the stress axes vary from place to place. NNE-SSW—NE-SW extension is predominant, however, although locally, perpendicular extensional direction can also be estimated (Fig. 6). Based on the new structural data, there is no striking difference between the Early Jurassic and younger Jurassic stress field and deformation style.

D2 phase in the Gerecse and Pilis Hills: Early Cretaceous (Late Berriasian—earliest Albian, 142–110 Ma)

Visited outcrops connected to D2 phase: Ördögát and Bersek Quarries (1.3, 1.4)

This phase is connected to the formation of the clastic basin in the Gerecse and Pilis Hills. Few outcrop- or map-scale structures can be connected to this basin formation. Considering the stress field, three events are either coeval or just slightly post-dating this basin (Fig. 6). The relative chronology of the three events is not well-constrained: a more detailed work could lead to their separation into distinct phases. These phases were important in the structural evolution of the Gerecse Hills, but the separation from younger phases still need further work. Any of these stress fields rarely occur in the central and southern TR, partly because of the lack of Valanginian—early Aptian rocks. This indicates the attachment of D2 deformation to the particular clastic Gerecse sequence.

D2a: E–W to SE–NW extension

Few small-scale normal faults can be classified to this event. They were formed before the tilting of beds or during the burial of the sediments (Fodor, 1998; Horányi *et al.*, 2010; Fodor 2010). These small-scale structures are characterised by SE-NW extension (Fig. 6). Few fractures from the Vértes Hills can be attributed to this event: they were formed before the main folding phase.

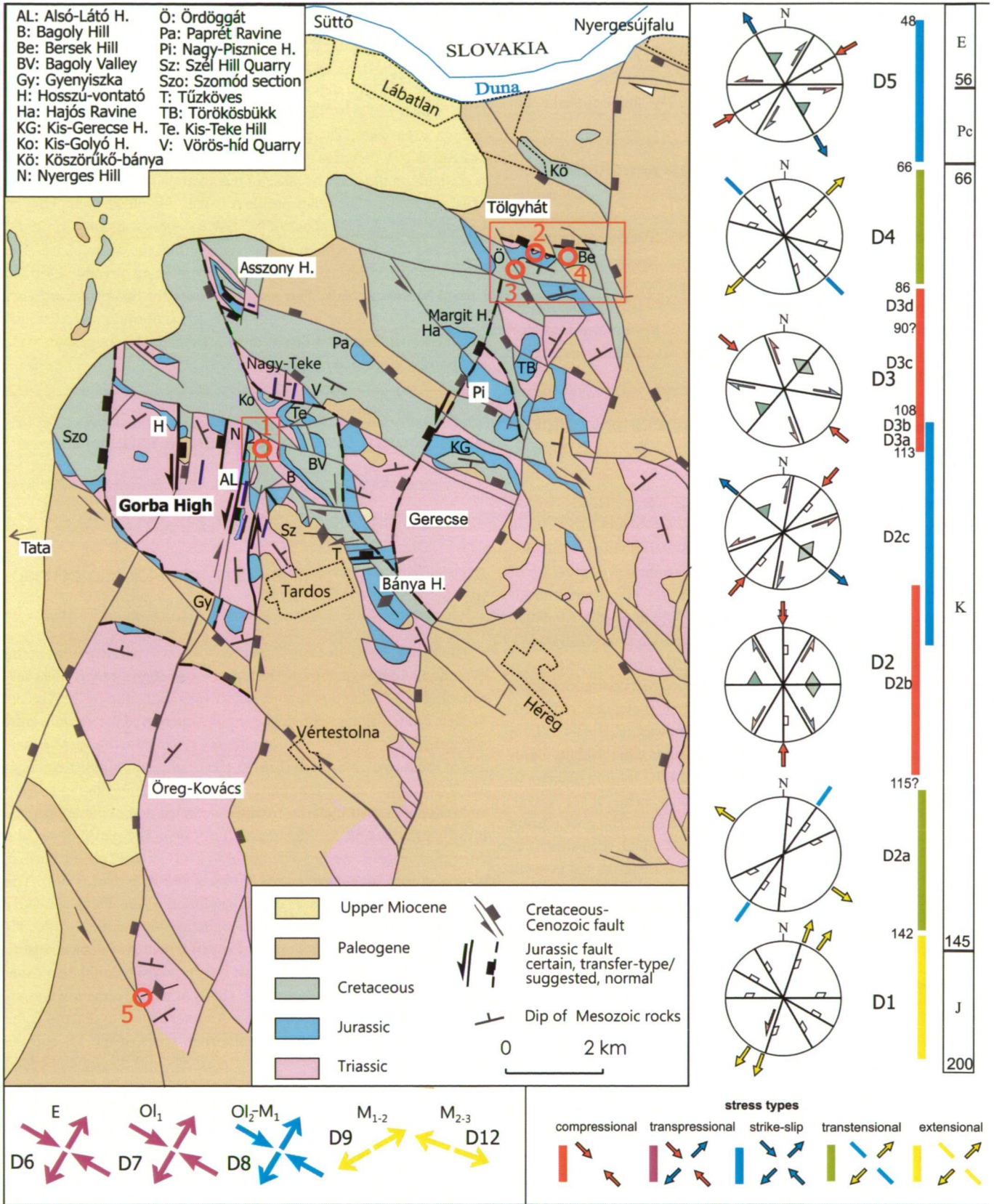


Fig. 6. Pre-Quaternary simplified geological map of the western and northern Gerecse Hills, after Fodor and Lantos (1998) and Fodor (2013), modified. Simplified fault pattern and stress axes are from Fodor (2008, 2013). Time scale is not proportional for the duration of the deformation phases.

D2b: N-W compression

The central part of the Gerecse Hills is often characterised by N-S compressional structures. These are ~E-W-striking folds, small-scale thrusts and NNW-SSE dextral and NNE-SSW sinistral strike-slip faults (Fig. 6) (Bada et al., 1996).

D2c: NE-SW compression and perpendicular extension

Strike-slip stress field characterised by NE-SW compression and perpendicular extension was detected in several localities of the Gerecse Hills. The direction of the maximal horizontal stress axis varies between NNE-SSW and ENE-WSW. E-W-striking sinistral and N-S-striking dextral strike-slip faults with NW-SE-directed folds and small-scale thrusts are characteristic (Fig. 6) (Bada et al., 1996; Sasvári, 2008, 2009a).

D3 phase: early Albian–Coniacian shortening (folds, thrust faults) 113–86 Ma

Visited outcrops connected to D3 phase: Környe Roadside stop (1.5), Vértessomló Church (1.6), Tatabánya, Terv road (1.7)

A series of mid-Cretaceous compressional deformation events led to the formation of the characteristic folded-imbricated structure of the central and southern Transdanubian Range. The orientation of compression was estimated on the basis of fold axes and calculated using fault-slip data. The direction of compression is generally NW–SE but it shows changes towards N–S (Fig. 6).

The deformation events could have occurred in a continuous manner but 4 individual sub-phases or events have been differentiated. The D3a event occurred before the folding, but was marked by a stress field similar to that of the folding. The first part of the folding represents the D3b event, while the termination of the folding belongs to the D3c event. While the D3b has early Albian age (ca ~113–108 Ma), the D3c was late Albian to Coniacian (108–86 Ma). The post-folding structures have been classified to D3d event, although such structures could also have been formed during later phases. Pre-tilt and post-tilt events mainly indicate coaxial deformation (stop 6, Vértessomló site), but a change of the compression in a clockwise sense could have occurred during the D3c and D3d events (Márton et al., 2009).

D4 phase: Santonian–Maastrichtian deformation (86–66 Ma)

In the southern-central TR a Senonian (Santonian to Campanian) sedimentary sequence covered the considerably deformed older rocks (Haas, 1999). The origin of the basin is not clear, compressional and extensional origin was also suggested (Tari, 1994). Few structural data in the southern TR could be connected to this phase, but its presence in the Gerecse Hills is questionable.

D5 phase: Paleocene(?) – Early Eocene strike-slip faulting (66?–48? Ma)

A strike-slip type deformation occurred in the Gerecse and Vértes Hills, which had an ENE–WSW compression and perpendicular extension stress axes. The major structures are sinistral faults in E–W or ESE–WNW direction (Fig. 6). The identification of these elements is difficult on the maps because of reactivation by dextral slip during Miocene events. The other problem is that this phase is not easy to separate from the D2c phase of NE-SW compression; Sasvári (2008) suggested that the two stress fields are in fact the same phase. The separation of D5 phase is easy when they affected already deformed (tilted) Mesozoic beds. The age constraints for this phase are very poor. It does not occur in Eocene rocks and deformed few Senonian sites in the southernmost TR, so these poor data may suggest the wide and poorly constrained time span.

4. Introduction to geodynamic interpretations

A brief notion to Alpine-Carpathian-Dinaric connection

The Late Jurassic to early Cretaceous was a dynamic period in the evolution of the Neotethys. In the tectonic-palaeogeographic units surrounding the TR there is firm evidence for subduction of the Vardar-Meliata branch of the Neotethys, partial obduction of the oceanic crust and thrusting of the evolving accretionary prism onto the passive margin of the down-going slab (Fig. 4) (Schmid et al., 2008; Kovács et al., 2010). This subduction-related process was connected to erosion and redeposition of material from the accreted and obducted nappes into flexural basins, in the close vicinity or in the periphery of the emerging orogenic wedge. The northern TR (Gerecse) clastic basin is clearly one of such depocentres (Császár and Árgyelán, 1994). The influence of these processes on the evolution of the TR is generally accepted, although the precise palaeogeographic position of the TR with respect to the subduction front is still a matter of debate. Just to mention two end-member scenarios: the thrust front could be outside the present-day TR (e.g. Tari, 1994; 1995) or the deformation was affected the TR (Csontos et al., 2005). Another aspect to discuss is the similarity of the stratigraphy and the rock types of the TR and the Northern Calcareous Alps, which is correctly and deeply embedded in Hungarian literature (Haas and Császár, 1987; Császár and Dosztály, 1994; Tari, 1994; Csontos and Vörös, 2004). It is another question, how many from the late Jurassic to Cretaceous deformation phases could be projected to the whole area of the TR. All these aspects will be compared with observations and models seen on the excursion stops.

The connection of the Early Cretaceous basin of the Gerecse Hills with the subduction of the Neotethys Ocean is an accepted model in the last 30 years. Its compressional origin was suggested by Balla (1981) in the first time. Since then, several authors have modified or

contributed to the basic geodynamic theory. Flexural origin of the foreland basin was suggested by Tari (1994, 1995) at the first time, and several other works arrived at similar interpretation (Császár and Árgyelán; 1994; Fogarasi 1995b; Mindszenty et al., 1995; 2001; Tari and Horváth, 2010). The exact position of the load has not been specified, yet. Most of the authors refer to NE-SW compression as the origin of the lithospheric flexure, which is supported by sediment transport from the NE (Sztanó, 1990; Fogarasi, 1995b). However, distribution of the partly eroded Albian lithofacies may refer to a deformation zone situated to the ENE of the Gerecse Hills (Császár, 1995; 2002). Thus, the exact compressional direction could have been anywhere between N-S and ENE-WSW and correspond to regional D2 deformation phase presented in the previous chapter.

In a regional scale, D3 was probably the phase when the TR became part of the Alpine nappe system (Horváth, 1993; Tari, 1994; Fodor et al., 2003). Within the Austroalpine system, the TR is the highest unit. It is to note that this tectonic position is different from those of the D2 phase, when the northern TR was not the highest unit but probably the lowest unit.

Further discussion of these geodynamic questions will be detailed in Chapter 5., after the presentation of the outcrop-scale observations.

5. Excursion stops

Stop 1. Tardos, Nyerges Hill

47°41'26.35"N, 18°26'3.17"E

This outcrop exposes the classical Hierlatz localities of the Gerecse Hills. This syn-tectonic sediment is bounded by Jurassic syn-sedimentary faults, which were only partially reactivated during the post-Jurassic (mainly Cenozoic) deformation).

Stratigraphy: Norian Dachstein Limestone, Sinemurian brachiopod-crinodal limestone (Dulai 1993)

Publications: Lantos (1997), Fodor and Lantos (1998), Horányi et al. (2010).

This stop is found 3km north from Tardos village, on the eastern end of the Nyerges Hill (Fig. 7a). Most of the hill consists of thick-bedded Upper Triassic Dachstein limestone which represent thick portion of the passive margin platform carbonate of the Neotethys. It is bounded on the east by a fault which separates the Sinemurian bioclastic limestone on the easternmost tip of the Hill (Fig. 7a, 7b, 7d). This particular rock type is limestone with crinoids, brachiopods, and small (but not dwarf) Ammonites (Fig. 7c), and may contain blocks from the nearby Triassic limestone. The matrix is red, yellow micritic limestone but the clast- and matrix-supported patches does not show clear organisation. This rock is considered as having been formed at the slope of syn-sedimentary fault or within neptunian dykes (Vörös, 1991). This fault-related rock is called Hierlatz Limestone in the Alpine literature. This rock frequently occurs only in fault-bounded fissure fillings and no stratiform counterparts occur. If it does, it is a bioclastic layer with sign of gravity flow transport (Lantos, 1997). Sedimentary dykes in similar strike are well-known from the surrounding hills. One dyke is located at the top of the hill, with 20-30cm width (Fig. 7a). In fact, all these structures occur in a narrow zone of N-S strike from Tardos up to 5km length (Vigh, 1961). Lantos interpreted this zone as the sign of a tectonically active Jurassic fault zone.

The contact is locally associated with calcite veins of 1-15cm thickness (Fig. 7d) but in other cases the Triassic and Jurassic limestones are cemented: the faults have been healed. The fault now vertical, but if one apply backtilting, the fault becomes steeply east-dipping (Fig. 7e).

The Jurassic limestone is bounded on the north and east by faults which separate it from Triassic limestone. In this way, the peculiar, fault-related sediment body has a triangular shape and bounded by all sides by faults (Fig. 7a). Because of the fault-related nature of the Hierlatz Limestone, and the locally healed contact with the Dachstein Limestone (Upper Triassic), we interpret all faults as Jurassic. Post-sedimentary reactivation is not excluded, but could be limited.

Similar, fault-bounded Hierlatz limestone occurs ca. 500m, southward, in the Gyökér Valley (Lantos, 1997; Fodor and Lantos, 1998; Horányi et al., 2010). Here the Early Jurassic syn-sedimentary fault is now dipping gently to the west. Backtilting to its original position brings the fault to its Jurassic steeply west-dipping position. In this location, the fault plane is covered by Early Jurassic limestone, cemented to the Dachstein Limestone (Upper Triassic) across the fault (Horányi et al., 2010). This proves that the original Jurassic contact



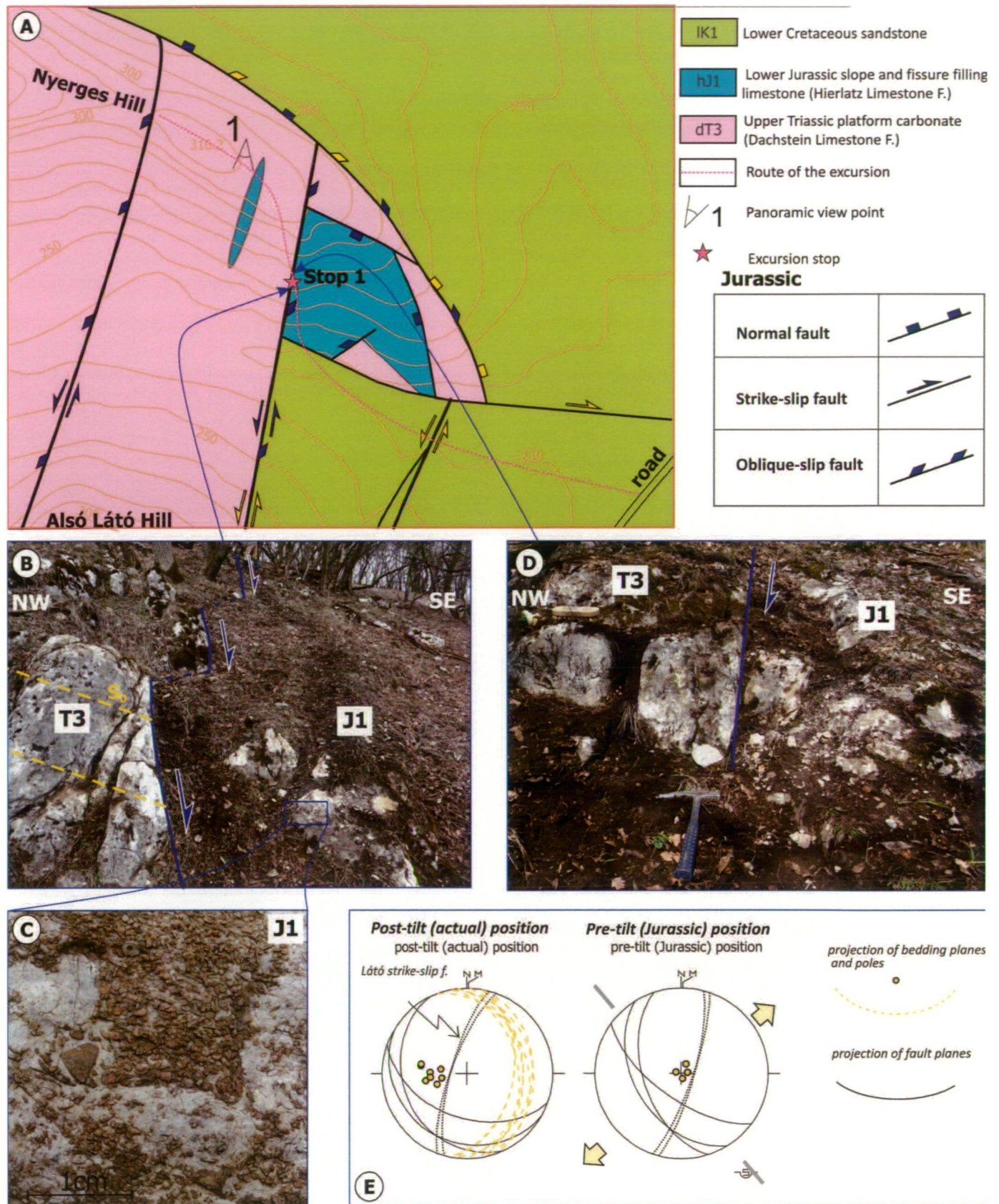


Fig. 7. Structural situation at Stop 1.1, Nyerges Hill, north from Tardos. A) Map of the Nyerges and Alsó-Látó Hill (Fodor and Lantos 1998, modified). B) Series of fault contacts between the Upper Triassic and Early Jurassic coarse bioclastic limestone (Hierlatz Fm.). C) Coarse crinoideal limestone and fine-grained matrix. D) Fault contact between the Upper Triassic and Early Jurassic coarse bioclastic limestone (Hierlatz Fm.). E) Fault data on stereographic projection from the Nyerges Hill (Fodor and Lantos 1998) at actual and Jurassic (back-tilted) position. Note sub-vertical character of the main Jurassic fault.

remained intact and was not reactivated. The other argument for Liasic slip is that the fault and both blocks are covered by very reduced uppermost Jurassic (Kimmeridgian? to Tithonian) limestone. Similar, gently west-dipping fault occurs at the foot of the Nyerges Hill.

The revealed fault geometry thus consists of steep N–S striking features, and NW–SE to WNW–ESE striking segments (Fig. 7e). These latter directions are typical in other localities, thus is considered as the main extensional structures while the N–S direction is regarded as transfer faults.

Stop 2. Lábatlan, Tölgyhát Quarry. Bathonian(?) to Callovian normal faults, dykes (168–163 Ma).

47°43'20.92"N, 18°30'45.80"E

The outcrop offers a view to a typical, more or less complete Jurassic succession. This quarry exposes deformation features, which have excellent time constraints and therefore are definitely Jurassic in age.

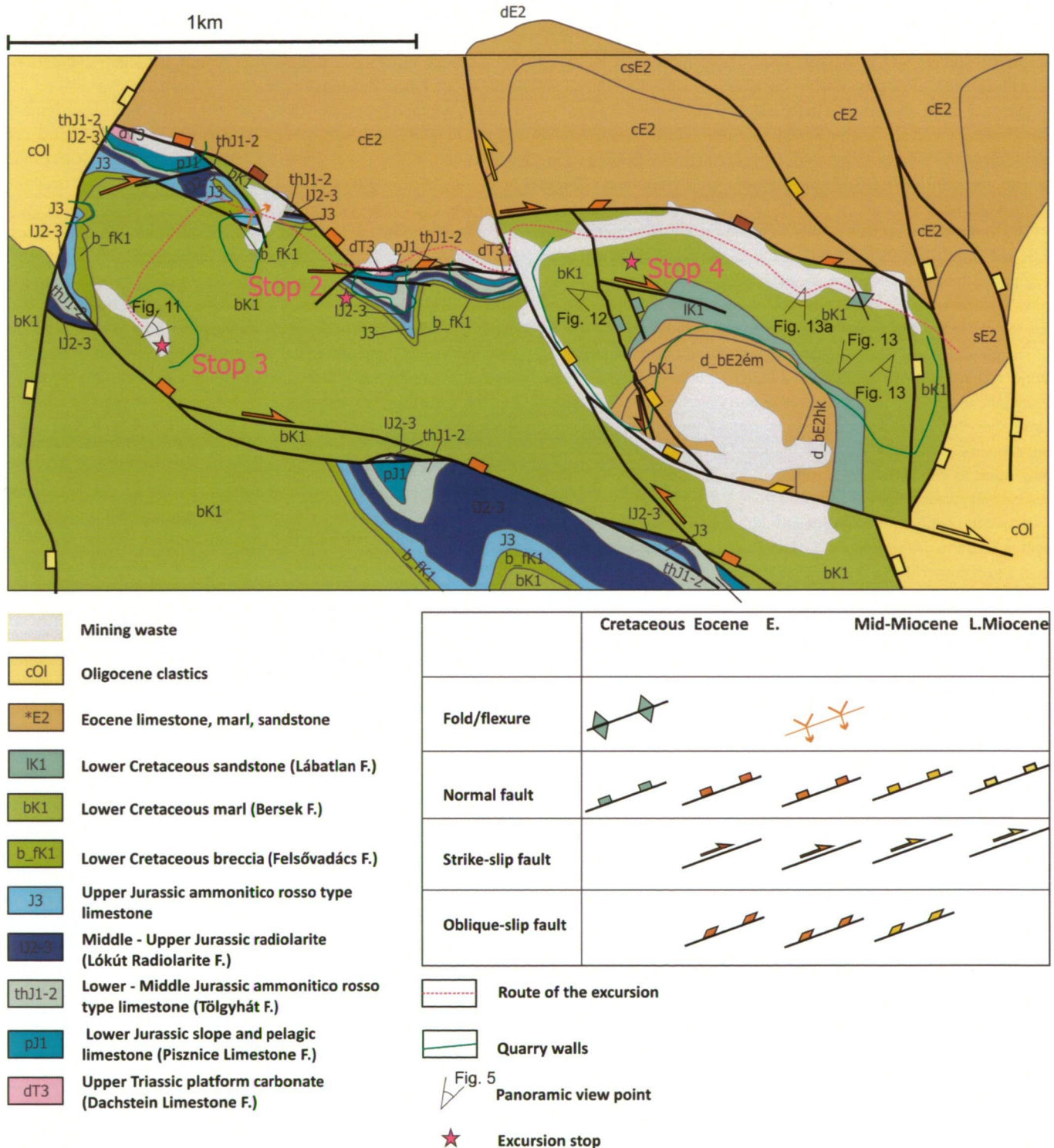


Fig. 8. Geological map for the stops 1.2, 1.3, 1.4 in the northern Gerecse Hills (after Albert, 20002 and Fodor 2009-2010 unpublished mapping results). White patches are damp sites of the quarries.

In addition, the geometrically complex connection between segmented faults, and related folds is worth to see.

General tectonic situation: dip to SSW by 15–20°.

Stratigraphy: At the bottom of the small quarry the Upper Triassic Dachstein Limestone is exposed (Fig. 8). The shallow marine limestone contains molluscs (*Megalodus* sp.) and probably has Rhaetian age (Fülöp et al. 1969). The lowermost Jurassic seems to be missing, and the following 15m thick yellow or grey unit still represents a shallow marine limestone containing crinoids, brachiopods or Ammonites. This limestone gradually changes to well-bedded pink limestone of 10m thickness which has stylonitic and wavy bedding planes with clay seams and nodules with manganese crust. This is overlain by the Toarcian black and yellow clay of 0,5m thickness, which is the equivalent of manganese ore of other sites in the TR. The following 2-3m is composed of thin-bedded marlstone and limestone nodules. It is followed by the classical “ammonitico rosso”, the red, Ammonite-bearing nodular limestone of late Early to mid-Jurassic age (Cresta and Galácz, 1990, Tölgyhát Fm).

The topmost bed surface of this formation is a highly bioturbated pale red limestone. Bioturbation occur as wavy, max. 20 cm long cylindrical tubes of 1–4cm in diameter (Fig. 9b). Occasionally burrows contain infilling sediments of whitish marlstone. This surface has the appearance as a poorly developed hardground.

The ca. 2m thick “chert” layers are composed of laminated limestone, which was partially silicified during the diagenetic process (Fig. 9a); a phenomenon which was already observed by Vigh (1961) and Dosztály (1998). Laminae are parallel but can show thinning, pinching out and very small angle cross lamination. This sedimentary structure may point to deposition from sediment gravity flow although deep sea currents cannot be ruled out.

Above the radiolarite, a 1m thick middle Oxfordian redeposited bed occurs (Bárány, 2004; Főzy and Meléndez, 2013). The upper Oxfordian and Kimmeridgian seems to be missing, and only the Tithonian is represented by purple, or white pelagic micritic limestone beds (Főzy and Szinger, 2013). They are exposed above the quarry and in a small ravine to the south. Finally, the last outcropping beds are the conglomerate of the basal member of the Gerecse Cretaceous clastic sequence (Felsővadács Member).

Earlier structural works: Sasvári et al. (2009), Fodor (2013)

Jurassic structures

Age of fractures

The deformation elements are beautifully exposed on the upper beds of the Tölgyhát Formation, displace few basal beds of the Lókút Radiolarite but do not disturb the main part of the chert layers and definitely do not cut the unique “Oxfordian breccia” layer. Therefore the observed deformation features post-dates the Tölgyhát Limestone of Bajocian age (Cresta and Galácz, 1990), and are Bathonian to Callovian in age although an extension into the earliest Oxfordian cannot be ruled out.

Fault geometry

The top beds of the Tölgyhát Fm are cut by small-scale faults, infilled sedimentary dykes and joints (Fig. 9c, d). In a number of cases, faults with clear vertical separation have sediment infill in their deeper parts, so they are part of the class ‘sediment infilled fractures’ (Beacon

et al., 1999), like the dykes. In the case of joints, sediment fill was not observed.

All these fractures have variable strike and their along-strike geometry depend on this strike. The most common direction is W–E to WNW–ESE; faults, dykes and joints belong to this class. NW–SE striking infilled faults and dykes are also present. These two classes have straight to slightly wavy geometry both along strike and dip. On the other hand, NE–SW directed infilled fractures and joints are generally highly curved, and connect two other fractures from the previous sets. Dip is in both directions for the E–W to NW–SE striking fractures, with dip degree from 50° to 90°, while NE–SW joints are sub-vertical. Fractures are sometimes planar, but small undulations and protuberances are equally present.

Dyke width ranges from 0.5 to 8 cm (Fig. 9d). Infilling sediments are red to white marlstone, silicified marlstone and reddish brown or white chert. Wider dykes contain angular to subangular clasts of the host Tölgyhát Limestone (Fig. 2d, e). In some cases, clasts from the overlying chert also occur in the dyke infill.

Faults have few cm to 50 cm displacement (Fig. 9c). In all cases, the hanging wall blocks contain chert and intercalated silicic claystone layers which either do not appear in the footwall or their thickness is smaller. Ductile drag of these growth layers is ubiquitous. The best example is the largest fault, where dip degree of the lowermost chert bed reaches 50°, and decreases upward from bed to bed. Along this fault, the hanging wall thickening of the first 3-5 beds is very clear; and the lowermost two beds almost filled the void created by the fault movement.

Kinematics, stress field

Faults show apparent normal separation, except for one, which has thickening in footwall and dip toward the hanging wall. In one case, the geometry of overlapping fractures can indicate dextral or dextral oblique slip (Fig. 9b). Opening of one dyke is connected to sinistral motion. Few slickenside lineations are present, in the form of calcite fibres on fault planes (Fig. 9f). Because these faults have no continuation in the higher Lókút Fm., their post-Oxfordian reactivation can be excluded, so the fibres are Jurassic in age. These slickenside fibres show normal separation on WNW–ESE and sinistral to normal-sinistral on NW–SE trending faults. Together with other observations, this would suggest a coherent kinematic picture, with W–E trending dextral, WNW–ESE trending normal or dextral-normal, and NW–SE trending normal-sinistral faults. Stress calculation would indicate NNE–SSW trending tension. However, this data should be taken as approximation because of small number of kinematic indices.

Rheology of deformation

There are a number of evidences for the soft state of cherty siliceous sediments at the time of deformation, and also for the partially lithified status of the underlying limestone. Slight thickness variation and bend can still occur in the third to fifth chert layers from the base, but higher up no traces of deformation occur. It unequivocally demonstrates syn-sedimentary origin of the fault displacement. Ductile drag of the basal chert layers and some dyke infill indicates soft state of sediment at time of deformation. Because of the complexity of cementation and the mobility of silica gel this state could existed during the (early) lithification process. The underlying limestone was in an advance state of cementation because of ability to be fractured along straight planes. On the other hand, protuberances on fault walls indicate a certain plas-

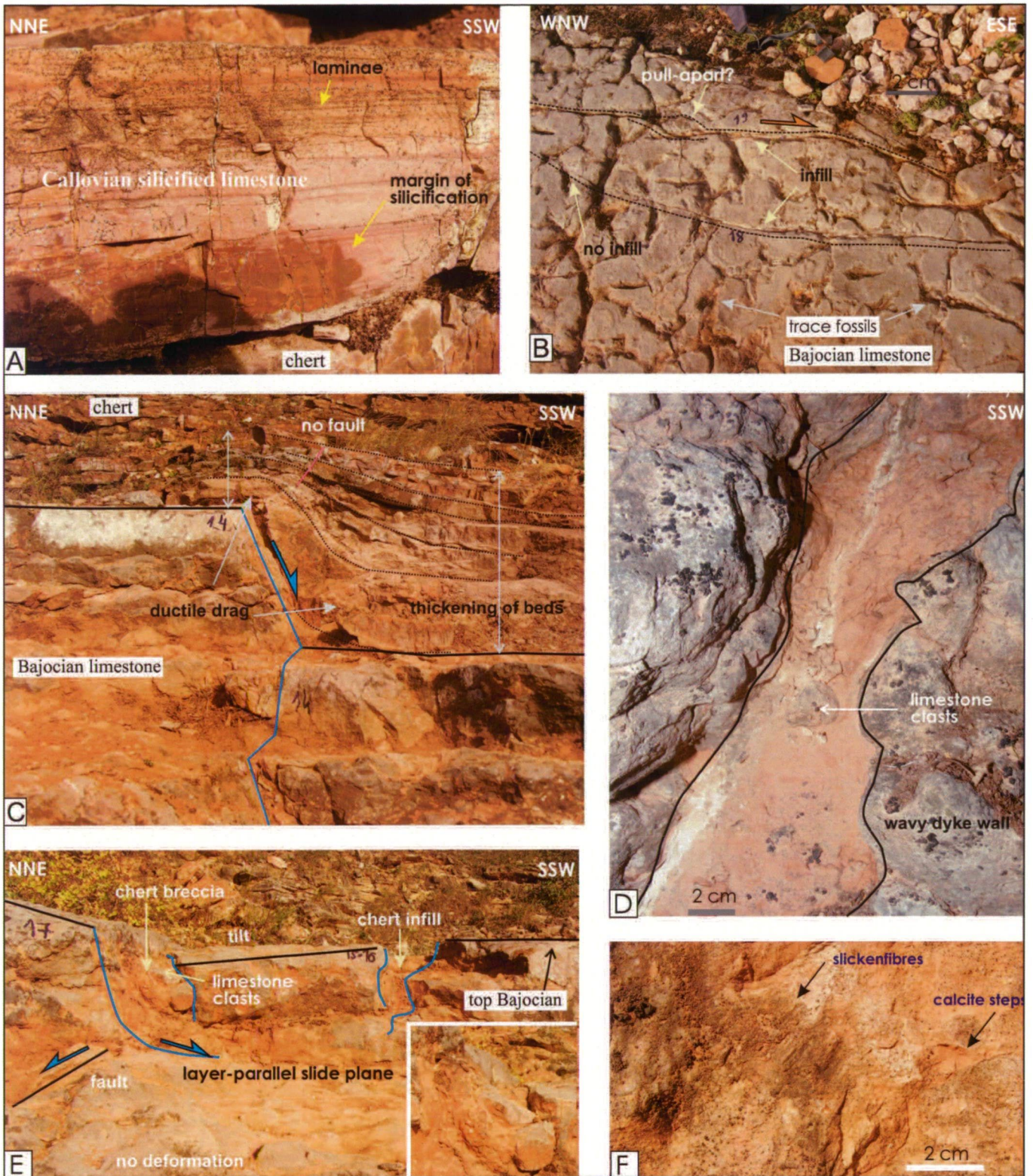


Fig. 9. Structures of the Tölgyhát Quarry, Stop 1.2. A) Laminated, partly silicified limestone (Lókút Radiolarite Fm.) probably deposited by sediment gravity flow. B) Trace fossils(?) on the highest bedding plane of the Tölgyhát Formation, connected to poorly developed hardground. Sediment-filled fractures could open due to dextral shear. C) The largest syn-sedimentary fault of the quarry. The normal fault contains beds with increased thickness in the hanging wall, and the fault does not continue in the higher beds of the chert. D) Jurassic dyke with silicified marlstone infill in the Tölgyhát Fm. E) Gravity slide of the higher Tölgyhát beds. Inset shows angular clasts of the Tölgyhát Fm. filling a dyke along the sliding plane. Note pronounced downward shallowing of the slide plane. F) Jurassic calcitic slickenfibres on the largest fault plane.

tivity of the limestone, which was not fully indurated. In conclusion, the deformation was syn-sedimentary for the basal parts of the radiolarite and can be classified as syn-lithification type for the underlying limestone.

Origin of the structures: Sedimentary versus tectonic deformation

Few faults certainly cut downward at least 3-5m across the mid-Jurassic limestone which favours their true tectonic origin rather than being simple sedimentary deformation. On the other hand, non-tectonic origin is clear for few faults. The northernmost faults do not continue downward but curved strongly and the displacement was probably transferred to bedding plane slip (Fig. 9e). The hanging wall block was tilted toward the fault and dismembered by additional faults, dykes. This structure can be considered as sedimentary slide with rotating hanging wall block. It is not excluded that sliding was triggered by true faulting, because one fault underlays the slide.

Segmented fault zone and folds

Sasvári et al. (2009) documented in great detail two peculiar features of the quarry. One is a E–W trending fault zone which cut across the eastern quarry wall. Although their observations are correct in several details, and followed here, our interpretation is slightly different. The fault zone consists of two main south-dipping segments, one sub-vertical fault and several, smaller gently north-dipping faults. Beds are rotated between these small faults which detach onto the marl unit. The sub-vertical fault cut the limestone above but no below the marl unit. The two main fault segments are planar in the limestone units, but do not continue in the Toarcian marl and clay layers (Kisgerese Fm.). Instead, they form a continuous, folded unit, which have variable thickness, and the black clay can thin out completely. The complete displacement can be in the order of 3m. This geometry demonstrates that the displacement was accommodated by planar discrete faults in limestone and ductile structures in the marl-clay unit.

The structural geometry is typical for along-dip segmented normal faults and the associated fault-related fold (Khalil and McClay, 2002; Koyedole et al., 2003; Fodor et al. 2005b). The two brittle planar fault segments were formed approximately at their present position and are en echelon in dip direction of the deformation zone. The continuous marl unit can be considered as clay smear dragged along the fault plane, or more precisely at the overstep zone of the two fault segments. The north-dipping small faults occur above the marl unit and can be considered as antithetic faults of the main zone. Rotation of the faults and the intervening blocks are typical near along-dip segmented faults (Rykkeldid and Fossen, 2002; Willsey et al., 2002; Fodor et al., 2005).

The western quarry wall exposes the strongly deformed marl-clay unit which is cut by curved listric faults restricted only to the marl level. Marl layers are strongly tilted oppositely to listric faults, while the whole overlying limestone shows a general flexure. Few steep faults cut the marl and overlying limestone. Within-marl faults indicate E–W extension.

In both cases, the sharply different rheological behaviour of the marl unit with respect to limestones is without doubt. This unit could form good detachment horizon which separated the faults above and below this level, and could be deformed in macroscopically ductile manner between fault segments. The question is when the marl-clay

unit had this exceptional rheological character. Because of the present-day cemented nature of the marlstone, the ductile deformation could be a relatively early feature before the complete diagenesis. The E–W trending en echelon faults are parallel to the Callovian small normal faults, so a temptation is possible to rank the E–W faults as Jurassic, although no firm evidence support this idea. On the other hand, the curved faults are sub-perpendicular to the E–W faults and their age is difficult to determine.

The observed structural geometry of the Tölgyhát and of other quarries is used for a general, simplified model for the deformation style in the Gerecse Jurassic and early Cretaceous rocks (Fig. 10). The structural pattern consists of fault segments which are in en echelon geometry both along strike and dip. Fault-related folding is very pronounced in the Toarcian Marlstone and in the Bersek Marl (Fig. 10). Simple drag folds are ubiquitous in marly lithology. The other type of folds occurs between along-dip segmented faults, like in the case of the Tölgyhát quarry. Fold limbs can be very steep approaching the dip of the limiting faults. Faults can flatten to sub-horizontal in the marlstone unit. Antithetic faults can be accompanied by folds, too, and in this way synclines occur between conjugate faults. All these deformation features are possible because of different rheological character due to the contrasting marlstone and limestone lithology. The structural pattern warns that observation of folds is not necessarily the expression of regional contraction but could only be connected to local rheological conditions, and can reflect extensional or strike-slip setting.

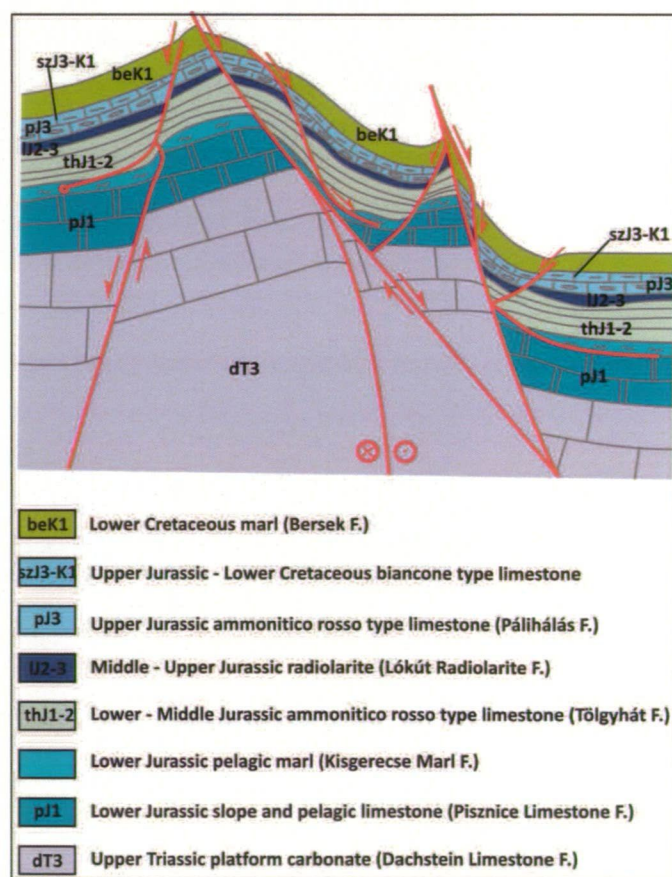


Fig. 10. Model for the deformation of the Jurassic and early Cretaceous sediments. Structural pattern involves along-dip segmented faults, fault-related folds and drag folds, the two latter are mainly connected to Toarcian and Valanginian marlstone units, where ductile deformation was possible.

Stop 3. Lábatlan, Ördögát quarry. Early Valanginian slides

47°43'18.45"N, 18°30'18.62"E

The main attraction of this site are early Cretaceous (Valanginian) sedimentary deformation features, slides and related faults and foliation. In the outcrop the mid-Berriasian to earliest Barremian Bersek Marl can be studied in details (Fig. 5, 8). The bearing of deformation features for basin geometry, evolution and broader geodynamic interpretation will be discussed in this and in the next outcrop.

Rock type, stratigraphy: Bersek Marl Formation, late Berriasian to Hautrivian. Its age is best constrained by Cephalopods (Főzy and Janssen, 2009) and nannoflora (Fogarasi, 2001) mainly from the classic Bersek quarry. Local position is close to the base, (ca. 20–25m from the base of the formation) and nannoflora also support lower Valanginian (Fogarasi, 2001). Carbonate content of the marl layers, reflected by their resistance against weathering, is highly variable. Few centimetre-thick fine to medium-grained sandstone beds intercalate among 10–40 cm thick marl layers. Many small sandstone beds have sharp base with sole marks. They are normally graded, rarely horizontal to cross-lamination can be observed. Their transition to the overlying marls is rather abrupt. In the marl large (up to 1-2 cm in diameter), sand-filled winding, bed-parallel burrows are common. The interpretation of the sandstones as turbidites is well accepted.

Earlier studies: Balkay (1955), Fülöp (1958), Császár (1992-2000 unpublished mapping) Fogarasi (2001), Albert (2000-2002: unpublished map compilation), Sasvári (2008), Sasvári (2009a, b), Fodor (2009-2010: unpublished mapping).

General tectonic situation: dip to SSE by 8–10°.

Deformation features: The main features of the marl sequence are rock packages which have larger dips than the „normal” layers (Fig. 11a, c green layer packages). Dip degree can reach 30 in these blocks. The internal structure of such blocks is quite regular, tabular beds are parallel to each other but bending can occur at package terminations (Fig. 11b, c). They can terminate sharply to underlying gently tilted beds or bend gradually from sub-horizontal to steep position.

The packages have shear contact at their lower side, while the upper contact seems to be a gently curved erosional surface. The lower contact is generally sharp, but the slide plane is not easy to study and measure (dig out): the sub-horizontal and moderately dipping layers seem to be welded, cemented to each other (Fig. 11b, c, d, f). No (rare) calcite steps have been formed or preserved along these surfaces. Fault planes are layer-parallel sub-horizontal, or gently cut across layers.

The upper surface is generally slightly erosional, and thus become weakly undulatory. The relief is only a few decimetres deep, but the width of these gentle troughs is several tens of meters). The overlying beds commonly onlaps on their flanks, therefore thin pinching out units can be distinguished (Fig. 11a, b, e). Overlying marl layers are as continuous and parallel as the ones at the bottom of the outcrop.

Three main packages are recognised in the 15 m high quarry. The lowest package 1 is the largest, with vertical thickness of about 6-8 m. It contains parallel tilted layers with sharp basal plane, which climbs upward toward the NW (Fig. 11a, b). Near the SE end, the dip of layers gradually decreases, and flatten to sub-horizontal. The welded basal shear plane is well visible below the tilted package (Fig. 11c). Further to the SE, the basal shear surface can continue parallel to bedding but it is not well exposed. Two oblique shear planes occur

above the basal surface, both step up over several layers (Fig. 11b, f). The lower shear plane cut few tilted beds but terminates upward. The higher shear plane (small low-angle fault) detach downward to an undeformed clayey marl layer, so it seems to be a secondary feature. At the higher termination of this low-angle shear, a wedge-shape marl unit occur (Fig. 11f). Within the main oblique package, internal faults and shear zones can be seen, where marl layers were dragged into the shear zone (Fig. 11d). The slip increased the tilt of the layers. The contacts along the faults are welded and are very similar to “normal” sedimentary contact between layers. Tilt of beds in package 1 was toward the ESE, while the dip of the basal faults and internal shear surfaces is mainly to the east or west (Fig. 11i). Close to the lower shear surface, a dense network of gently dipping planes is visible (Fig. 11c). They have slightly curved or sigmoidal shape, and cut the bedding planes.

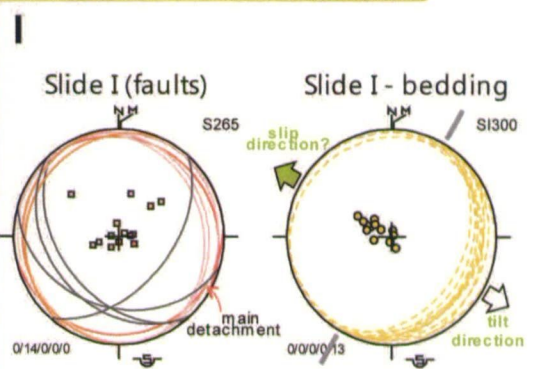
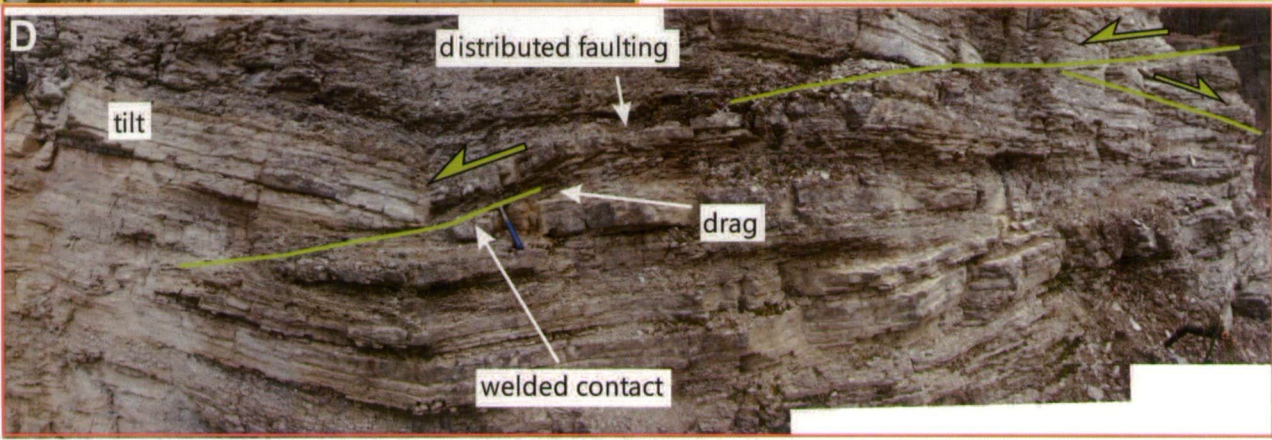
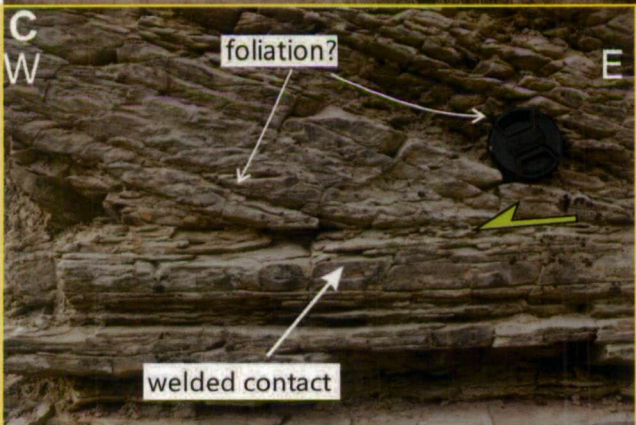
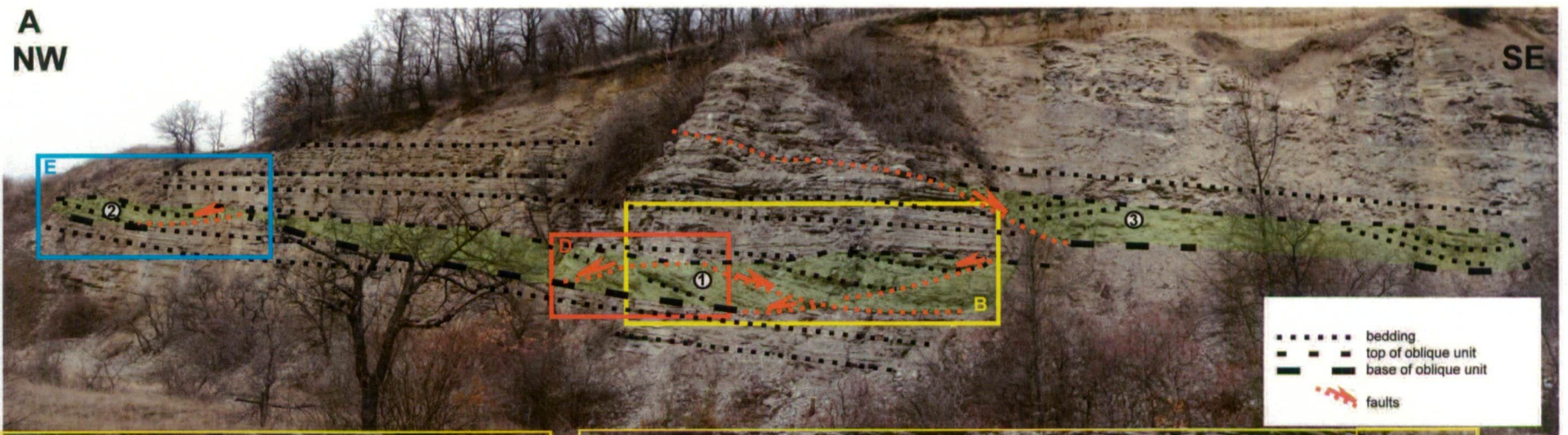
Package 2 is found in the NW corner and the tilt and basal displacement seems to be (relatively modest and) oblique to the main quarry wall (Fig. 11a, e). Correlation of sandstone units indicates normal displacement along anastomosing faults. It is possible that package 1 and 2 would be the same, but their transition is difficult to observe and is cut by an erosional surface. For package 2 we have no measured data but slip could be westward.

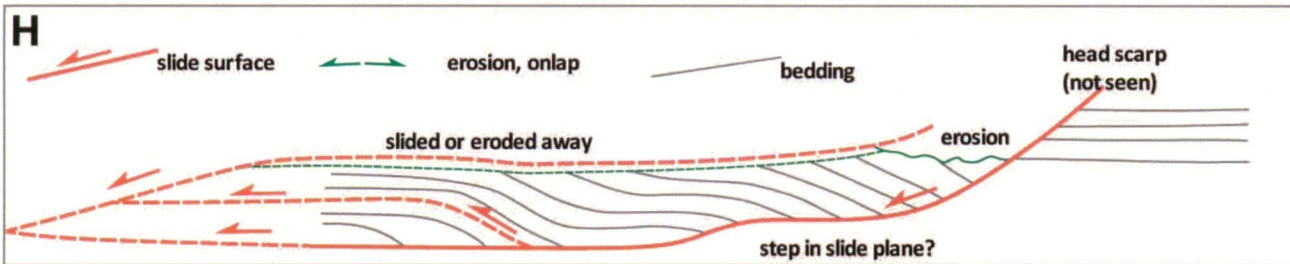
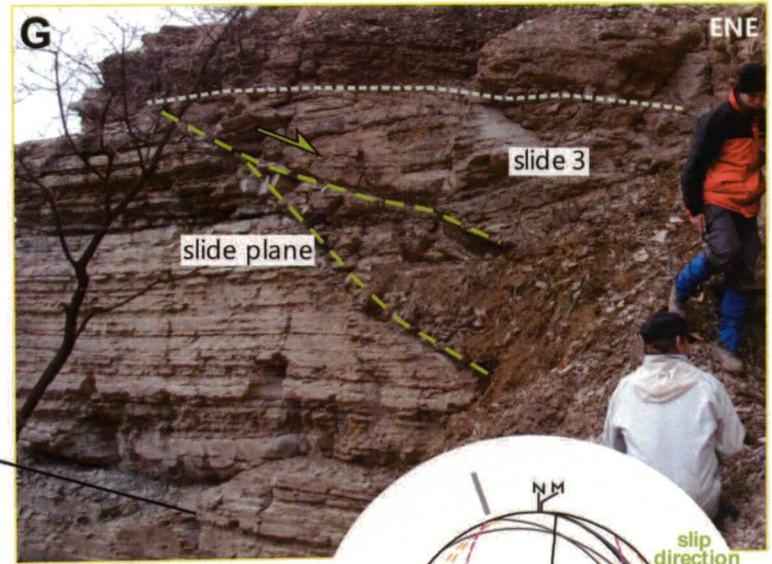
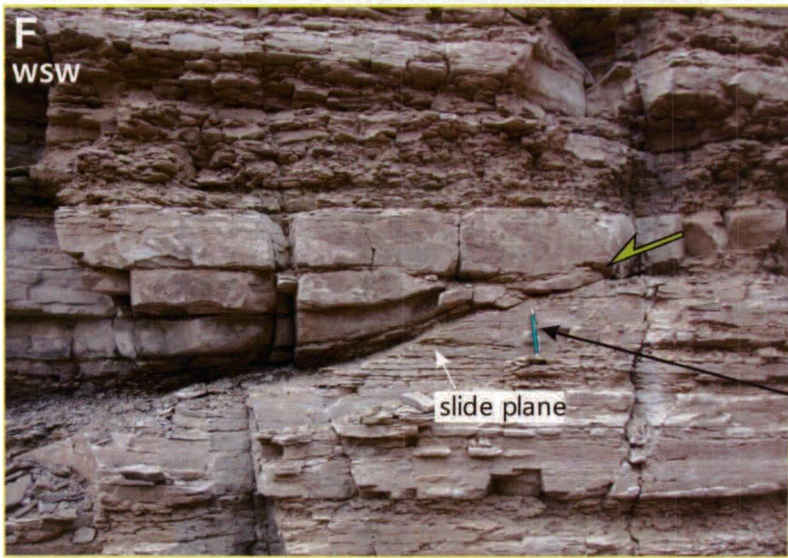
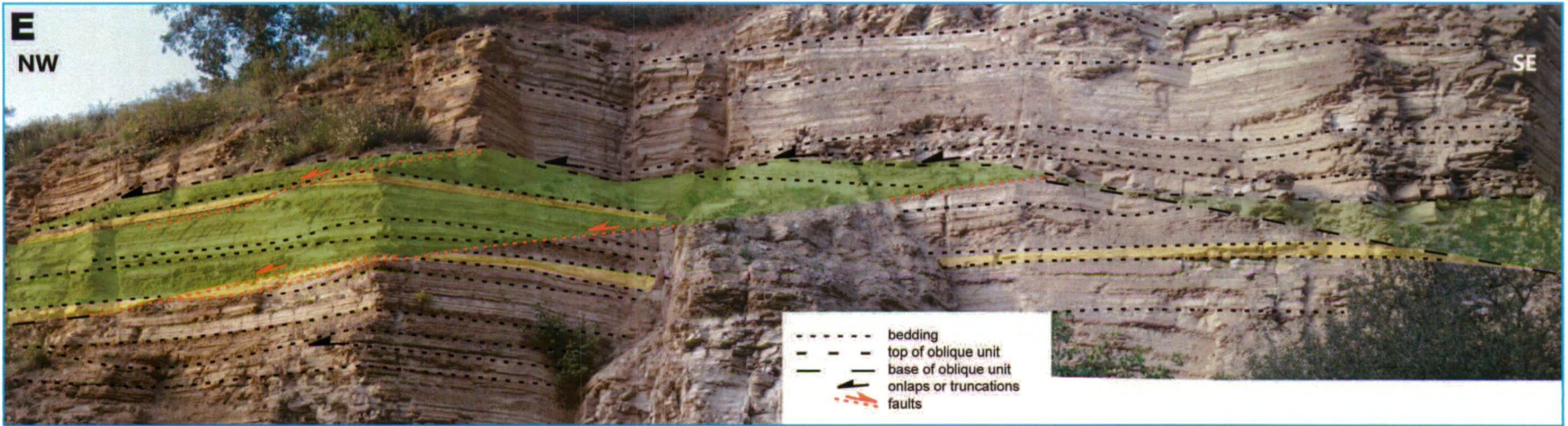
Package 3 is in the highest stratigraphic position, occurs above package 1 in the SE part of the quarry (Fig. 11g). The exposed thickness is about 2m. Its basal plane has two branches, both dips ENE, while the deformed beds dip SW (Fig. 11i). The package is covered by sub-horizontal layers.

Interpretation

Balkay (1955) who was the first recognizing the strange bedding contacts, was uncertain on the origin, hesitating between tectonic and non-tectonic origin. Sasvári (2008, 2009a,b) interpreted as thrust-related duplexes with roof thrust and basal thrust and regarded late Aptian to Albian the age of deformation.

Our interpretation favours non-tectonic syn-sedimentary deformation origin. Welded (cemented) nature of basal shear planes across footwall and hanging wall layers and also along intra-package faults (Fig. 11d) suggest an origin at early stage of burial, (before cementation) not after the complete diagenesis. Geometry of basal contacts, and the locally observed normal separation (Fig. 11e, f, g) are more consistent with normal displacement than basal thrust detachment. The gradual change from tilted to sub-horizontal strata within the packages also point to minor rotations in more plastic than rigid state. The small secondary low-angle faults however may help this deformation and accommodate the rotation of sedimentary packages above the basal slide plane. The gently concave, eroded nature of upper contact argue for some weak submarine erosion and not for an upper tectonic contact, which should be the case for thrust-duplex systems. We interpret that part of the tilted layers bulging out due to deformation were removed by currents because of their semi consolidated character. What is more important these currents were unable to level off all topographic differences, therefore sediment accumulate in the shallow troughs above the deformed units, indicated by the onlapping beds. These features indicate deformation during the deposition and not in a later event (e.g. during the post-sedimentary deformation event(s) of late Aptian to Albian age). The packages can be considered as slide units, and their base as basal detachment/slide surfaces. Some of the low-angle faults may rep-





Previous double page: Fig. 11. Sedimentary deformations in the Ördögát quarry (Stop 1.3), Valanginian Marlstone (Bersek Fm.). A) View of the north-eastern quarry wall. B) Detail of slide 1, with intra-slide secondary faults, eroded top and thinning overlying package. C) Bottom slide plane of package 1, where the footwall and hanging wall packages are welded. Note slightly sigmoidal fractures which are interpreted as S-C structures by Sasvári (2008). D) Secondary fault within slide package 1 with dragged and welded layers. E) Slide package 2 at the northern corner of the quarry. Note clear normal separation of yellow sandy layers. F) Detail of the secondary slide plane and scar-filling marlstone at slide 1. G) Slide package 3 with two sub-parallel slide planes. H) Model for the quarry showing major slide planes, their potential continuations outside of the quarry and sediment deformation related to slide plane irregularities.

resent the head scarp itself, while others are just internal extensional structures within the rotating-gliding unit (cf. Bradley and Hanson 1998; Frey-Martinez et al. 2005; 2006; Alsop and Marco, 2011). The main message is that these structures indicate the upper extensional part of the slide-complexes, the lower compressional ones with the slope-toe folds are not exposed in this area. With other words, the grey Bersek Marl represents the upper portion of a submarine slope.

The sigmoidal dense network of fractures was interpreted as being S-C shear bands (Fig. 11c) by Sasvári (2009a), which was related to the general thrust character of the main basal contacts. However, along few of such small fracture planes normal displacement can be seen. This is in contradiction to thrust character and more in agreement with postulated normal slip. We attribute these structures to the slide-related deformation process although the exact linking mechanism remains hidden.

Model

In sum, we consider all structures are part of different slide blocks, which were displaced along the basal detachments. It seems to us that for the slide unit 1, the head scarp surface is not outcropping but only the middle part of the slide blocks (Fig. 11h). The smaller slide planes, visible at the SE end of the slide unit 1 seem to be secondary slide planes embedded within the larger slide unit. Slide scar for slide 1 was filled with background marl sediment which is the triangular grey marl package just above the slide plane (Fig. 11b, f).

The onlaps on the flanks of the gentle depressions above the slides testify the erosion and later infill. The basal detachment surface of unit 1 cut down more steeply to N then climbed up in low-angle in the same direction revealing either a lateral or the frontal ramp of the slide. The undeformed and tilted blocks were cemented together during successive burial which equally indicate an early deformation feature. The data on slide direction is scattered but not in agreement with southerly or south-westerly gravity transport. In our interpretation gravity transport could be toward ENE, or WNW: none of these directions is in line of supposed sediment transport direction (i.e. from (N)E to (S)W; Sztanó, 1990; Fogarasi, 1995a).

Stop 4. Lábatlan, Bersek Hill quarry. Valanginian–Barremian slides, syn-sedimentary and syn-lithification faults, Eocene and post-Eocene reactivation

47°43'20.33"N, 18°31'29.13"E

In addition to the excellent outcrop (Fig. 8) of the major part of the Bersek Marl Formation (Fig. 5), the main attraction of this site is the variable early Cretaceous synsedimentary deformation features, slides

syn-sedimentary and syn-lithification faults and their reactivation in Eocene and post-Eocene times. The early Cretaceous basin geometry and basin evolution and broader geodynamic interpretation will be also discussed.

Earlier studies: Balkay (1955), Fülöp (1958), Félegyházi and Nagymarosy (1991), Fogarasi (1995a, b; 2001) Albert (2000–2002: unpublished map compilation), Főzy and Janssen (2009), Sasvári (2008, 2009a), Fodor (2009–2010: unpublished mapping), Császár et al. (2012).

General tectonic situation: dip to SW by 8–10°.

Stratigraphy: Bersek Marl Formation, Late Berriasian to Hauterivian, Lábatlan Sandstone Formation, Barremian–Aptian, Dorog Formation (Middle Eocene, Lutetian).

Rock types, lithofacies

In the huge quarry the Bersek Marl and the lower part of the overlying Lábatlan Sandstone is cropping out (Fig. 12). The marl can be divided into the lower grey and the upper purple units, which differ not only in colour, but in lithology, i.e. the grey marl contains cm thick sandstone beds, but these are totally missing from the purple marl.

Both in the grey and purple marl carbonate content varies significantly as reflected by alternations of argillaceous and calcareous marl layers. Occasionally the carbonate content is as high, that some beds can be regarded as pelagic limestones. Oxygen and carbon isotope signal confirms the variation of the carbonate content as well. The two types of marls make up couplets, which based on varying thickness, are organized into larger bundles of about 4–5 pairs and 16–17 pairs (Fogarasi, 1995b).

Sandstone occurs in the lower part of the succession in the grey marl as cm-thick fine- to medium-grained interbeds (Fig. 12). It is worth emphasizing that the purple marl lacks any sandy intercalations. In contrary in the overlying Lábatlan Formation, sandstone form 10–40 cm thick beds where they alternate with fair amount of purple to green silty marl. In both cases sandstones are sharp-based, often poorly graded, various elements of incomplete Bouma sequences (Ta, Tab, Tabc and Tac) can be observed. Sole marks, like flute and prod marks are also common indicating transport most likely from E to W. The greenish gray sandstone beds of the Lábatlan Formation comprise thickening upwards units of a few metres (Fogarasi, 1995a).

Fossils, Age

In the Bersek Marl aptychi and internal moulds of ammonites, belemnites can be collected. The rich, but poorly preserved ammonite assemblage contains forms of Spitidiscus, Neocomites, Barremites, Phylloceras, Lytoceras, Neocomites and Anahamulina, providing a firm base of age determinations (Főzy and Janssen, 2009). Other macrofossils are not common. Trace fossils are, however, also frequent, particularly in the purple marl comprising a Zoophycos type ichnofacies (Fucoidea, Zoophycos, Chondrites, Palaeodyction, etc.).

Based on the ammonite, belemnite and nannoplankton biostratigraphy the age of the grey marl is late Berriasian to Valanginian, the fossil-rich purple marl is Hauterivian and the sandstone is of Barremian (Fogarasi, 2001; Főzy and Fogarasi, 2002; Főzy and Janssen, 2009).

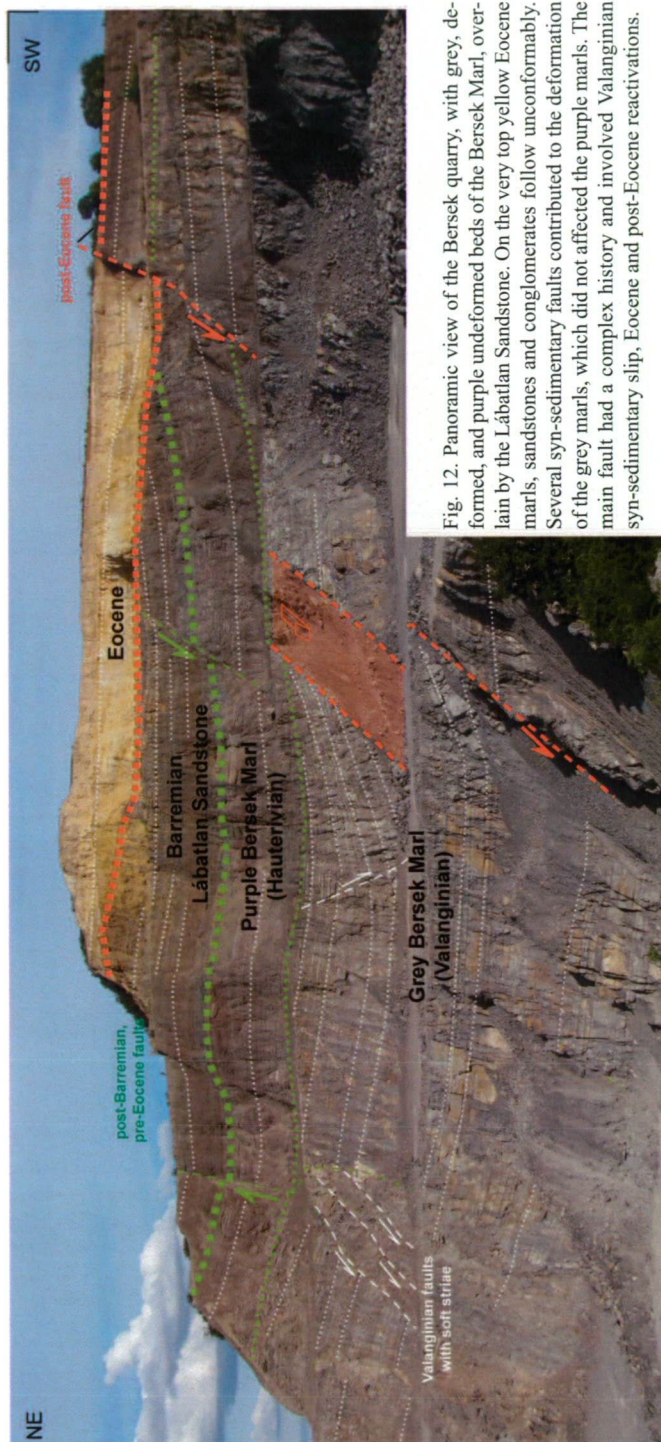


Fig. 12. Panoramic view of the Bersek quarry, with grey, deformed, and purple undeformed beds of the Bersek Marl, overlain by the Lábattlan Sandstone. On the very top yellow Eocene marls, sandstones and conglomerates follow unconformably. Several syn-sedimentary faults contributed to the deformation of the grey marls, which did not affect the purple marls. The main fault had a complex history and involved Valanginian syn-sedimentary slip, Eocene and post-Eocene reactivations.

Sedimentary environments

Palaeo-water depth can be estimated from the presence of the calcite-made aptychi and the lack of aragonite-shells of ammonites. Thus it is inferred that depositional depth might have been between ACD and CCD, whatever that meant in the Early Cretaceous (Kázmér, 1987).

The varying carbonate content of the marl is primarily regarded as the result of varying bioproduction in the photic zone, thus may reflect orbitally-controlled climatic forcing during deposition. At the same

time fluctuation of precipitation governed both the amount of nutrients and terrigenous influx to the basin. Therefore “dilution-cycles” i.e. increasing rate of muddy plumes to pelagic carbonate mud, were also climatically controlled. Based on cyclostratigraphic analyses of clay marl and calcareous marl bed-pairs and bundles of about 5 pairs, it was concluded that the depositional environment was mainly influenced by precession and excentricity (Fogarasi, 1995a).

The cm thick sand beds in the grey marl were products of sandy turbidity currents. Their rather coarse grain size and poor grading indicate relatively close source of the powerful currents. The presence of small and larger backfilled slump scars, rotational blocks, low-angle truncation surfaces (see details below) point to deposition on an actively forming submarine slope. There bypass, and as low sedimentation rate as 10 mm/ka was characteristic during the Valanginian. During the Hauterivian coarse sediment input to the basin ceased. Only horizontally persistent marl beds were present, which do not inform about the relief of the basin floor. Most likely it became flat.

In the Barremian input of coarse clastics increased significantly. Deposition was mostly governed by gravity mass movements, i.e. turbidity currents, sandy and muddy debris flows. Shortly after the onset of Barremian a 5 m slump-fold unit formed, indicating the recurrence of slopes to the area. Sandy turbiditic successions known from the Bersek Hill comprised only small lobes with low sand to shale ratio. Palaeocurrent directions from E to W (in present sense) were measured from sole marks, while fold axes in the sandy slumps indicates transport towards SW (Fogarasi, 1995a, b).

In two nearby wells an up to 400 m thick sand-dominated succession of massive, thick-bedded turbidites to conglomerates (Császár, 1995; Árgyelán, 1995) characterized by high net to gross ratio reveals a mid-fan environment. The topmost, conglomeratic part of the succession – proven to be Early Albian in age, follows above 30 m of siltstones. These interpretations suggest that a deep-sea fan existed from Barremian to Early Albian in the area of northern Gerecse. However, the overall thickness is rather small for such a long-lasting fan in an actively fed flysch-like basin. From sedimentological point of view it is fairly plausible that there was a gap with condensed deposition between Barremian and Late Aptian, not documented so far, and in Late Aptian to Early Albian a new fan might have developed.

Syn-sedimentary deformational structures and their interpretation

Several types of deformation features from 1 cm to hundred meters in size can be studied in the quarry: they reflect the changing rheology of the sediments during their deposition and burial. They probably belong to sedimentary deformation features, syn-sedimentary faults (Fig. 13a, b) and/or slides, syn-lithification faults, and post-cementation faults and folds.

In the grey marl the cm-thick sandstone layers commonly contain a set of small, parallel displacement zones, which cannot be followed to the next sandstone bed (Fig. 13d). Within the sandstone, the fault planes are not visible, and they can occur in the intercalating marls as closed fractures. In addition displacement lines at the upper and lower boundaries of the sandstone bed are not aligned but are in an echelon along dip direction. The extensional character is clear, and deformation developed when the sandstone beds were partly consolidated (cemented), but were still in plastic state. This is the reason these are called syn-lithification faults. The age of deformation could be Hautri-



Fig 13. Sedimentary deformation features in the Bersek Marlstone (Valanginian part). a) Panoramic view of large synsedimentary listric faults and small sets of rotated blocks, interpreted as a slide-scars. b) Close up of deformed beds below and above one of the large synsedimentary faults. c) Strike-section of a slide-scar with low-angle internal shear surfaces and onlapping beds postdating deformation. d) Small normal faults fragmented and rotated brittle sandstone layers between plastically deformed, not faulted marl beds. These are indicating gravity-related, i.e. slope-directed extension before diagenesis. e) Another very small low-angle shear surface and the rotated beds above. f) Close-up of a head scarp with stretched and teared beds and small extensional features in the headward region. All views are toward the SSE except for F, which is looking to ESE.

vian to Barremian, before the maximal burial at Albian to Cenomanian (Sasvári 2009a, b). Post-deformation cementation sealed the early displacement features. Compaction affected the conjugate fracture set and increased their angle to obtuse angle. The faults are NE–SW trending, which could be perpendicular to the paleoslopes envisaged by Fogarasi (1995b).

The quarry is crosscut by several faults which generally have curved (listric) geometry (Fig. 13a, b). The dip of such surfaces varies from very gentle to moderate, and dips typical for normal faults (60°) are very rare. The dip direction is generally to ward to NNE but opposite dip to the (S)SW also occurs. These surfaces are overlain either by a set of strata parallel with the surface itself or by a set of dipping beds. These beds are also seemingly unconformably overlain by beds which parallel to the lower undeformed strata (Fig. 13a, c, e, cover photo). The low-angle erosional surfaces are mostly part of listric faults of varying size from a few cm to several tens of metres. The oblique bedsets rotated along the upper segment of these faults, thus small openings developed at the head region, which were filled by beds of different dip. All these structures are interpreted as large gravity slides. The slid blocks generally kept their coherency and the scarps could be filled with new sediment package.

The common occurrence of these slides point to slope instability. Small fissures with cm-scale offset near to head scarps, and several meter to tens of meter long/wide slump scars developed (Fig. 13c, cover photo). Truncations are mostly related to basal slide surfaces, which are small listric faults, merging/fitting finally to bedding planes. Toe-thrusts or folds related to slumping are not present in the marl. These morphologic elements can be formed only on (submarine) slopes, and the presence of the scars with the lack of thrust indicates the upper portion of the slope (Fogarasi, 1995b).

The deformation occurred and gradually ceased coevally with the early Cretaceous clastic sedimentation: the best argument is that the gray marl is strongly deformed: erosional surfaces, large packages with different dip angles and syn-sedimentary faults are present, while beds of the purple marl are laterally persistent, just weakly affected by the above mentioned sediment deformation features and syn-sedimentary faults (Fig. 12).

At the case of the largest structure one can hardly determine if it would be a large gravitational slide or a syn-sedimentary fault. The structure cut across the whole quarry (Fig. 12, 13a). In the Valanginian level the hanging wall beds are considerably tilted away from the



Fig. 14. Soft striae on Valanginian fault plane, which indicates deformation (faulting and slip) of non-cemented sediment.

fault, and show pronounced thinning toward the fault. This part of the structures is sealed by Hautrivian red marls. The thickening away from the fault may point to syn-sedimentary slip. On the fault plane, “soft” slickenside lineations (Fig. 14) point to plastic state of the footwall at the time of deformation in the Valanginian.

The next stage of deformation tilted and displaced the complete exposed Cretaceous sequence including the Barremian Sandstone before the mid-Eocene. Following this slip event, the Barremian was eroded from the footwall block. The fault was reactivated during the Eocene, because soft striae also occur at the contact of Cretaceous and Eocene, and several small syn-sedimentary faults occur in the Eocene at immediate vicinity of the fault. Finally, the fault was reactivated after the mid-Eocene.

There is another type of deformational structure in the Lábatlan Sandstone. The contact of the purple marl and the sand dominated series is a wide-spread erosional surface. It is overlain by an internally complex, partly chaotic, partly folded unit of 5 m thickness. It is built up of strata like the overlying undeformed sandstones and marls. The folded unit is understood as a major slump-fold unit (Fig. 13e, f). Where it is possible to measure fold axes suggest movements towards the SW (Fogarasi, 1995b). The age of this sediment deformation is Barremian.

Consequences for basin geometry

Observations in both the Ördögát and Bersek quarries indicate important sediment deformation features, namely gravity slides, which occur at variable size but the largest can affect the whole Bersek Marl sequence. Slide scars occur and were filled by the successive sediment packages. This intensive sediment deformation events could be associated with syn-sedimentary faulting along which thickening occur in the hanging wall. Thrust and slump folds do not occur in the marl, but only in the overlying Barremian Sandstone.

It is speculated that considerable slope instability during Valanginian was related to structural movements controlling basin morphology. This idea is in line with most of the previous works, which considered the Gerecse Cretaceous clastics as having deposited in a foreland basin (Tari, 1994; 1995; Császár and Árgyelán 1994). Most of these works suggested that a basin plain and a prograding submarine fan were fed from the N or NE by sediment gravity flows. Using the vergency of slump folds, Fogarasi (1995b) suggested that the preserved sequences deposited on S to SW facing submarine slopes, close to the source of clastics. On such slopes gravity slides would have southerly or south-westerly direction, like the slump folds.

However, several observations contradict this scenario. The gravity slides of the Ördögát Quarry are not consistent with southerly sliding, but indicate eastward, westward or northward slide. Most (but not all) pre-Hautrivian sliding planes in Bersek dip to the N–NE and not to the S–SW. The large syn-sedimentary fault of the Bersek quarry has hanging wall to the NE. These remarks led us to suggest that the deposition of the Bersek Marl occurred on the south-western rather than the north-eastern side of the foreland basin.

This position would be in agreement with results from mapping and stratigraphic works. The Bersek Marl gradually thinning and pinches out only ca. 6,5–7,2 km south-west from the Bersek Quarry. The missing marl was not eroded, because there is a time-equivalent rock formation which replaces the Bersek Marl, which was not deposited in locations farther than 7km to the SW. In that region, the marl is replaced by a very much reduced

limestone or calcareous marl, which has thickness of 2–3m in most outcrops (Császár et al. 1998, Főzy et al. 2013). The very much condensed sedimentation is marked by the presence of hard ground above the limestone, below the Barremian Lábatlan Sandstone. Such reduced sedimentation would be typical for the forebulge side of a foreland basin, and not for a location relatively close to the thrust fronts.

This additional argument supports our hypothesis that the preserved Bersek Marl outcrops represent the south-western side of the foreland basin, already on the north-facing slope, descending from the forebulge region. This north-facing slope did not prevent the deposition of thin sandstone layers within the marl while the transporting gravity flows could climb slightly upslope. Their small volume, but relatively coarse grain size provides further support of the idea (Edwards et al., 1994; Covault and Romans, 2009) This paleogeographic position would imply that the active thrust front was in a large distance from the Bersek Hill and thus from the Gerecse Hills in general.

Stop 5. Környe, roadside panoramic view to the east. Albian?–Coniacian? fold

47°34'20.14"N, 18°19'32.49"E

This short stop offers a panoramic view to a typical fold which occur below the so-called Turul statue of Tatabánya town, at the southernmost Gerecse Hills (Fig. 2). The highway M1 is just passes below the rocky cliff. The fold is part of the structural elements of the regional D3 phase (Fig. 6).

Stratigraphy: Upper Triassic Dachstein limestone is folded, late Cretaceous to Paleogene denudation surface cut it.

Earlier works: Bada (1994)

Tectonic features

The fold is exposed by a N–S running Cenozoic fault, most probably an Early Miocene sinistral fault (Fig. 15). The fold is open, the dip of the limbs are not more than 30°. The southerly dip is quite rare and not typical in the Gerecse and Vértes Hills. There are slickensided bedding planes, which are the result of flexural slip folding. These data indicate NNW–SSE shortening. North from the cave other blocks have southerly dip and may be connected to the fold by reverse faults. This shortening direction is close to compressional stress axes deduced for the D3 phase (Fig. 6). The age of the deformation is poorly constrained in the location, just a pre-Paleogene age is clear (older

than the denudation surface). Projection of regional time constraints would indicate Albian to Coniacian age.

Few, meter-scale reverse faults with fault-ramp-flat geometry occur near the hinge of the fold. The fault slip data indicate NE–SW compression (Bada, 1994), probably belonging to D2 phase of latest Aptian to earliest Albian.

Introduction to the Vértesomló Line and the structure of the northern Vértes Hills (Stops 6 and 7)

The northern part of the Vértes Hills and the southernmost Gerecse Hills are cut by the E–W striking Vértesomló Line (Fig. 16) (Balla and Dudko, 1989) or Szár-Somlyó Line (Taeger, 1909). In this work the more precise Vértesomló Thrust name has been used. The fault is on the surface for about 8–9km in the Vértes hills; Véressomló is the westernmost outcrop. In its eastern continuation the fault runs within the upper Triassic carbonates and was reactivated or cut during the Cenozoic deformation phases. The fault is covered by Palaeogene deposits west from Vértesomló and this part can be imaged on the basis of boreholes; the fault trace was mapped by Császár et al. (1978), revised by Fodor et al. (2005a) and Fodor (2008).

The main characteristics of the fault is that the northern block contains upper Triassic, Jurassic carbonates, a hiatus in the Valanginian–early Aptian and the latest Aptian to earliest Albian Tata limestone, while the southern block contains the Albian to Cenomanian clastic-carbonatic sequence above the Tata limestone (Fig. 16, Stop6-1). This geometry was considered to indicate a south-vergent thrust (Császár et al., 1978). Detailed mapping in the central part of the zone revealed a complex strike-slip faulting close to the main contact (Maros 1988). On the other hand, Balla and Dudko (1989) considered the fault as a Miocene sinistral fault. In fact, the upper Triassic transitional unit shows a ca. 6km of apparent map-view sinistral separation, the origin of which will be discussed during the stop 7.

North of the Vértesomló Line additional structural elements were mapped (Fig. 16). Several folds can be reconstructed on the basis of dip data. Such an anticline was detected just north of the stop 1.6, Vértesomló (Eper Hill) where the reduced Jurassic sequence and the Cretaceous Tata Formation occur on both fold limbs. The folds are dissected by NW–SE striking dextral faults. One such fault constitutes the narrow ridge of the Vitány castle, the other occurs in the Stop 1.7 near the Szarvas-kút. These faults do not displace the main Vértesomló Fault just merge it suggesting their transfer fault origin. The

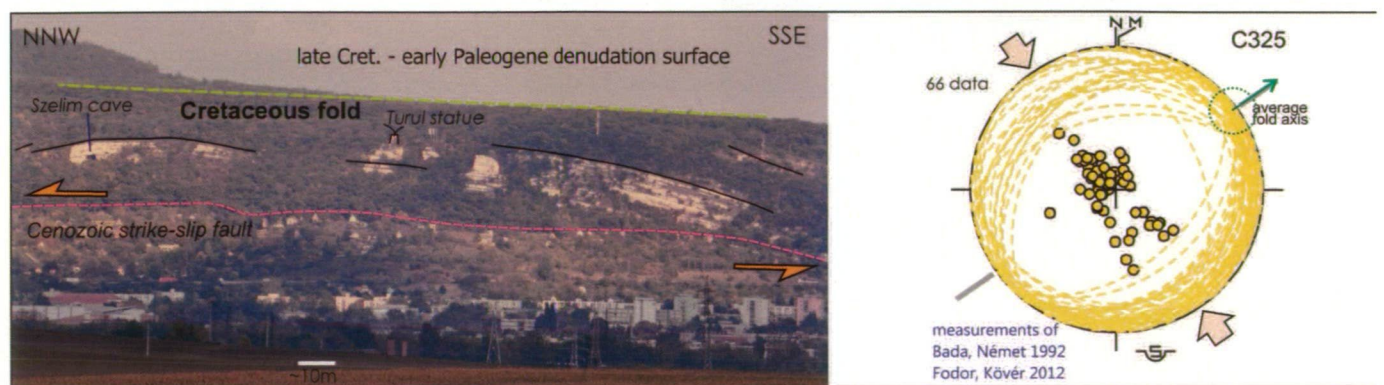


Fig. 15. Panoramic view of the fold below the Turul statue above Tatabánya town. The gentle fold belongs to D3 deformation phase and deforms upper Triassic Dachstein Limestone. The cliff itself is bounded by sinistral strike-slip fault which could belong to D6 or D8 deformation phase, probably reactivated during the Late Miocene (D12) as normal fault.

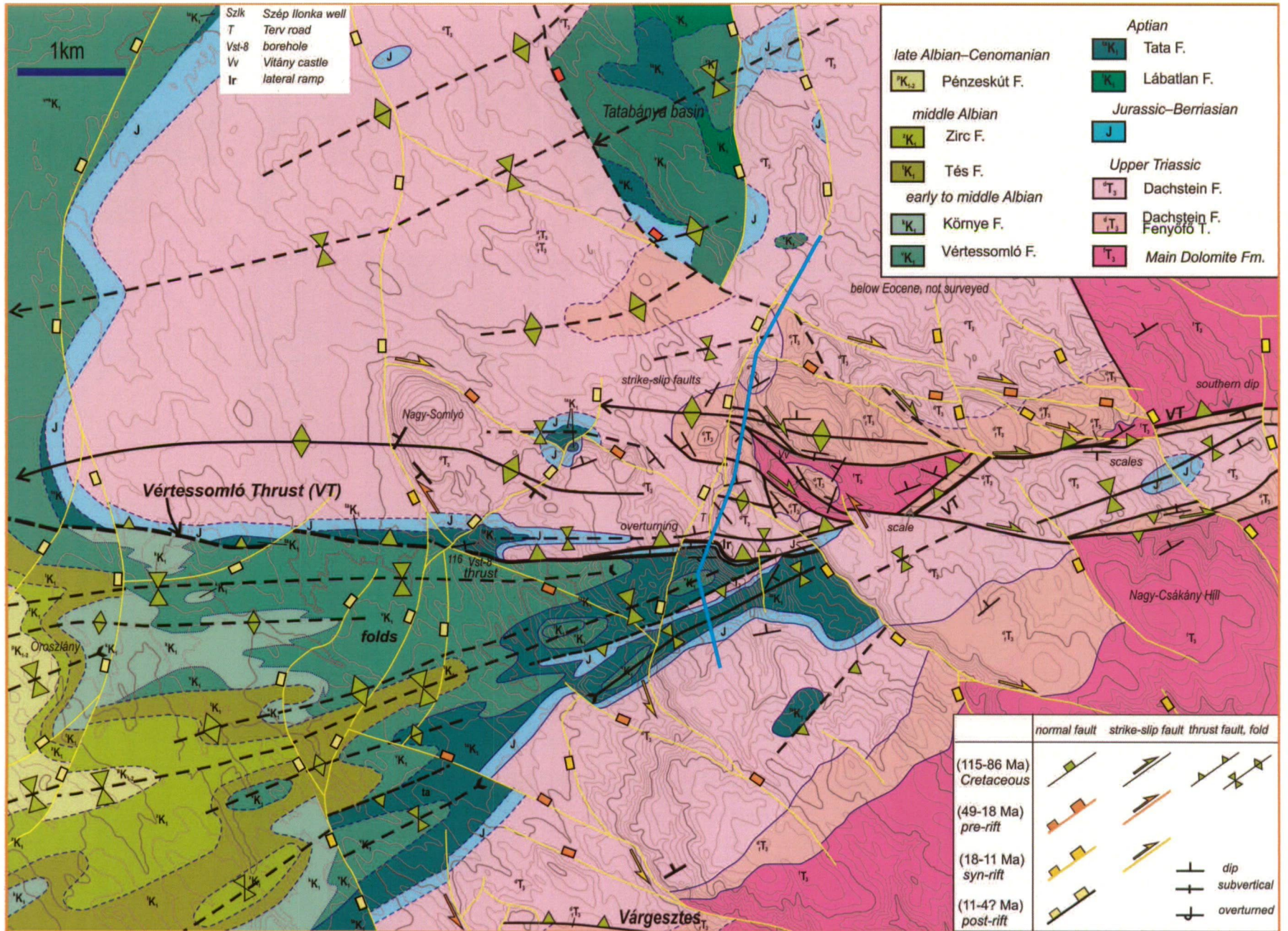


Fig. 16. Map of pre-Cenozoic formations of the northern Vértess Hills, Tatabánya Basin and the surroundings of the Vértessomló Thrust, after FODOR et al. (2005a). Note that the Vértessomló thrust is connected to a series of folds of the Mesozoic rocks.

block south from the main fault is also folded, and the mid-Cretaceous formations basically form a syncline with smaller parasitic anticlines. Most of the folds have gentle westward axial plunge both in the northern and southern block.

Stop 6. Véressomló, church hill. Albian to Coniacian fold, the Vértessomló thrust.

47°30'25.14" N, 18°22'31.11" E

This and the following outcrop introduce you to the problem of the Vértessomló Line, a fault with the largest map-view separation within the Transdanubian Range (Fig. 16). The small valley below the church of Vértessomló exposes several decametric folds which are in the im-

mediate vicinity of the main fault. From the small-scale feature, the deformation history of the folded layers can be reconstructed.

Stratigraphy: latest Aptian to earliest Albian Tata limestone (crinoidal limestone) (Császár 1995, 2002).

Earlier works: Taeger (1909), Császár et al. (1978), Balla and Dudko (1989), Fodor et al. (2005a), Fodor (2008)

Folds and faults

The westernmost surface outcrop of the Vértessomló Fault is near the Vértessomló. On the surface, the crinoidal limestone shows moderately closed folds with a slightly overturned southern limb and gently south-dipping northern limbs (Fig. 17). The steep limb is cut by

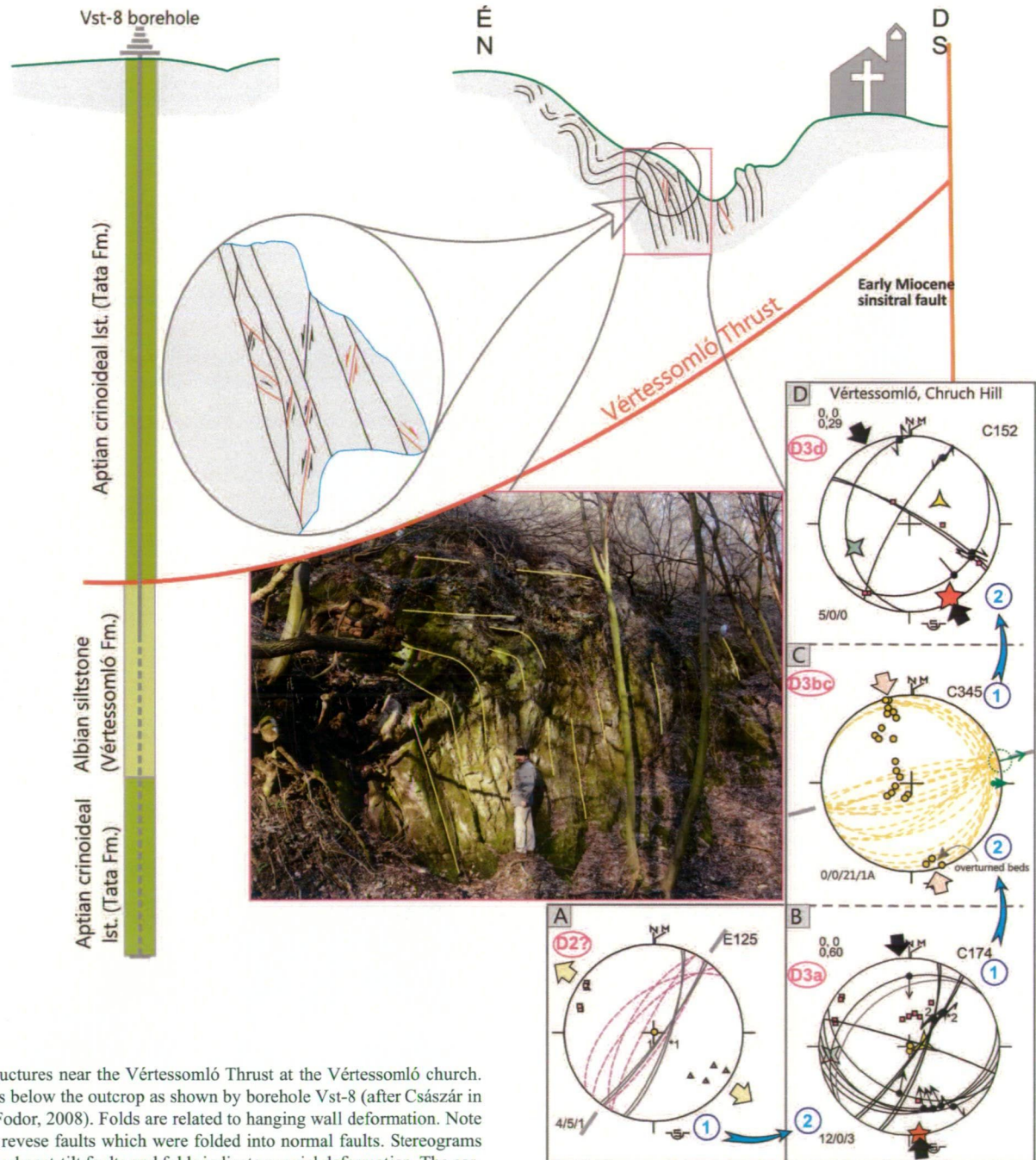


Fig. 17. Structures near the Vértessomló Thrust at the Vértessomló church. The thrust is below the outcrop as shown by borehole Vst-8 (after Császár in Budai and Fodor, 2008). Folds are related to hanging wall deformation. Note pre-folding reverse faults which were folded into normal faults. Stereograms for pre-tilt and post-tilt faults and folds indicate coaxial deformation. The earliest event is pre-folding fracturing by SE-NW extension (D2a phase).

conjugate faults which make small angle to the layers and show normal kinematics. Steep bedding planes equally bear striations and calcite steps. Backtilting the faults to horizontal bed position reveals that conjugate faults become reverse ramp faults, while horizontal bedding planes functioned as small detachments. These faults represent a pre-folding event before the main folding, as the first increment of shortening deformation (Fig. 17). Similar tilt test suggests that other faults were formed after the folding, as the last step. The calculated stress axes and estimated shortening directions are closely parallel and indicate roughly N–S compression. This correspond to regional D3 deformation phase.

Just above the folds, the Vértessomló Vst-8 borehole encountered a thrust of the Cretaceous Tata Formation upon the Vértessomló Formation (Fig. 17) (Császár, 1995; 2002). The Tata Formation is slightly older, the underthrust Véressomló Siltstone is early Albian. The surface folds could develop above this thrust and in agreement with reverse kinematics.

Tilt test suggests that few fractures do not fit to the D3 phase and were formed before the folding started. The fractures could be classified into phase D2, and occurred in a narrow time span, in the earliest Albian. They could be the far-field echo of the clastic foreland basin formation of the Gerecse Hills.

Stop 7. Tatabánya, Szarvas-kút, Terv road. Albian to Coniacian folds, the Vértessomló thrust.

47°30'25.14" N, 18°24'25.05" E

East from Véressomló, the next surface segment of the Vértessomló Fault is found near the Terv road, Tatabánya (Maros, 1988) (Fig. 16). The road cuts three times the fault, because it has two curved segments. Along the road and in the valley below, the north-dipping Cretaceous limestone is followed by north-dipping Triassic limestones. The younger formations dip below the older ones in each case (Fig. 16, 18). Reduced slices of Jurassic occur between the Cretaceous and Triassic in 1-3m thick lenses. At the Jurassic-Triassic boundary surface dextral-reverse slickenlines represent the most direct kinematic data for the Vértessomló Line, which is thus interpreted as an oblique-slip thrust.

The rocks in the footwall of the thrust are strongly folded in a narrow zone (MAROS 1988). The fold shape changes suddenly (Fig. 19a, b, c), and, northwards, overturned limbs occur. Fold hinges vary between E–W and NW–SE; this feature was interpreted as sign of several folding phases by Maros (1988). On the other hand, SE plunging fold hinges occur at a place where the fault itself changes its strike from E–W to NW–SE (Fig. 16). Thus this short segment may represent a lateral ramp, whose kinematics was dextral or reverse-dextral. Some of the folds could have been distorted along this lateral ramp from an original, E–W direction. Small Jurassic rock slivers are involved in the zone of the Vértessomló Thrust, as is the case on the western slope of the 433m high hill (Fig. 18a).

In a small quarry below the Terv road reverse ramp faults were described by Maros (1988). Striae indicate NW–SE compression. Further to the south, near the Szarvas-kút a small anticline with a Triassic core occurs. Near the Szép Ilonka well the Mesozoic succession dips to the north. Thus the area south from the Vértessomló Thrust is marked by E–W trending folds (Fig. 18a) partly seen on the surface, partly followed by borehole data.

In the road cut a below, a 10x30m large Triassic limestone block is found between the deformed Cretaceous limestone beds. It was interpreted as a block incorporated within the main fault during the deformation (Maros, 1988). In fact, at the contact the Cretaceous limestones show normal drag which is consistent with slickenside data. So we interpret this block as slid down from the tip of the overthrust Triassic during a much younger deformation event.

The thrusting and folding post-date the latest Aptian – earliest Albian Tata limestone. The other time constraint is that the folds are cut by the late Cretaceous to early Paleogene denudation surface. The mid-Eocene sequence covers the southern folded block of the thrust and thus post-date it. The first sediments are abrasional gravel, which occur on the Cretaceous: one outcrop is seen in the road curve 200m SE from the folds, just above the Szarvas-kút. The gravel contains large pebbles, and cobbles of Triassic limestones which derived from the hanging wall of the thrust (Fodor and Bíró, 2004). Bioperforation (*Lithophaga?* sp.) indicate marine cliff along the thrust line which was the source of clasts transported away from this rocky shore (Fig. 19e).

The kinematics, timing and the model of the Vértessomló Thrust

Because of the west-plunging fold hinges around the Vértessomló Thrust (VT), the formations become younger in a westwards direction and the southern syncline widens. Figure Stop7-3 shows that the formation boundaries in the northern anticline jump westwards with respect to the same boundaries in the syncline. As a consequence, the apparent sinistral separation of the formation boundaries along the VT can be produced uniquely by folds, without a brittle fault, and the lack of knowledge about the folds may lead to misinterpretation of the map-scale separation.

Disregarding the folds, the apparent sinistral separation in map view could have been produced by variable kinematics, including dextral slip (Fig. 20). The true separation of a fault is uniquely based on the recognition of two displacement markers on two sides of the fault. One such marker is the intersection line of the Vértessomló Thrust and the displaced Mesozoic beds. In the case of pure dextral slip, the apparent displacement is also dextral on a horizontal plane (AA1=BB1=BM1 vector on Fig. 20c). However, the apparent displacement would be sinistral (BM3) if a dip-slip reverse separation (AA3) had occurred (Fig. 20c). The boundary between the apparent dextral (BM2) and sinistral (BM3, BM4) displacement is the displacement vector which is parallel to the intersection line (Fig. 20c). Despite apparent sinistral displacement, the real slip is dextral-reverse in all cases between B3 and B5 (BM3, BM5).

The research of the detailed mapping resulted in two independent arguments for the dextral-reverse kinematics of the Vértessomló Line: (1) direct fault kinematic data above the Terv road (Stop 1.7), and (2) the determination of a NNW–SSE compressional stress field in closely spaced outcrops (Fig. 6, 17; Bíró 2003, Fodor and Bíró, 2004; Fodor et al., 2005a). At stop 6, the reconstruction of deformation history would imply several episodes and basically show coaxial deformation. The direction of compression was perpendicular or slightly oblique to the Vértessomló Line for the whole phase and induced a pure reverse or an oblique dextral-reverse slip.

The timing of the Vértessomló Line varies among authors. Balla and Dudko (1989) assumed Miocene slip because they believed that the VL cut the Paleogene rocks, too. However, the mapping work

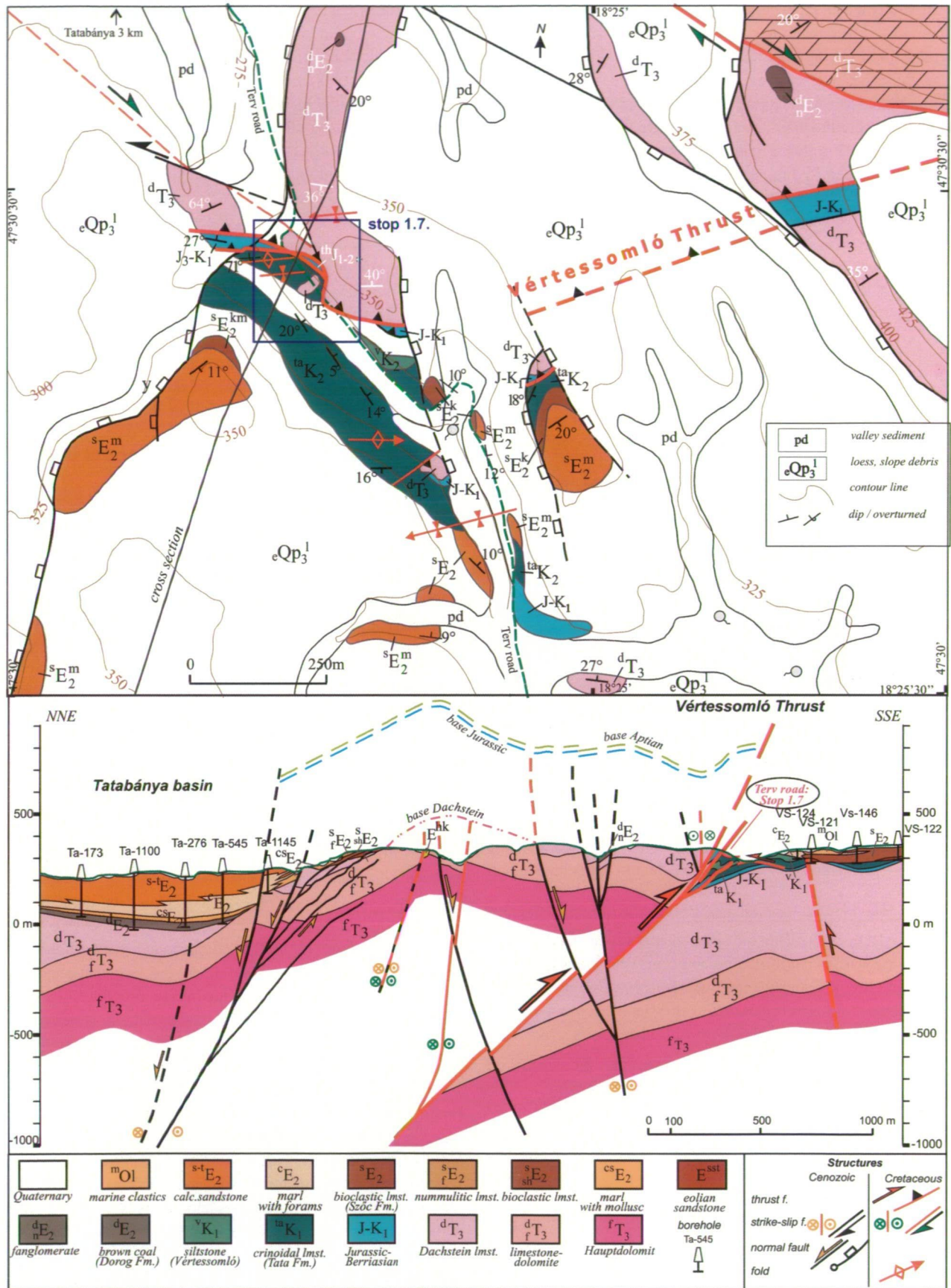


Fig. 18. A) Geological map of the Vértessomló Thrust, near Szarvas-kút, Tatabánya, after FODOR AND BÍRÓ (2004), using the data of MAROS (1988), P. TÁLAS (unpublished). B) Cross section through the Vértessomló Thrust (near the Szarvas-kút, Tatabánya) and the southern margin of the Tatabánya Basin (after Fodor et al. 2005a).

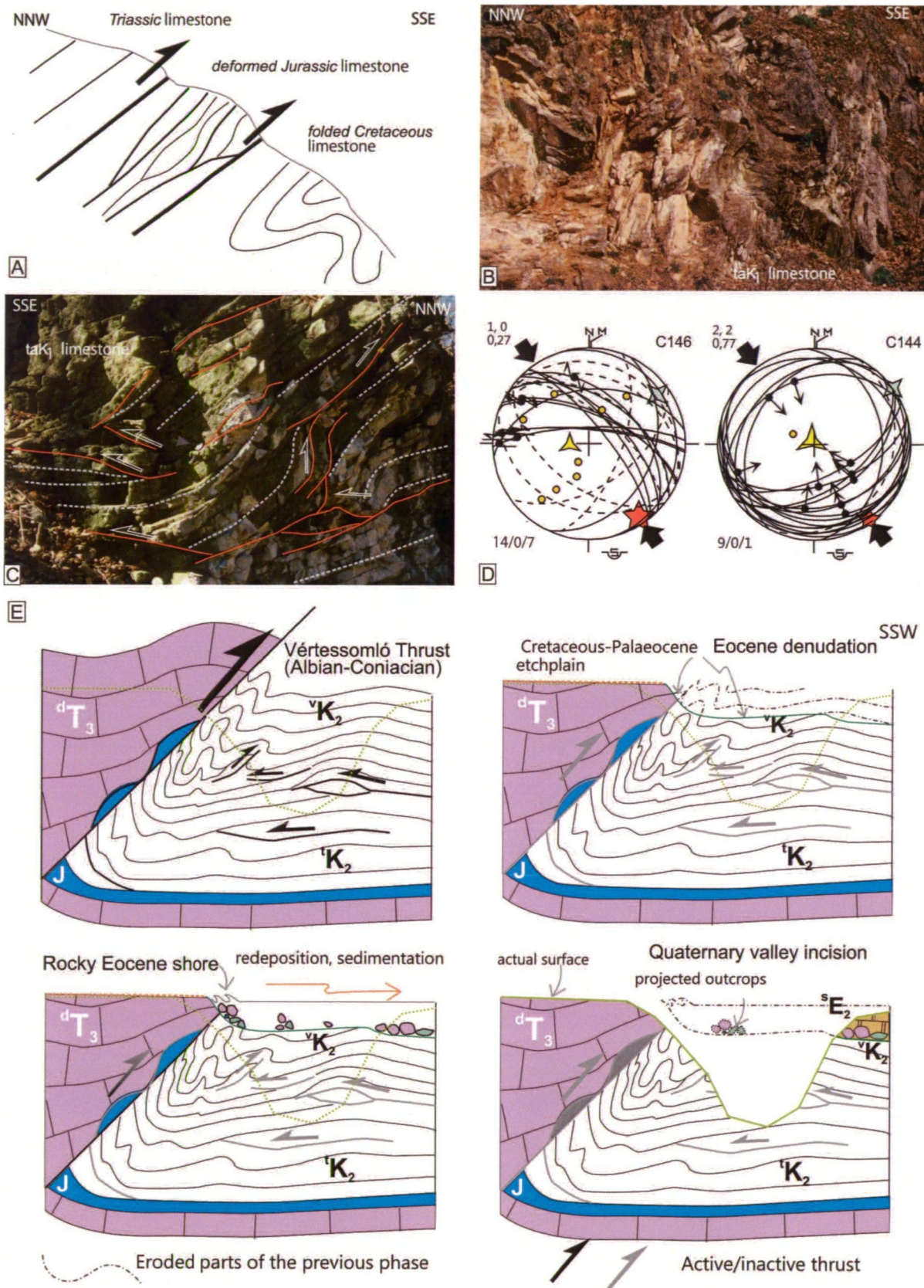


Fig. 19. Structures at the Vértessomló Thrust, terv road, south of Tatabánya (after Fodor, 2008, and Fodor and Biró, 2004). A) sketch of structural position of the Mesozoic rocks above the road. B) Strong folding of Aptian to earliest Albian Tata limestone. C) Flat-ramp fault geometry ca. 150m below the main thrust. D) Stereograms of faults measured directly at the main Vértessomló Thrust (A) and at the ramp faults (C). E) Evolution of the Vértessomló Thrust through time showing 4 major steps, like (1) Albian-Coniacian thrusting, (2) late Cretaceous to Palaeocene etchplain formation and Early Eocene denudation, (3) development of mid-Eocene rocky shore along the former thrust and transport of Triassic boulders away from the inactive fault line (4) Quaternary valley incision.

demonstrated that the VL and the Miocene fault make a small angle, just exactly near Stop 6. At other locations the VL is covered by Eocene. Fodor and Bíró (2004) demonstrated that the central segment of the Vértessomló Thrust (at Stop 1.7) was sealed by the basal Eocene beds. Pocsai and Csontos (2006) suggested Aptian slip on the basis of sedimentological features. Császár (1995) demonstrated that tectonic repetition in the Vst-8 borehole is not older than middle Albian. Although the Aptian initiation cannot be ruled out, the mapping work suggests that the activity of the Vértessomló Thrust started in the early Albian and continued during the Cenomanian–Coniacian(?) (Fodor et al. 2005a, Fodor 2008). In this case, all the deformation could belong to different events of the D3 phase. Traces of earlier D2

structures was found in Stop 1.6, while several faults of Cenozoic age cut across the VT.

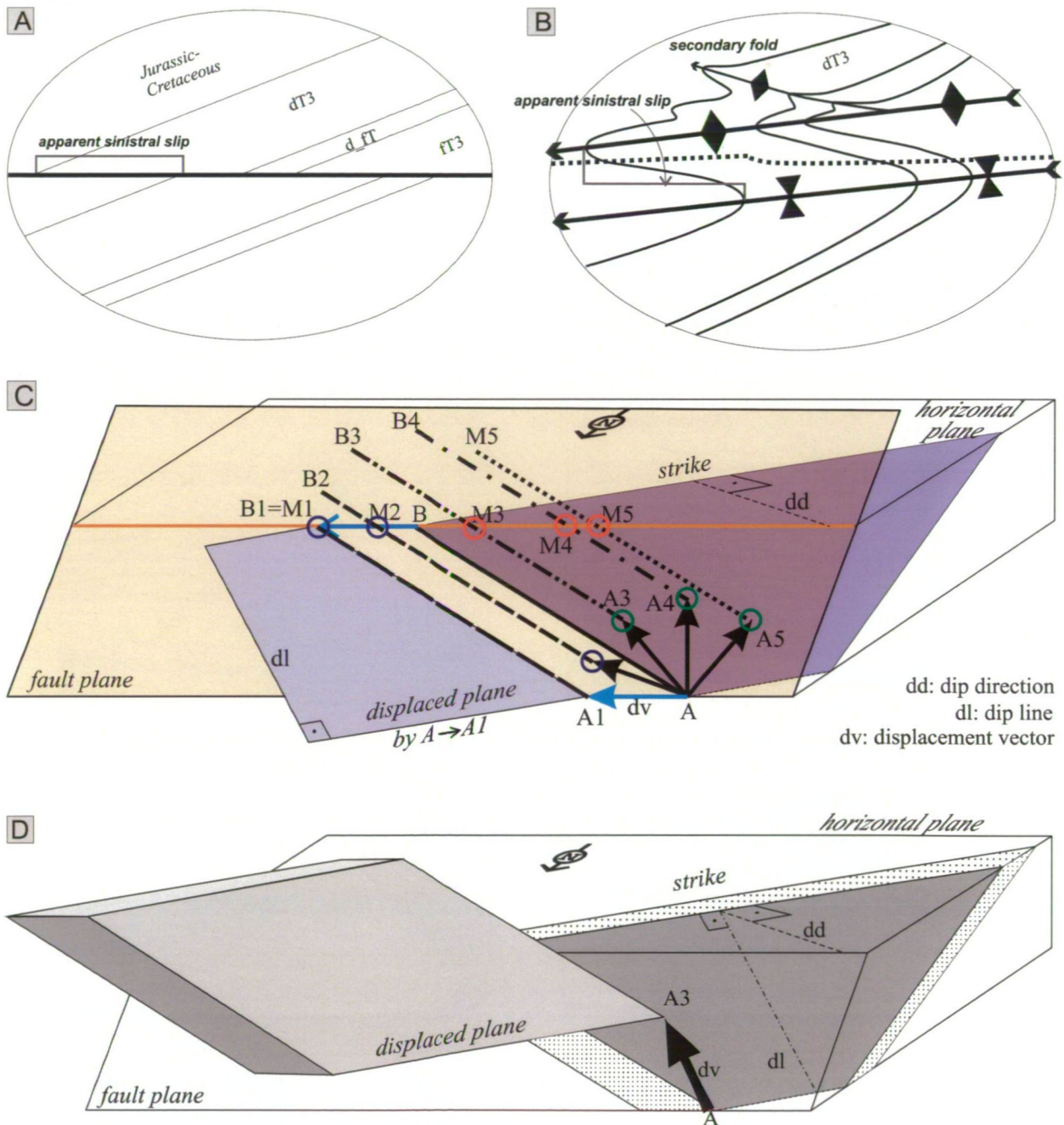


Fig. 20. Model for the kinematics and apparent map view displacement of the Vértessomló Thrust (Fodor, 2008). A) the slip is apparently sinistral. B) Such situation is possible with folding and gentle westward axial plunge. C) Possible displacement vectors of the intersection line AB of the Vértessomló Thrust and Mesozoic beds. Note the change in apparent displacement on horizontal (map) view between M2 and M3 map-view displacements. D) Block model for the displacement scenario AB—A3B3, which is a dextral-reverse slip (A-A3) with sinistral map separation (B-M3).

6. Discussion – Geodynamic evolution

Jurassic basin evolution started in the Hettangian, and differentiation of the Triassic carbonate platform (Fig. 10, 21a) occurred in the Sinemurian. Syn-sedimentary dykes and small faults (Fig. 9) indicate extensional deformation, which can be related to the early rifting event of the Alpine Tethys, far to the west. The direction of extension was probably NNE–SSW. Some map-scale syn-sedimentary faults can be delineated on the basis of completeness of the Jurassic successions (Fig. 6, 7, 8). The WNW–ESE faults could be normal faults, while the N–S striking elements could be transfer faults with oblique-slip (sinistral) character. The model, which was adopted proposed for both the Gerecse (Lantos, 1997) and for the nearby Vértes Hills (Fodor, 2008).

After the Toarcian “black shale event”, nodular and Bositra limestones deposited in the half-grabens (Tölgyhát and Eplény Fm). These depressions have origin from the Early Jurassic and possibly were re-activated during the mid-Jurassic. This unit was thinner toward the tilted blocks and was missing completely from their edges, which represented topographic highs. The complete lack of Dogger limestone can indicate submarine currents and not emergence above sea level. The maximum thickness could be around 50m. Bathonian is nowhere documented biostratigraphically from the Gerecse, so this period was probably marked by non-deposition.

In most geodynamic models, late Middle to Late Jurassic times was marked by the subduction of the Neotethys Ocean (Fig. 4) (Plašienka, 1997; Neubauer et al., 2000; Frisch and Gawlick, 2003; Csontos et al., 2005; Schmid et al., 2008; Kovács et al. 2010). Although no Jurassic structures were analysed in detail, earlier models envisioned N–S to NE–SW directed compression for the Gerecse Hills (Csontos et al., 2005; Palotai et al., 2006).

As discussed in Fodor (2013) and presented in stop 1.2, the structural observations are not really consistent with a compressional stress field or the presence of S- to SW-vergent reverse/thrust faults of late Jurassic age in the Gerecse Hills. In contrast, the few observed brittle elements can be considered as extensional or transtensional features, normal, oblique-normal or even strike-slip faults. During the late Jurassic, the fault pattern consisted of WNW–ESE and closely N–S trending faults, which could be inherited from the previous, Early Jurassic rifting phase. The former structures could be normal faults while the latter ones could play the role of (sinistral) transfer faults.

Normal or oblique-slip faulting induced slightly differential subsidence in fault-bounded blocks, which could be asymmetric. The produced space was partially filled by late Middle to Late Jurassic formations, whose stratigraphic completeness and thickness variations reflect this slightly differentiated basin floor topography (Fig. 21a). Fossil contents, their preservation, encrustation and fragmentation also demonstrate the existence of relatively higher areas, located probably at block edges. However, the overall pelagic environment was kept, and no clastic input occurred. Emergence to near-photoc zone could be possible only in the Early Tithonian, when a peculiar coquina with abundant crinoid content formed (Főzy et al., 1994; Fodor and Főzy, 2013).

Local extension related to bending or folding is a common phenomenon both in outcrop-scale folds and within larger plates (Ramsey and Hubert, 1987). The outer, stretched arc of a fold can be filled by min-

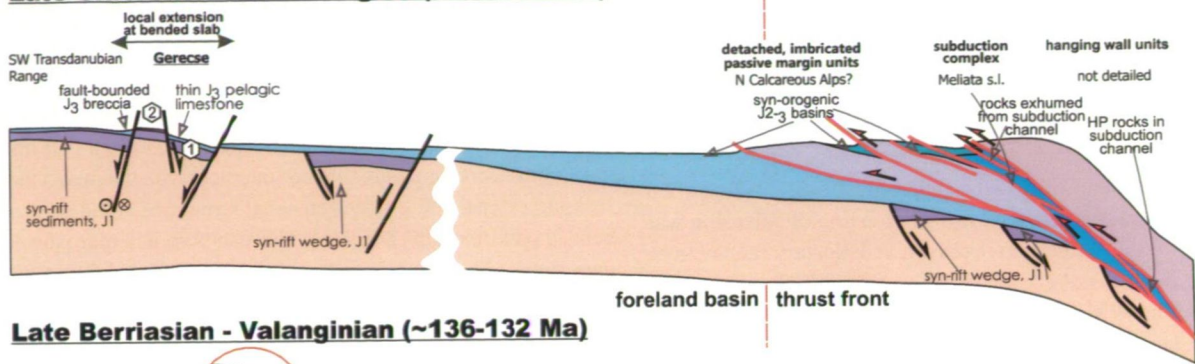
eral veins or sediment (Fossen, 2010). Localised extension can occur on the most bended part of a footwall plate, which is subjected to underthrusting. This can be the case in flexural (foreland) basins, where extensional faulting, associated with slight increase in sediment thickness could occur on forebulge limb of the basin, on the opposite side of the loading thrust sheets (Bradley and Kidd, 1991). Our observations in the Gerecse Hills could be consistent with the model that Late Jurassic extensional or transtensional structures could form on the bended part of a slab (Fig. 21a). The slab was, in a more distal location, subject to overthrusting by the emergent Alpine-Carpathian-Dinaridic nappe pile (Fig. 3, 21a) (Csontos and Vörös 2004). However, the fossil content, lithofacies and thickness data indicate that the position of the Gerecse was very far from any active deformation front (Fodor and Főzy, 2013). The central and southern part of the TR was equally part of this local deformation, although could be located even farther from the thrust front (Fig. 21a). Despite this considerable distance, local extensional deformation can indicate that loading was already active during this time period. This distant position changed during the successive Early Cretaceous deformations and basin formation (Fig. 21b).

The emerging orogenic arc could incorporate slices of accreted sediments of the subducting Meliata Ocean and fragments of its crust (Fig. 3, 21a, b). These slices could be found in the Inner Western Carpathians (Mello et al., 1997), in the Bükk Mountains (Csontos, 1988; 2000), in the northern Calcareous Alps (Gawlick and Frisch, 2003) and in the Dinarides and Hellenides (Robertson, 2002; Pamić et al., 2002; Liati et al., 2004; Gartzos et al., 2009). Distal margin of the down-going slab was gradually incorporated in the footwall of the ocean-derived thrust units. The imbrication of this distal margin could be associated with very low to low degree of metamorphism, as it was probably the case in the Bükk Mountains (Csontos 1999) and also in the Eastern Alps (Gawlick et al., 1994).

In the Northern Calcareous Alps, the imbricated distal margin and ocean-derived units served a source for the late Jurassic flexural (foreland) type basins (Gawlick et al., 1999; Mandl, 2000; Gawlick and Frisch, 2003; Frisch and Gawlick, 2003). Deposition mechanisms involved different gravity mass movements from large-scale slides through debris flows to turbidity currents. The change in sedimentation pattern prograded from south to north (in present direction) and was younging from Callovian to earliest Cretaceous. These gravity-flow dominated successions were deformed soon after deposition, gradually incorporated into the Jurassic nappe pile, and partly eroded. Such actively forming sedimentary basins, and the resulted nappe pile were projected into our model section, to visualise the possible structure of the loading orogenic wedge, and also the large and necessary distance between the actively forming orogen and the Jurassic rocks of the Gerecse. The NCA and the Gerecse Jurassic basins were probably never positioned in one section; it is more probable that the Jurassic basins of the Bükk or of other Dinaridic units were part of the actively shortening margin.

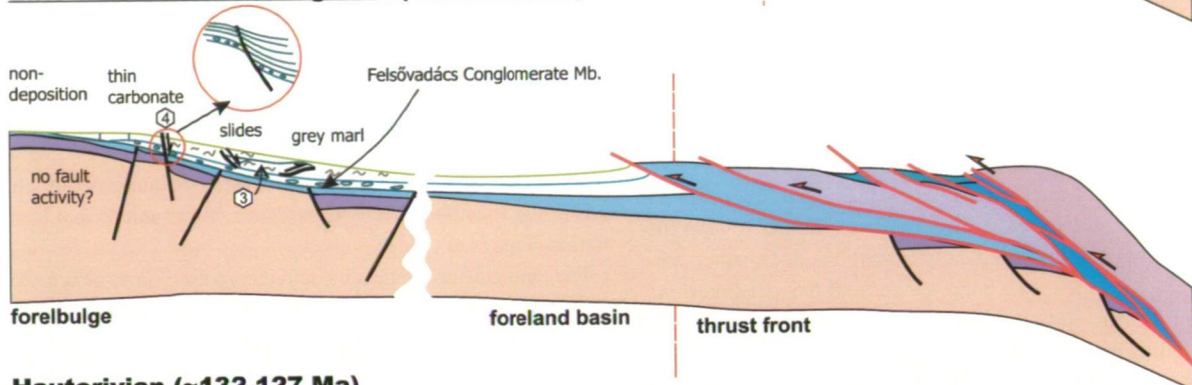
There are few beds in the Gerecse and Pilis Hills, which could be a far-field echo of this Alpine tectono-sedimentary process (Bárány, 2004; Csontos et al., 2005). One is the Middle Oxfordian breccia bed (stop 1.2). The others are few beds with locally derived olistoliths in the Pilis Hills (Palotai et al., 2006). These redeposition events were regarded as direct signs for the birth and progressive evolution of important thrust faults (Csontos et al., 2005), or even real nappes in the

Late Oxfordian - Kimmeridgian (~160-152 Ma)



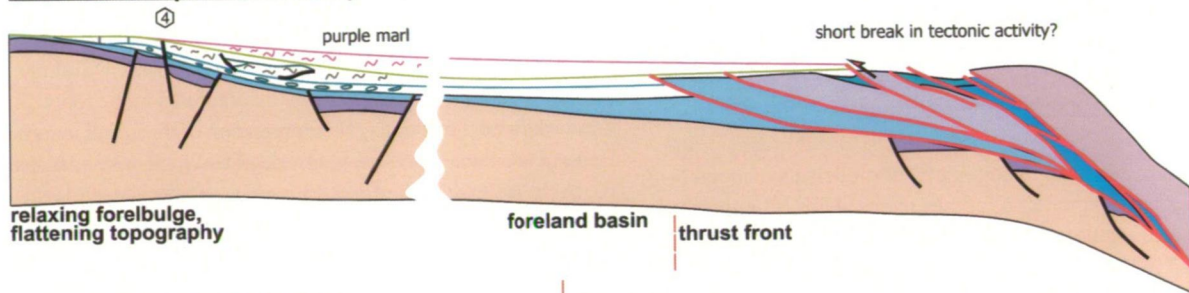
(A)

Late Berriasian - Valanginian (~136-132 Ma)



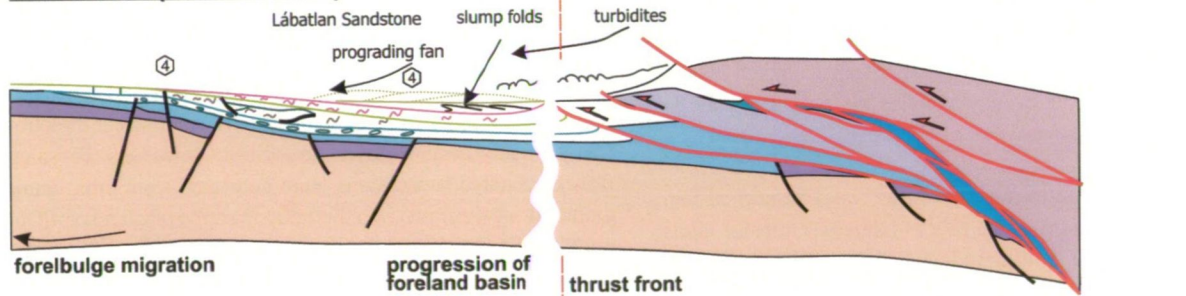
(B)

Hauterivian (~132-127 Ma)



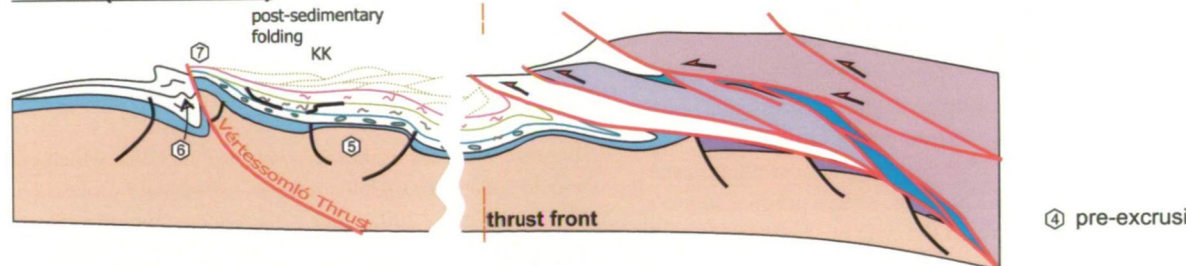
(C)

Barremian (~127-121 Ma)



(D)

Albian (~112-99 Ma)



(E)

④ pre-excision stop

Fig. 21. Geodynamic model for the position of the Gerecse through the Late Jurassic to mid-Cretaceous tectonic evolution. Note decreasing distance of the Gerecse Hills from the orogenic wedge. Units within this wedge were not necessarily in section with the Gerecse. A) After Fodor and Főzy (2013). B) Beginning of the clastic sedimentation in the late Berriasian, formation of foreland flexural basin. C) Condensed sedimentation, tectonic quiescence(?) during the Hauterivian. D) Input of coarse clastics into the basin. E) Post-sedimentary folding from the Early Albian to Coniacian by D2b,c and D3 phases.

TR (Sasvári, 2009b), or at least as an indirect sign, a far-field echo of NCA contractional deformation (Bárány, 2004; Palotai et al., 2006). However, the different thickness, and particularly the uniqueness of the mid-Oxfordian bed clearly indicate a large distance of the Gerecse from the deformation front; e.g., from the actively imbricated Alpine-Carpathian-Dinaridic margin. This means that considering the structural position of the NCA and Gerecse Hills with respect to the loading orogenic front was dramatically different (Fig. 21a); the former was close or within the orogenic wedge, while the Gerecse was located much further away from the active thrust front. **These relative positions should be considered in paleotectonic reconstructions.**

The situation changed considerably by the end of the Berriasian, when the thrust front advanced toward the foreland and also the content and topography of the nappe pile changed. In the Northern Calcareous Alps it resulted in the drowning of carbonate platforms (Gawlick and Schlagintweit, 2007), while in Gerecse Hills this is the time of termination of the Late Jurassic to Berriasian carbonate sedimentation and the change to mixed siliciclastic-carbonate sedimentation. The formation of the Felsővadács Conglomerate Member marks the beginning of the overall clastic sedimentation. It is possible, although not proven unequivocally, that clasts of this far-traveled gravity flow unit had the same or similar platform carbonate source in the Gerecse as in the NCA (Császár et al., 2008). The following Early Cretaceous (Valanginian to early Albian) basin evolution was dominated by clastic input from the approaching thrust front while the subsidence of the basin was caused by the increasing effect of the loading nappe pile (Fig. 21b) (Tari, 1994).

The Gerecse remained on the southern side of this flexural basin during the Valanginian-Hautrivian (Fig. 21b, c). The instable slope was deformed progressively by large slides with dominantly northern vergency. More to the south (toward the forebulge) the marly sediments interfinger with a carbonate sequence of only a few meters in thickness (Fig. 21b). These rocks mark the southern boundary of the marly basin. During this phase of evolution we do not know rocks which were formed on the northern (orogene) side of the basin, which could be located still in a large distance from the present outcrops.

From the Barremian onwards coarse clastics dominated over the marl deposition (Fig. 21d). The active thrusting got revitalized, thus the distance between the Gerecse and the frontal thrusts decreased. As a consequence sedimentation took place in the vicinity of the orogen-ward slope of the basin in form of submarine fans. The depositional slope of the mid-fan could be deformed by slump complexes with south-westerly vergency (Fig. 21d). The depocenter and probably also the southern margin of the basin were shifted to the south and condensed deposits of the former forebulge area got covered by sandy turbidites. This shift is typical for foreland basins. Probably the last event was the occurrence of the mid-fan deposit (Köszörükőbánya Member, Sztanó, 1990) near the Aptian-Albian boundary. **By this time the Gerecse clastic basin approached the orogenic wedge**, although the distance from the thrust front could remain considerable. The southern margin of the basin could shift further to the south. The forebulge could be located in the southern TR, where bauxitic deposition could be connected to emergence and denudation (Mindszenty et al. 1995; 2001).

The Gerecse clastics show notable similarity to the Rossfeld beds of the Eastern Alps which equally had ophiolite in its source area (Decker et al., 1987). However, this similarity does not mean that

Rossfeld and Gerecse occupied the same position with respect to the emerging orogenic wedge.

In the Gerecse Hills, folding, strike-slip and thrust faulting can be documented only after the termination of the sedimentation sometimes in the early Albian. One example of such folds is present in the Bersek quarry (Fülöp, 1958) while others were documented by Sasvári (2008, 2009a, b) and Bada et al. (1996). The structures could belong to phases D2b and D2c of Fodor (2010) and marked by N-S or NE-SW compression. These events deformed the whole Gerecse area, although large-scale thrusting seems to be missing (or wait for discovery). With the post-sedimentary deformation, the long-lasting, “Meliata-related” evolution of the Gerecse Hills ended.

From the early Albian, the northern TR was influenced by the effect of a new deformation phase, the D3 phase. The major structures are the large-scale folds of the TR (Fig. 21e), while during the excursion we will visit some important map-scale structures in stops 1.5-7. In the southern and central TR the major structures are NE-SW trending elements. However, in the northern Vértes Hills, the E-W trending Vértessomló Thrust seems to be an exception. As we discussed in stops 1.6, 1.7, this line was a south-verging thrust with possible dextral component of slip. The structure could be somewhat younger than the majority of the TR D3 structures while they are Early Albian (113-108 Ma), and the VT could be mid-Albian to Coniacian (108-86 Ma). This later timing could explain the slightly oblique strike and kinematics of the VL.

The TR occupied a completely different tectonic position during the D3 deformation phase than during the D2 phase. The TR was in the lower position in the latter and higher position in the former phase. This needs a major reorganisation of the subducting and overriding plates. We follow the suggestions of Stüwe and Schuster (2010) and others that a major strike-slip fault operated during this time (Frank and Schlager, 2006; Stüwe and Schuster 2010). The large shift placed the TR and its foreland-type Early Cretaceous basin in the rear of the subduction, in the highest position. In the same time, the style of subduction could also change and finally led to the formation of the Austroalpine nappe pile. It is to note that this reorganisation did not affect the NCA. On the other hand, a somewhat similar change occurred in the Gemer-Meliata area, where the occurrence of some units (Silica and related nappes) would need major change in thrust geometry and the overriding units and could have similar interpretation (Plašienka, 2000; Deák-Kövéér 2012). Although the nature, timing, and extent of this reorganisation needs further studies, the contrasting tectonic position of the TR during the early and “middle” Cretaceous deformation phases is one of the main issues of this study.

References

- Alsop, G. I., Marco, S. (2011): Soft-sediment deformation within seismogenic slumps of the Dead Sea Basin. *Journal of Structural Geology*, 33, 433–457.
- Árgyelán, G. (1995): Petrographical and petrological investigations of the Cretaceous clastic sediments of the Gerecse Mountains, Hungary. *Általános Földtani Szemle*, 27, 59–83.
- Árgyelán, G., Császár, G. (1998): Törmelékes króm-spinellek a gerecsei jura képződményekben. *Földtani Közlöny*, 128/2-3, 321–360.
- Bada, G. 1994: A paleofeszültségtér fejlődése a Gerecse hegység és kelet-délkeleti előterének területén. (Evolution of the paleostress field in the Gerecse Hills and their southern and southeastern vicinity). Master thesis, Eötvös University, Dept. Applied and Envir. Geology 147 p. (in Hungarian).
- Bada, G., Fodor, L., Székely, B., Timár, G. 1996: Tertiary brittle faulting and stress field evolution in the Gerecse Mts. N. Hungary. *Tectonophysics*, 255, 269–290.
- Balkay, B. (1955): Über einen Untertyp der Gesteinsbewegung. *Földtani Közöly*, 85, 2, 153–156.
- Balla, Z. (1981): Magyarország kréta – paleogén képződményeinek geodinamikai elemzése. *Általános Földtani Szemle*, 16, 89–180.
- Balla, Z., Dudko, A. (1989): Large-scale Tertiary strike-slip displacements recorded in the structure of the Transdanubian Range. *Geophysical Transactions* 35, 3–64.
- B. Árgyelán G. 1996: Geochemical investigations of detrital chrome spinels as a tool to detect an ophiolitic source area (Gerecse Mountains, Hungary). *Acta Geologica Hungarica*, 39, 341–368.
- Bárány, M. (2004): A jura-kréta határ gravitációsán átülepített képződményei az Északi-Gerecseben. MSc thesis, Eötvös University, Dept. General Geology, Budapest, 74 p.
- Beacon, L. E., Anderson, T. B., Holdsworth, R. E. (1999): Using basement-hosted clastic dykes as syn-rifting palaeostress indicators: an example from the basal Stoer Group, northwest Scotland. *Geological Magazine*, 136, 301–310.
- Bíró, I. 2003: A Vértessomló-i-törésvonal szerkezetföldtani vizsgálata a vértesi Mária-szurdok környékén. MSc thesis, ELTE Regionális Földtani Tanszék, 73 p.
- Bradley, D., Hanson, L. (1998): Paleoslope Analysis of Slump Folds in the Devonian Flysch of Maine. *Journal of Geology*, 106, 305–318.
- Bradley, D.C., Kidd, W.S.F., (1991): Flexural extension of the upper continental crust in collisional foredeeps. *Geological Society of America Bulletin*, 103, 1416–1438.
- Budai, T., Vörös A. (1992): Middle Triassic history of the Balaton Highland: extensional tectonics and basin evolution. *Acta Geologica Hungarica*, 35, 237–250.
- Covault, J. A., Romans, B. W. (2009): Growth patterns of deep-sea fans revisited: Turbidite system morphology in con ned basins of the Quaternary California Borderland. *Marine Geology* 265, 51–66.
- Cresta, S., Galács, A. (1990): Mediterranean basal Bajocian ammonite faunas. Examples from Hungary and Italy. *Memoire Descrittive della Carta Geologica d'Italia*, 40, 65–198.
- Császár, G. (1986): Dunántúli-középhegységi középső-kréta képződmények rétegtana és kapcsolata a bauxitképződéssel. *Geologica Hungarica series Geologica*, 23, 295p.
- Császár, G. (1995): A gerecsei és a vértesi-előterű kutatás eredményeinek áttekintése. *Általános Földtani Szemle*, 27, 133–152.
- Császár, G. (2002): Urgon formations in Hungary. *Geologica Hungarica ser. Geologica* 25, 209 p.
- Császár, G., Árgyelán, B. G. (1994): Stratigraphic and micromineralogic investigations on Cretaceous Formations of the Gerecse Mountains, Hungary and their palaeogeographic implications. *Cretaceous Research*, 15, 417–434.
- Császár, G., Haas, J., Jocháné-Edelényi, E. (1978): Bauxite geological map of the Transdanubian Range, 1:100 000. Geological Institute of Hungary.
- Császár, G., Haas, J., Halmaj, J., Hámor, G., Korpás, L. (1982): A középső és fiatal alpi tektonikai fázisok szerepe Magyarország tektonikai fejlődésében. *MÁFI Évi jelentés*, 1980-ról, 509–516.
- Császár, G., Galács, A., Vörös, A. (1998): The Jurassic of the Gerecse Mountains, Hungary; facies and Alpine analogies. *Földtani Közöly*, 128/2, 397–435.
- Császár, G., Schlagintweit, F., Piros, O., Szinger B. (2008): Are there any Dachstein Limestone fragment in the Felsővadács Breccia Member? *Földtani Közöly*, 138/1, 107–110.
- Császár, G., Haas, J., Sztanó, O., Szinger B. (2012): From Late Triassic passive margin to Early Cretaceous active continental margin of dominantly carbonate sediments in the Transdanubian Range, Western Tethys. *Journal of Alpine Geology*, 54, 33–99.
- Csontos, L. (1988): Etude géologique d'une portion des Carpathes Internes, le massif du Bükk (Nord-est de la Hongrie), (stratigraphie, structures, métamorphisme et géodynamique). Ph.D. thesis, University Lille Flandres-Artois, n° 250, 327 pp.
- Csontos, L., (1999): Structural outline of the Bükk Mts. (N. Hungary). *Földtani Közöly*, 129, 611–651.
- Csontos, L. (2000): Stratigraphic reevaluation of the Bükk Mts. (N. Hungary). *Földtani Közöly*, 130/1, 95–131.
- Csontos, L., Vörös, A. 2004: Mesozoic plate tectonic reconstruction of the Carpathian region. *Palaeogeography, Paleoclimatology, Palaeoecology*, 210, 1–56.
- Csontos L., Sztanó O., Pocsai T., Bárány M., Palotai M., Wettstein E. 2005: Late Jurassic – Early Cretaceous Alpine deformation events in the light of redeposited sediments. *Geolines* 19, 29–31.
- Deák-Kövr, Sz. (2012): Structure, metamorphism, geochronology and deformation history of Mesozoic formations in the central Rudabánya Hills. Ph.D. Thesis, Eötvös University, program for Geology and Geophysics, 162p.
- Decker, K., Faupl, P., Müller, A. (1987): Snyorogenic Seidmentation on the Norhtern Calcareous Akps during the Early Cretaceous. In: Flügel, H.W., Faupl, P. (eds.): *Geodynamics of the Eastern Alps*. Franz Deuticke, Vienna, 126–141.
- Dercourt, J., Zonenshain, L. P., Ricou, L. E., Kazmin, V. G., Lepichon, X., Knipper, A. L., Grandjacquet, C., Sbertshikov, I. M., Geyssant, J., Lepvrier, C., Pechersky, D. H., Boulin, J., Sibuet, J. C., Savostin, L. A., Sorokhtin, O., Westphal, M., Bazhenov, M. L., Lauer, J. P., Bijuduval, B. (1986): Geological evolution of the Tethys belt from the Atlantic to the Pamirs since the Lias. *Tectonophysics*, 123/1–4, 241–315.
- Dosztály, L. (1998): Jura radiolaritok a Dunántúli-középhegységben. (Jurassic radiolarites in the Transdanubian Range). *Földtani Közöly*, 128/2, 273–295.
- Dulai, A. (1998): Hettangian and Early Sinemurian (Early Jurassic) brachiopod fauna of the Pisznice Limestone in the eastern Gerecse Mts. and in the Kálvária Hill at Tata. *Földtani Közöly*, 128/2-3, 237–263.
- Edwards, D. A., Leeder, M. R., Best, J. L., Pantin, H. M. (1994): On experimental reflected density currents and the interpretation of certain turbidites. *Sedimentology*, 41, 3, 437–461.
- Félegyházy, L., Nagymarosy, A. (1991). New data on the age of the Lower Cretaceous formations in the Gerecse Mountains (Hungary). *Geologica Carpathica* 42, 123–126.
- Fodor, L. (1998): Late Mesozoic and early Paleogene tectonics of the Transdanubian Range. XIVth CBGA Congress, Vienna, Austria, p. 165, *Geol. Survey of Austria*.
- Fodor, L. (2008): Structural geology. In: Budai T., Fodor L. (eds.): *Geology of the Vértes Hills*. Explanatory book to the Geological Map of the Vértes Hills 1:50000. Magyar Állami Földtani Intézet, 145–202, 282–300.
- Fodor, L. (2010): Mezozoos-kainozoos feszültségmezők és törésszerek a Pannon-medence ÉNy-i részén – módszertan és szerkezeti elemzés (Mesozoic-Cenozoic stress fields and fault patterns in the northwestern part of the Pannonian Basin – methodology and structural analysis). Doctoral work of the Hungarian Academy of Sciences, 129p.
- Fodor, L. (2013): Deformation of the Late Jurassic sediments in the northern Gerecse Mountains. In: Főzy, I. (ed.): *Late Jurassic – Early Cretaceous fauna, biostratigraphy, facies and deformation history of the carbonate formations in the Gerecse and Pilis Mountains (Transdanubian Range, Hungary)*. Institute of Geosciences, University of Szeged, GeoLitera Publishing House, in press.
- Fodor L., Bíró I. (2004): Eocene abrasional rocky shore along the Cretaceous Vértessomló thrust (Szarvas-kút, Vértes Hills, Hungary). *Magyar Állami Földtani Intézet Évi Jelentése*, 2002, 153–162.

- Fodor, L., Főzy, I. (2013): Late Middle Jurassic to earliest Cretaceous evolution of basin geometry of the Gerecse Mountains. In: Főzy, I. (ed.): Late Jurassic–Early Cretaceous fauna, biostratigraphy, facies and deformation history of the carbonate formations in the Gerecse and Pilis Mountains (Transdanubian Range, Hungary). Institute of Geosciences, University of Szeged, GeoLitera Publishing House, in press.
- Fodor, L., Lantos, Z. (1998): Liassic brittle structures in the Gerecse. *Földtani Közlöny*, 128, 2–3, 375–396.
- Fodor, L., Koroknai, B., Balogh, K., Dunkl, I., Horváth, P. (2003): Nappe position of the Transdanubian Range Unit ('Bakony') based on new structural and geochronological data from NE Slovenia. *Földtani Közlöny*, 133, 535–546.
- Fodor, L., Bíró, I., Albert, G., Lantos, Z. (2005a): New structural observations along the Vértessomló Line and implications for structural evolution of the Transdanubian Range (western Hungary). *Geolines* 19, 38–40.
- Fodor, L., Turki, S. M., Dalob H., Al-Gerbi A. (2005b): Fault-related folds and along-dip segmentation of breaching faults: syn-diagenetic deformation in the south-western Sirt basin, Libya. *Terra Nova*, 17, 2, 121–128.
- Fogarasi, A. (1995a): Cretaceous cyclostratigraphy of the Gerecse Mt. Preliminary results. *Általános Földtani Szemle*, 27, 43–58.
- Fogarasi, A. (1995b): Sedimentation on tectonically controlled submarine slopes of Cretaceous age, Gerecse Mts., Hungary – working hypothesis. *Általános Földtani Szemle*, 27, 15–41.
- Fogarasi, A. (2001): Lower Cretaceous calcareous nannoplankton stratigraphy of the Transdanubian Range. PhD. Thesis, Eötvös University, Dept. General and Historical Geology, 95 p.
- Fossen, H. (2010): *Structural Geology*. Cambridge University Press, 463.
- Főzy, I. (1993): Upper Jurassic ammonite biostratigraphy in the Gerecse and Pilis Mts. (Transdanubian Central Range, Hungary). *Földtani Közlöny*, 123, 4, 441–464.
- Főzy, I., Fogarasi, A. (2002): The Lower Cretaceous biostratigraphy of the Bersek Hill (Gerecse Mts, Transdanubian Range) on the basis of the ammonites and nannofossils. *Földtani Közlöny*, 132, 293–324.
- Főzy, I., Janssen, N. M. M. (2009): Integrated Lower Cretaceous biostratigraphy of the Bersek Quarry, Gerecse Mountains, Transdanubian Range, Hungary. *Cretaceous Research*, 30, 78–92.
- Főzy, I., Meléndez, G. (2013): Oxfordian ammonites from the Gerecse and Pilis Mountains (Hungary). In: Főzy, I. (ed.): Late Jurassic – Early Cretaceous fauna, biostratigraphy, facies and deformation history of the carbonate formations in the Gerecse and Pilis Mountains (Transdanubian Range, Hungary), Institute of Geosciences, University of Szeged, GeoLitera Publishing House, in press.
- Főzy, I., Szinger, B. (2013): Upper Jurassic—earliest Cretaceous fossil localities of the Gerecse and Pilis Mountains (rocks and fossils) In: Főzy, I. (ed.): Late Jurassic–Early Cretaceous fauna, biostratigraphy, facies and deformation of the carbonate formations in the Gerecse and Pilis Mountains (Transdanubian Range, Hungary), Institute of Geosciences, University of Szeged, GeoLitera Publishing House, in press.
- Főzy, I., Kázmér, M., Szente, I. (1994): A unique Lower Tithonian fauna in the Gerecse Mts, Hungary. *Paleopelagos Special Publication*, 1, 155–165.
- Frank W., Schlager W. (2006): Jurassic strike-slip versus subduction in the Eastern Alps. *International Journal of Earth Sciences*, 95, 431–450.
- Frey-Martinez, J., Cartwright, J., Hall, B. (2005): 3D seismic interpretation of slump complexes: examples from the continental margin of Israel. *Basin Research*, 17, 83–108.
- Frey-Martinez, J., Cartwright, J., James, D. (2006): Frontally confined versus frontally emergent submarine landslides: A 3D seismic characterisation. *Marine and Petroleum Geology*, 23, 5, 585–604.
- Frisch W., Gawlick H.-J. (2003): The nappe structure of the central Northern Calcareous Alps and its disintegration during Miocene tectonic extrusion – a contribution to understanding the orogenic evolution of the Eastern Alps. *International Journal of Earth Sciences*, 92, 712–727.
- Fülöp, J. (1958): Die kretazeischen Bildungen des Gerecse-Gebirges. *Geologica Hungarica*, series Geologica, 11, 1–124.
- Fülöp, J., Géczy, B., Konda, J., Nagy, E., Hetényi, R. (1969): Földtani kirándulás a Mecsek-hegységben, a Villányi-hegységben és a Dunántúli-középhegységben. *Magyar Állami Földtani Intézet*, 68 p.
- Galács, A. (1988): Tectonically controlled sedimentation in the Jurassic of the Bakony Mountains (Transdanubian Central Range, Hungary). *Acta Geologica Hungarica*, 31, 3–4, 313–328.
- Galács, A., Vörös, A. (1972): Jurassic history of the Bakony Mts. and interpretation of principal lithological phenomena. *Földtani Közlöny*, 102/2, 122–135.
- Gartzos E., Dietrich V.J., Migiros G., Serelis K., Lymperopoulou Th. (2009): The origin of amphibolites from metamorphic soles beneath the ultramafic ophiolites in Evia and Lesvos (Greece) and their geotectonic implication. *Lithos*, 108, 224–242.
- Gawlick H.-J., Frisch W. (2003): The Middle to Late Jurassic carbonate clastic radiolaritic flysch sediments in the Northern Calcareous Alps: sedimentology, basin evolution and tectonics – an overview. *Neues Jahrbuch Geol. Pal. Abhandlungen*, 230, 163–213.
- Gawlick, H.J., Schlagintweit, F. (2006): Berriasian drowning of the Plassen carbonate platform at the type-locality and its bearing on the early Eoalpine orogenic dynamics in the Northern Calcareous Alps (Austria). *International Journal of Earth Sciences*, 95, 451–462.
- Gawlick, H.-J., Krystyn, L., Lein, R. (1994): Conodont colour alteration indices: Paleotemperatures and metamorphism in the Northern Calcareous Alps – a general view. *Geologische Rundschau*, 83, 660–664.
- Gawlick, H. J., Frisch, W., Vecsei, A., Steiger, T., Böhm, F. (1999): The change from rifting to thrusting in the Northern Calcareous Alps as recorded in Jurassic sediments. *Geologische Rundschau*, 87, 644–657.
- Haas J. (1988): Upper Triassic carbonate platform evolution in the Transdanubian Mid-Mountains. *Acta Geologica Hungarica* 31: 299–312.
- Haas, J. (1999): Late cretaceous isolated platform evolution in the Bakony mountains (Hungary) *Geologica Carpathica*, 50, 3, 241–256.
- Haas, J., Császár, G. (1987): Cretaceous in Hungary: paleogeographic implications. *Rendiconti della Società Geologica Italiana*, 9, 203–208.
- Haas, J., Kovács, S., Krystyn, L., Lein, R. (1995): Significance of Late Permian-Triassic facies zones in terrane reconstructions in the Alpine-North Pannonian domain. *Tectonophysics*, 242, 19–40.
- Haas J., Budai T., Csontos L., Fodor L., Konrád Gy. (2010): Pre-Cenozoic geological map of Hungary, 1:5000000. Geological Institute of Hungary.
- Haas, J., Hámor, G., Jámor, Á., Kovács S., Nagymarosy, A., Szederkényi, T. (2013): *Geology of Hungary*. Regional Geology Reviews, Springer 244p.
- Horányi, A., Takács, Á., Fodor, L. (2010): Sedimentological and structural geologic observations at the eastern slope of the Gorba High („Gyökér ravine”, Western Gerecse Mts., Hungary). *Földtani Közlöny*, 140/3, 223–234.
- Horváth, F. 1993: Towards a mechanical model for the formation of the Pannonian basin. *Tectonophysics*, 225, 333–358.
- Khalil, S.M., McClay, K.R. (2002): Extensional fault-related folding, north-western Red Sea, Egypt. *Journal of Structural Geology*, 24, 743–762.
- Konda, J. (1988): Lókúti radiolarit Formáció, Gerecse, Lábtalan, Margit-hegy, Margit-tető. *Magyarország geológiai alapszervevényei*. Magyar Állami Földtani Intézet, 4 p.
- Kovács, S. (1982): Problems of the “Pannonian Median Massif” and the plate tectonic concept. Contributions based on the distribution of Late Paleozoic–Early Mesozoic isopic zones. *Geol. Rundschau*, 71/2, 617–639.
- Kovács, S., Ozsvárt, P., Palinkaš, L., Kiss, G., Molnár, F., Józsa, S., Kővér, Sz. (2010): Re-evaluation of the Mesozoic of the Darnó Hill (NE Hungary) and comparison with Neotethyan accretionary complexes of the Dinarides and Hellenides – preliminary data. *Central European Geology*, 53/2–3, 205–231.
- Koledoye, A.B., Aydin, A., May, E. (2003): A new process-based methodology for analysis of shale smear along normal faults in the Niger Delta. *American Association of Petroleum Geologists Bulletin*, 87, 1–19.
- Lantos, Z. (1997): Sediments of a Liassic carbonate slope controlled by strike-slip fault activity (Gerecse Hills, Hungary). *Földtani Közlöny*, 127/3–4, 291–320.
- Liati, A., Gebauer, D., Fanning, C.M. (2004): The age of ophiolitic rocks of the Hellenides (Vourinos, Pindos, Crete): first U–Pb ion microprobe (SHRIMP) zircon ages. *Chemical Geology* 207, 171–188.
- Maros, Gy. (1988): Tectonic survey in the Vitány-vár area, W Hungary. *Ann. Report of the Geological Institute of Hungary from 1986*, 295–310.
- Márton, E., Haas, J., Fodor, L. (2009): Outline of the tectonic history of the Transdanubian Range between 150 and 50 Ma based on paleomagnetic observations. *Proceedings of the 7th Meeting of the CETeG*, Pécs, Hungary, p. 52.
- Mindszenty, A., Szóts, A., Horváth A. 1989: Excursion A3: Karstbauxites in the Transdanubian Midmountains. — In: Császár G. (szerk.): *Excursion Guidebook IAS 10th Regional Meeting*, Budapest. Budapest, pp. 11–48.

- Mindszenty, A., D'Argenio, B., Aiello, G. (1995): Lithospheric bulges at regional unconformities. The case of Mesozoic-Tertiary Apulia. *Tectonophysics* 252, 137-161.
- Mindszenty, A., Csoma, A., Török, Á., Hips, K., Hertelendi, E. (2001): Rudistid limestones, bauxites, paleokarst and geodynamics. The case of the Cretaceous of the Transdanubian Central Range. *Földtani Közöly*, 131/1-2, 107-152.
- Mello, J., Elecko, M., Pristaš, J., Reichwalder, P., Snopko, L., Vass, D., Vozárová, A., L'udovít G., Hanzel, V., Hók, J., Kováč, P., Slavkay, S., Steiner A. (1997): Explanatory book to the geological map of the Slovak karst area 1:50000. Slovak State Geological Institute of Dionýz Štúr 255 p.
- Neubauer, F., Genser, J., Handler, R. 2000: Eastern Alps: Result of a two-stage collision process. *Mitteilungen der Österreichischen Geologischen Gesellschaft*, 92, 117-134.
- Oravec J., Véghné Neubrandt E. (1961): A Gerecse- és Vértes hegységi felső triász dolomit- és mészkő öszlet. (Upper Triassic dolomite and limestone formations of the Gerecse and Vértes Mountains). *Magyar Állami Földtani Intézet Évkönyve*, 49/2, 291-294, (in Hungarian).
- Palotai M., Csontos L., Dövényi P. (2006): Field and geoelectric study of the Mesozoic (Upper Jurassic) occurrence at Kesztlőc. *Földtani Közöly* 136/3, 347-368.
- Pamić, J., Tomljenović, B., Balen, D. (2002): Geodynamic and petrogenetic evolution of Alpine ophiolites from the central and NW Dinarides: an overview. *Lithos*, 65, 113-142.
- Plašienka, D. (1997): Cretaceous tectonochronology of the Central Western Carpathians, Slovakia. *Geologica Carpathica*, 48, 99-111.
- Plašienka, D. (2000): Paleotectonic controls and tentative palinspastic restoration of the Carpathian realm during the Mesozoic. *Slovak Geological Magazine* 6/2-3, 200-204.
- Pocsai, T., Csontos L. (2006): Late Aptian-early Albian syn-tectonic facies-pattern of the Tata Limestone Formation (Transdanubian Range, Hungary). *Geol. Carpathica* 57, 15-27.
- Ramsay, J. G., Hubert, M. I. (1987): *The Techniques of Modern Structural Geology. Volume 2. Folds and Fractures.* Academic Press, London, 309-700.
- Robertson A. H. F. 2002: Overview of the genesis and emplacement of Mesozoic ophiolites in the Eastern Mediterranean Tethyan region. - *Lithos* 65, 1-67.
- Rykkeliid, E., Fossen, H. (2002): Layer rotation around vertical fault overlap zones: observations from seismic data, field examples, and physical experiments. *Marine and Petroleum Geology*, 19, 181-192.
- Sasvári Á. (2008): Shortening-related deformations in the Gerecse Mts, Transdanubian Range, Hungary. *Földtani Közöly*, 138/4, 385-402.
- Sasvári, Á. (2009a): Explanation of an 'extraordinary rock deformation' - sheared structures in the Ördögát Quarry of the Transdanubian Range, Hungary. *Földtani Közöly*, 139, 3-4, 341-352.
- Sasvári, Á. (2009b): Középső-kréta rövidülési deformáció és szerkezeti betemetődés a Gerecse területén. PhD Thesis, Eötvös University, Dept. General and Applied Geology, 164 p.
- Sasvári, Á., Csontos, L., Palotai, M. (2009): Structural geological observations in Tölgyhát quarry (Gerecse Mts., Hungary). *Földtani Közöly* 139, 55-66.
- Schettino, A., Turco, E. (2011): Tectonic history of the western Tethys since the Late Triassic. *Geological Society of America Bulletin*, 123/1-2, 89-105.
- Schmid, S. M., Fügenschuh, B., Kissling, E., Schuster, R. (2004): Tectonic map and overall architecture of the Alpine orogen. *Swiss Journal of Geosciences*, 97/1, 93-117.
- Schmid, S. M., Bernoulli, D., Fügenschuh, B., Matenco, L., Schuster, R., Schefer, S., Tischler, M., Ustaszewski, K. (2008): The Alpine-Carpathian-Dinaridic orogenic system: Correlation and evolution of tectonic units. *Swiss Journal of Geosciences*, 101, 139-183.
- Stampfli, G., Borel, G. (2002): A plate-tectonic model for the Palaeozoic and Mesozoic constrained by dynamic plate boundaries and restored synthetic oceanic isochrons. *Earth and Planetary Science Letters*, 196, 17-33.
- Stüwe K., Schuster R. (2010): Initiation of subduction in the Alps: Continent or ocean? *Geology*, 38, 175-178.
- Szabó, J. (1998): Paleogeográfiai és paleoökológiai következtetések egy késő-sinemuri gastropoda-fauna kapcsán (Hierlatzi-Mészkő, Nagy-Teke-hegy, Gerecse). *Földtani Közöly* 128, 211-222.
- Szives, O., Fözy, I., (2013): Early Cretaceous ammonites from the carbonate formations of the Gerecse Mountains (Hungary). In: Fözy, I. (ed.): Late Jurassic - Early Cretaceous fauna, biostratigraphy, facies and deformation history of the carbonate formations in the Gerecse and Pilis Mountains (Transdanubian Range, Hungary), Institute of Geosciences, University of Szeged, GeoLitera Publishing House, in press.
- Szatanó, O. 1990: Submarine fan-channel conglomerate of Lower Cretaceous, Gerecse. *Neues Jahrbuch Geol. Paläont. Mh.* 7, 431-446.
- Tari G. (1994): Alpine tectonics of the Pannonian basin. - Ph.D. thesis, Rice University, Houston, Texas, U.S.A. 501 p.
- Tari, G. (1995): Eoalpine (Cretaceous) tectonics in the Alpine/Pannonian transition zone. In: Horváth, F., Tari, G. & Bokor, Cs. (eds.): Extensional collapse of the Alpine orogene and Hydrocarbon prospects in the Basement and Basin Fill of the Western Pannonian Basin. AAPG International Conference and Exhibition, Nice, France, Guidebook to field trip No. 6. Hungary, 133-155.
- Tari, G., Horváth, F. (2010): Eo-Alpine evolution of the Transdanubian Range in the nappe system of the Eastern Alps: revival of a 15 years tectonic model. *Földtani Közöly* 140/4, 483-510.
- Taeger, H. (1909): A Vérteshegység földtani viszonyai. *Magyar Királyi Földtani Intézet Évkönyve* 17, 1-256.
- Vigh, G. (1945): Részletes térképezés és kőületgyűjtés a tardosi Szelhegyen. *Földtani Intézet Évi Jelentése 1944-ről*, 27-29.
- Vigh, G. (1961): Esquisse géologique de la partie occidentale de la Montagne Gerecse. *Annales Instituti Geologici Publici Hungarici* 49, 2, 569-589.
- Vörös, A. (1991): Hierlatzkalk - a peculiar Austro-Hungarian Jurassic facies. In: Lobitzer, H., Császár, G. (eds.): *Jubiläumsschrift 20 Jahre Geologische Zusammenarbeit Österreich-Ungarn*, I.: 145-154.
- Vörös, A., Galász, A. (1998): Jurassic paleogeography of the Transdanubian Central Range (Hungary). *Rivista Italiana di Paleontologia*, 104/1: 69-84.
- Willsey, S.P., Umhoefer, P., Hilley, G.E. (2002): Early evolution of an extensional monocline by a propagating normal fault: 3D analysis from combined field study and numerical modeling. *Journal of Structural Geology*, 24, 651-669.

Post-conference excursion: Cenozoic deformation of the northern Transdanubian Range (Vértes Hills)

László Fodor^{1,2}, Szilvia Kövér¹

¹ Geological, Geophysical and Space Science Research Group of the Hungarian Academy of Sciences at Eötvös University, 1/c Pázmány Péter sétány, H-1117, Budapest, Hungary

² Department of Regional Geology, Eötvös University, 1/c Pázmány Péter sétány, H-1117, Budapest, Hungary
 lasz.fodor@yahoo.com, koversz@yahoo.com

Table of contents

1. Introduction.....	36
2. Geological setting of the Pannonian Basin.....	36
3. Cenozoic faulting in the Vértes Hills.....	39
4. Excursion stops.....	39
Stop 1. Várgesztes, castle.....	39
Stop 2. Csókakő, quarry and castle.....	39
Stop 3. Csákberény, Lóállás Hill.....	42
Stop 4. Gánt, open pit mine.....	44
Stop 5. Csákvár, Kőlik Valley.....	49
References.....	51

1. Introduction

The post-conference excursion connected to the 11th Meeting of the Central European Tectonic Studies Group in Várgesztes will give an insight into the complex post-Mesozoic structural evolution of the Transdanubian Range. The main points will include deformation features from Eocene to late Miocene with a notion to neotectonic deformation. Near the conference location, from the Várgesztes castle we can have a look to the Early Miocene strike-slip fault, one of the largest within the TR. Exposures of the southern boundary fault of the Vértes Hills offer the possibility to discuss rifting of the Pannonian Basin and neotectonic aspects as well. Excellent outcrops of the Gánt mining area expose diverse structures from the Early Miocene strike-slip faults to the Miocene syn-rift and post-rift faults. The main structural attraction of this site is a 3D view of fault relay ramps between oblique-slip faults. We will discuss the geometry and formation of late Miocene so-called post-rift grabens and the related sediment pattern. We tackle the origin of this post-rift deformation, which is not part of the classical concepts about the Pannonian basin. Visited stops and a brief description of topics which are planned to discuss are listed below (Fig. 1).

Várgesztes castle: Early Miocene dextral fault — displacement markers, small pull-apart depressions, Miocene strike-slip and normal faults, Eocene depression

Csókakő quarry and castle: Cenozoic basin-margin fault — geometry of and deformation within a fault zone, inheritance from early phase, comparison of fault and seismic data, question of neotectonic reactivation

Csákberény: graben-margin fault — geomorphological expression of the fault, direct comparison with seismic data nearby. Landscape evolution and neotectonic activity

Gánt open pit mines: Miocene strike-slip faults, oblique-slip normal faults, relay ramps — 3D view of faults with diverse kinematics, techniques of fault-slip analysis and field measurements, interaction of overlapping faults, superposition of different fault slip events, fluid flow and mineralisation along faults

Csákvár: basin margin fault of a late Miocene depression — appearance and message of eroded fault scarps, constraints on fault geometry and timing of fault activity from boreholes and seismic data set

2. Geological setting of the Pannonian Basin

The location of the field trip, the central part of the Pannonian Basin is situated within the Alpine, Carpathian, and Dinaric orogenic belt (Fig. 1). The main Miocene basin forming phase was preceded by several episodes of compressional to transpressional basin formation of Middle Eocene to early Miocene age (Fig. 1b, c). These are the regional D6 to D8 deformation phases of Fodor (2008). The related basins of Hungary were located in a retroarc position with respect to the Alpine-Carpathian thrust front (Tari et al. 1993). At that time the area of the future Pannonian basin was integral part of the compressional Alpine orogen.

During the second part of this transpressional basin evolution, an important fault zone cut through the entire Alpine-Carpathian orogen. The combined Periadriatic Fault (PAF) and Mid-Hungarian shear zone resulted in dextral displacement of 60–150 km and brought eastward the easternmost Alps, Western Carpathians NW Pannonia, the so-called AlCaPa block. This is the regional D8 phase. The dextral slip was associated with thrusting (Csontos and Nagymarosy 1998) (Fig. 1c). The major fault disrupted the former Paleogene basins and also the Mesozoic facies belts.

The Miocene basin system was formed due to lithospheric extension during the late early to late Miocene times, from 19 Ma (Royden and Horváth, 1988). Based on subsidence analysis and geophysical data, Royden et al. (1983) separated the syn- and post-rift phases, although recent structural analyses revealed a more complex evolution (Tari et al., 1992; Fodor et al., 1999; Horváth et al., 2006). The syn-rift phase of ~19–11 Ma resulted in the formation of numerous grabens filled with relatively thin syn-rift sediments of marine to brackish origin (Royden and Horváth, 1988; Tari, 1994; Csontos, 1995; Fodor et al., 1999) (Fig. 1d).

Crustal extension was followed by a post-rift phase characterised by thinning and updoming of the lithospheric mantle, thermal contraction, and related subsidence of the entire basin (Horváth and Royden, 1981) (Fig. 1e). Moderate faulting occurred in some parts of the basin, including the field trip area. Post-rift subsidence was compensated by intense sedimentation in the brackish to freshwater Lake Pannon during the late Miocene (Jámbor, 1989; Juhász, 1991). Deltaic to littoral sediments progressively filled up the lake, while all sub-basins became fluvial dominated by the end of the Miocene (Vakarc et al., 1994; Magyar et al., 2012).

The end of rift evolution was related to the end of thrusting along the Carpathian arc (Horváth et al., 2006), which occurred in the early late Miocene in the Eastern Carpathian segment (~9–10 Ma, Maženc and Bertotti, 2000). At the same time, however, the northern push exerted by the Adriatic microplate continued from the south. As the Pannonian Basin lithosphere had no free space to further extend eastward, a new phase of deformation started. This phase resulted in inversion of the basin and can be considered as neotectonic phase (Horváth, 1995; Bada et al., 1999).

Corresponding to this evolution, the central Pannonian Basin underwent several phases of Cenozoic faulting, resulted in a dense network of faults of variable orientation. One way to present this evolution is the usage of stress field data, which are briefly exemplified by simplified diagram on Fig. 1. During the Cenozoic, stress axes were gradually rotating in clockwise sense and governed the activity and kinematics of the fault pattern (Bergerat, 1989; Csontos et al., 1991; Fodor et al., 1999).

The Pannonian Basin holds considerable amount of hydrocarbon accumulations. Several of the above mentioned tectonic factors influenced the formation of source rocks, migration pathways and trapping (Royden and Horváth 1988; Horváth 1995). Just to mention some of them, Paleogene and Miocene subsidence resulted in source rock formation. Maturation of organic matter was enhanced by the important late Miocene (post-rift) subsidence. Penetrative Miocene faulting permitted the formation of extensive migration pathways. Traps are connected to faults, fault-related folds and neotectonic folds of varying age and kinematics. All of these features emphasize the importance

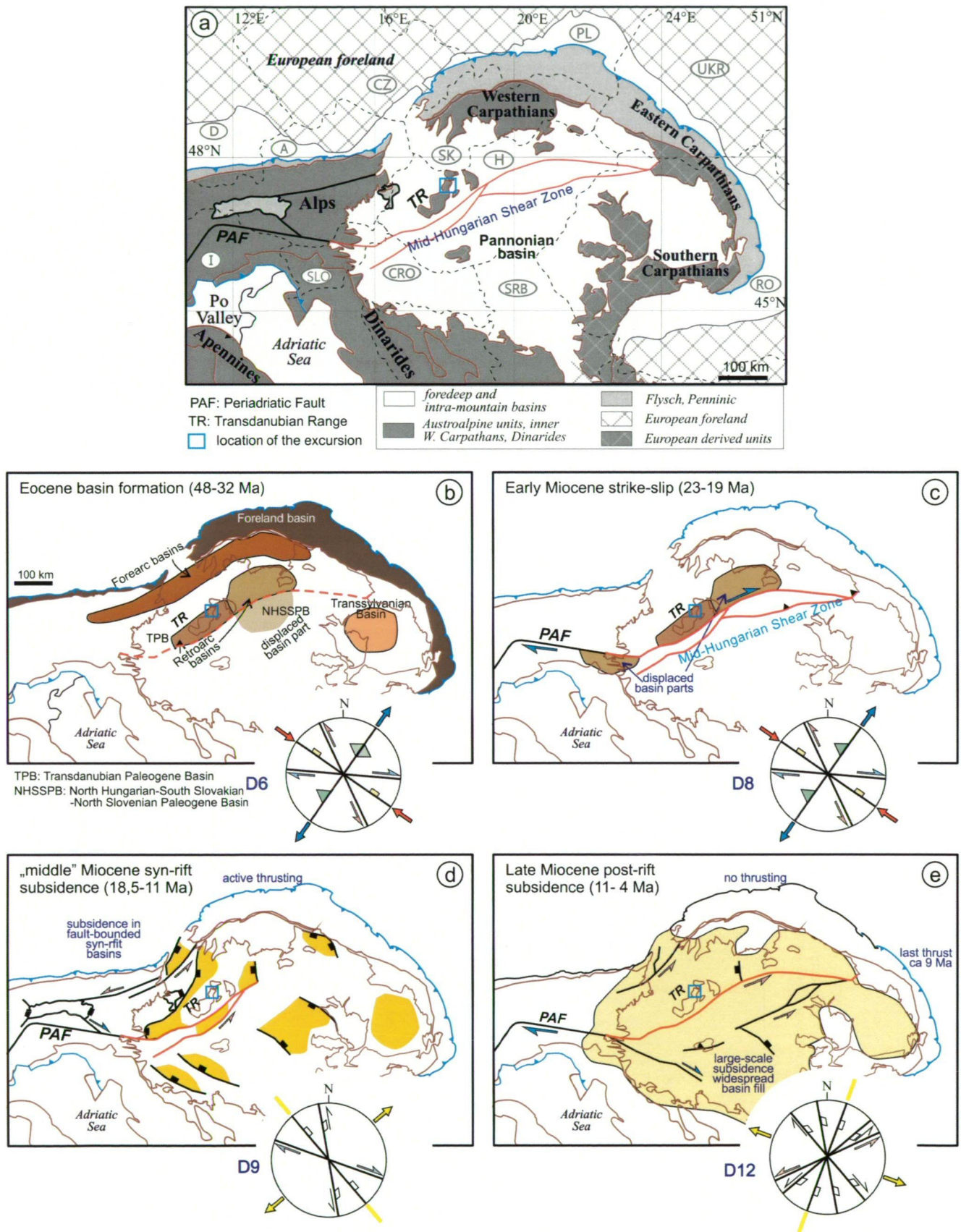
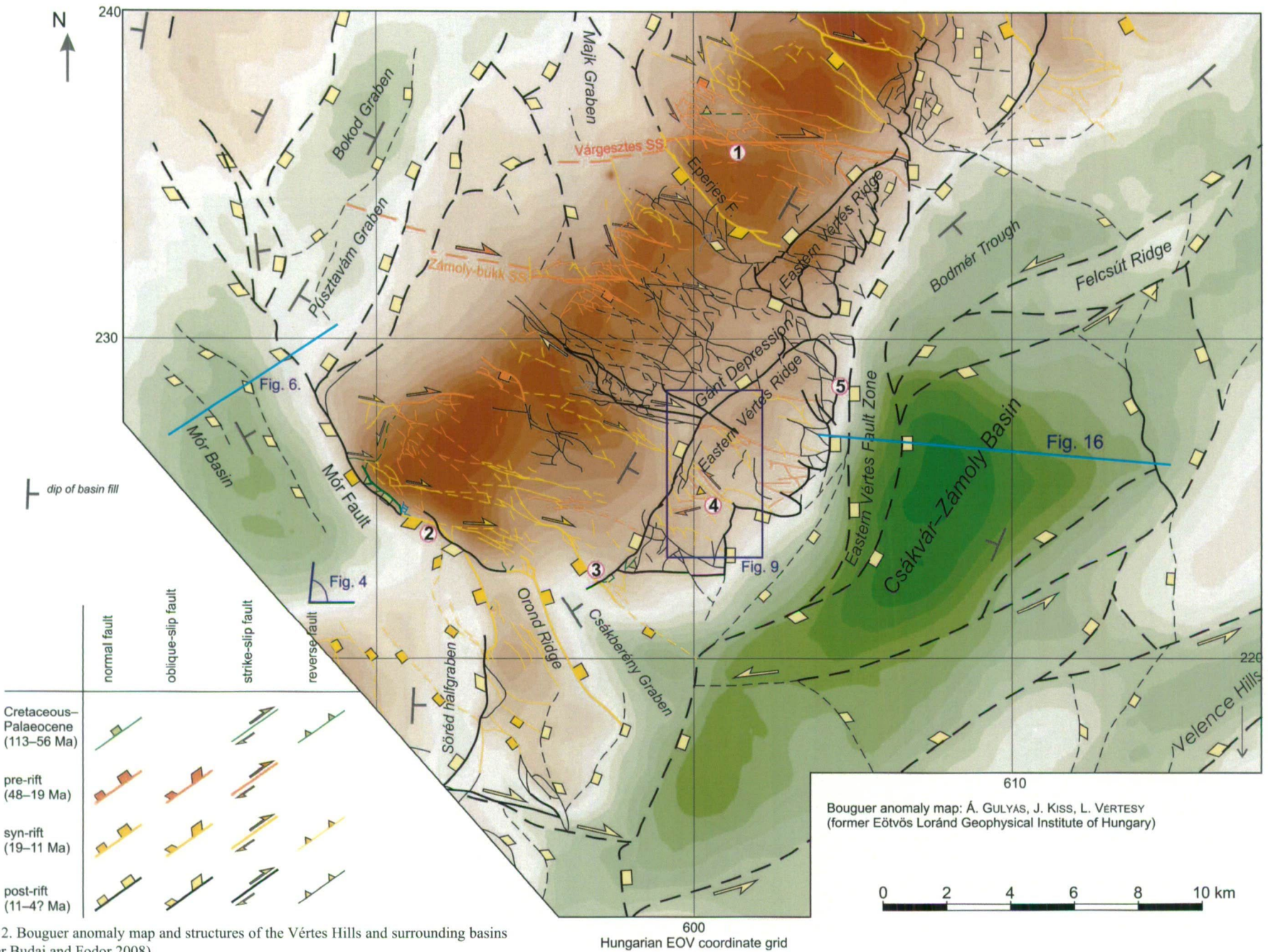


Fig. 1. Geodynamic setting and schematic structural evolution of the Pannonian Basin within the Alpine-Carpathian-Dinaridic orogen.



of understanding structural evolution of the Pannonian Basin, and of other sedimentary basin worldwide.

3. Cenozoic faulting in the Vértes Hills

The Vértes Hills are part of the Transdanubian Range (TR) which occupied a central position within the Pannonian Basin. The hills underwent the complex faulting evolution which is briefly outlined in the previous chapter and on Fig. 1. One way to study the Cenozoic deformation is the comparison of mapped faults and the gravity data. This is shown on Fig. 2, where the Bouguer anomaly map was placed below the fault pattern of the Vértes Hills and surrounding Cenozoic basins. As one can see the change in the anomaly map correspond to steep faults, and the negative values characterise the basins with Cenozoic sedimentary fill.

The oldest Cenozoic deformation phase, which was related to sedimentation, was the mid-Eocene basin formation. This D6 phase resulted in very gentle folds, namely two basins on the NW and SE limbs of the central Vértes ridge, which can be considered as an antiform. In the basins, the successions are thicker and more complete, while the central ridge was only inundated during the later part of the Eocene sedimentation. Few cross faults were associated with the folding, for example the Zámoly-bükk Fault (Fig. 2) and the marginal fault of the Csákberény graben (Stop 3).

The mid-to late Oligocene D7 phase resulted in amplification of NE–SW trending folds and the formation of the Mór fault (Stop 2, Fig. 2). The two major E– trending strike-slip faults are dextral in character and Early Miocene in age with occasional Eocene initiation. It is possible that these D8 dextral faults are the far-field echo of the major shear along the combined PAF–Mid-Hungarian Zone. The conjugate sinistral faults can be found near the dextral faults and in the Gánt area (Stop 4).

The syn-rift phase is marked by NW–SE striking normal or normal-oblique faults, like those in Stop 4. The Mór fault was reactivated (Stop 2) and the Eperjes faults accumulated ~200 m slip. The syn-rift phase was disrupted by a short-lived strike-slip phase (D11) between 12 and 10 Ma. There is no map-scale faults to this phase, but outcrop-scale reverse and dextral faults can locally be detected (Stop 4).

The post-rift deformation was surprisingly strong in the Vértes Hills and needs explanation. Important grabens and basins were formed at both sides of the Vértes Hills. In the eastern side the Zámoly Basin was filled up by several hundred meters of post-rift sediments of Late Miocene to earliest Pliocene(?) age. The suddenly subsiding basin was first accumulated lagunal or lacustrine marls than was filled by deltas from the NW. Final stage was marked by fluvial to terrestrial sedimentation (Csillag et al., 2008).

Deformation was coeval with basin-margin faulting, particularly along the western margin of the Zámoly Basin and along the Eastern Vértes Ridge. Syn-sedimentary character of faulting is based on borehole data, syn-sedimentary dykes and few seismic profiles. Stress data indicate E–W to SE–NW extension during this D12 phase (Fodor, 2008).

Neotectonic faulting in the Vértes Hills can be demonstrated by combined methodology including surface geological and geomorphological mapping, structural analysis, earthquake monitoring. All these

data suggest the neotectonic activity of some faults. The Mór Fault has a well-known historical seismic activity (Stop 2). Geomorphic and structural data also point to faulting along the Mór and nearby faults (Fodor, 2008; Fodor et al., 2007). The western margin fault of the Eastern Vértes Ridge could have Quaternary slip as revealed by geomorphic and borehole data (Stop3). Finally, the southern fault of the Felcsút ridge could be reactivated as reverse fault during the Quaternary. This slip changed the drainage pattern (Fodor et al. 2005).

4. Excursion stops

Stop 1. Várgesztes, castle. Panoramic view to Early Miocene dextral and sinistral fault, pull-apart depressions

47°28'4.34"N, 18°23'45.78"E

The top of the castle permits a panoramic view in several directions, and shows the general tectonic-morphological expression of the Cenozoic deformations in the central Vértes Hills. The main structure is the Várgesztes strike-slip fault which cut across the Vértes Hills in E–W direction. The fault has dextral separation as pointed out by the fault pattern, regional stress field evolution and displacement markers (Gyalog, 1992; Fodor, 2008). These latter are the displaced formation boundaries within the Triassic rocks and the basal Eocene unconformity (Fig. 3). The dextral slip was associated with the formation of small pull-apart depressions. These contained subsided packages of late Oligocene clastics which were encountered by shallow boreholes (Gyalog, 1992; Fodor et al., 2008). Because most of this soft sediment was eroded, the pull-apart depressions are present as a series of narrow valleys: one is just south from the castle hill.

Looking to the north, the morphological depression below Várgesztes village is bounded by faults or folds on each sides. The small depression was born in the Eocene, when the NW margin was gently folded and isolated a marginal marine lagoon from the open sea. After the Eocene and late Oligocene sedimentation, the north-eastern margin was cut by a NW–SE trending sinistral strike-slip fault which runs at the foot of rocky Eocene limestone cliffs. Finally, the SW margin is bounded by a Miocene normal fault.

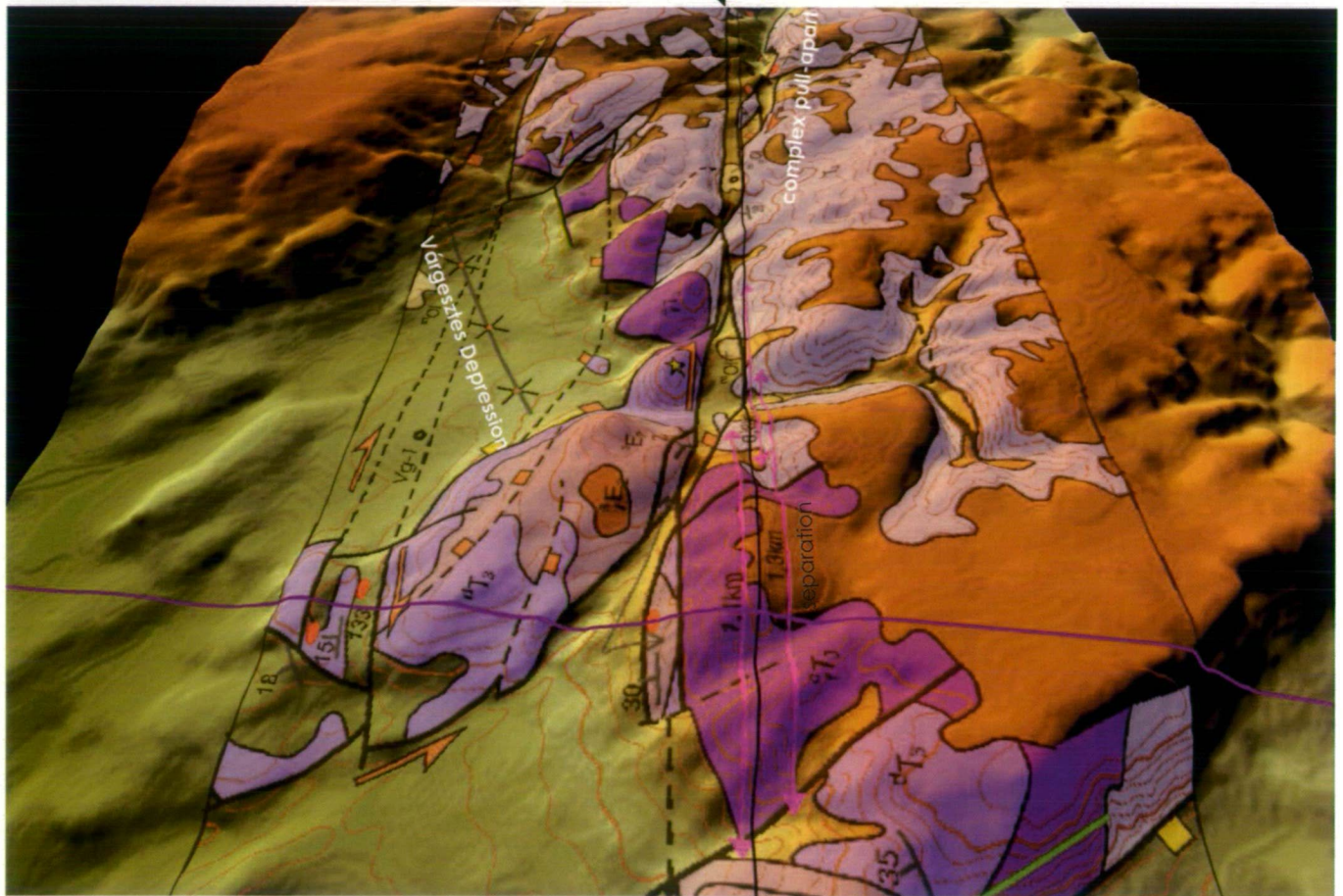
Stop 2. Csókakő, quarry and castle

Quarry: 47° 21' 31.91" N, 18° 16' 44.98" E

Castle: 47° 21' 37.12" N, 18° 16' 37.97" E

The Vértes Hills are limited by a major fault on their south-western side, called here as Mór Fault (Fig. 4). The curved, slightly segmented fault zone is expressed in the morphology as a steep slope of 100–250m height. The total displacement of the fault can reach 1000–1200m, taking into account borehole and seismic reflection data. The fault forms the NE boundary of the Mór graben (Fig. 2., 4). The fault has two closely spaced segments, which have different evolutions. The timing of slip events can be determined using combined data sets

Várgesztes Strike-slip Fault



- mO_1 deltaic to shallow marine clastics (Mány Fm.)
- E_2 shallow marine nummulitic limestone
- E_2 shallow marine bioclastic limestone (Szőc Fm.)
- red calcite vein (Eocene)
- T_3 platform limestone (Dachstein Fm.)
- T_3 transitional beds (Dachstein Fm., Fenyőfő Mb.)
- T_3 Hauptdolomit

- contour line
- T_{14} dip
- site for structural data
- Vgt-2 borehole
- Stop 2.1: Várgesztes, Castle

	normal fault	oblique-slip fault	strike-slip fault	fault-related fold
pre-rift (48-19 Ma)				
syn-rift (19-11Ma)				

Fig.3. Three dimensional view of the geological map of the Várgesztes castle wrapped onto digital elevation model. Note the morphological expression of the Várgesztes strike-slip fault. Map and structures are after Fodor et al. (2008) and Fodor (2008).

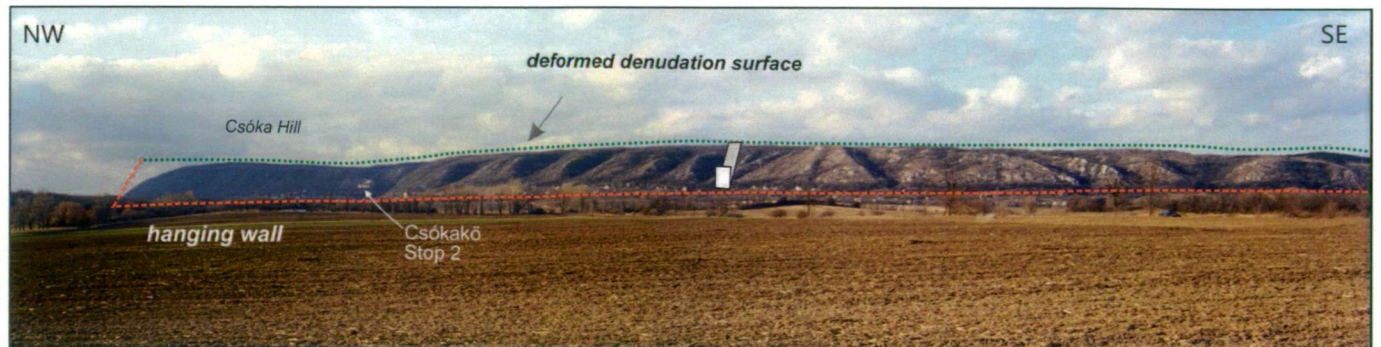
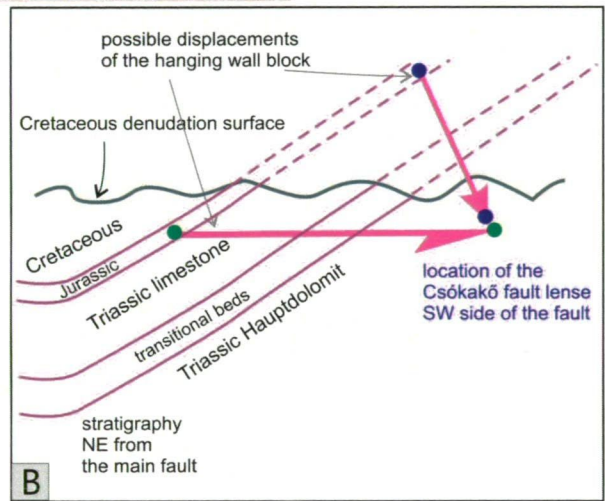
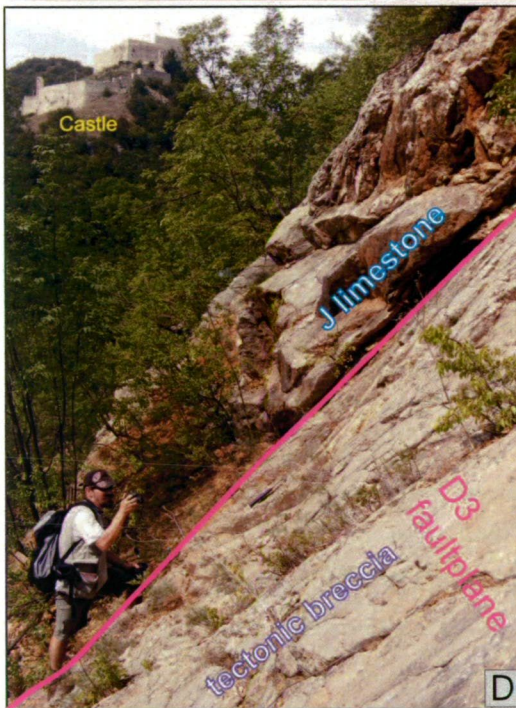
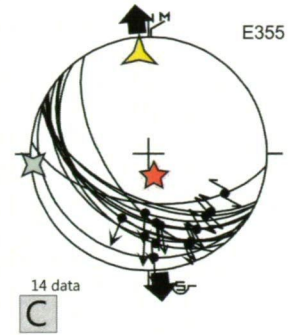
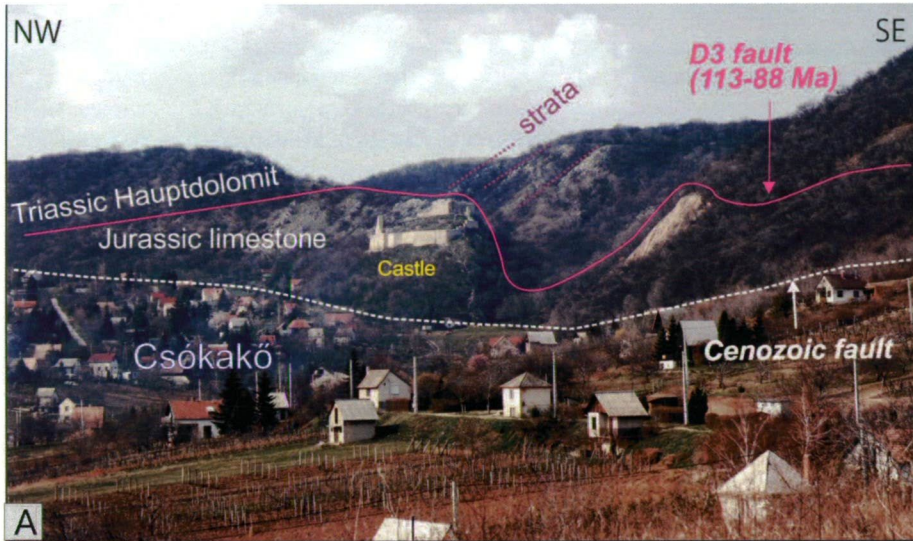


Fig. 4. View of the Mór boundary fault from the south. Note deformed denudation surface at the top of the hills.

Next page: Fig. 5. Structures near the castle hill and quarry of Csókakő. A) View from SE. B) Sketch explaining the possible slip of the Jurassic fault lens. C) fault-slip data from the quarry. D) Fault plane with Cretaceous and Cenozoic faulting events. E) View of the quarry with remnants of Jurassic fault lens.



from surface and subsurface sources. The stop will present aspects of this evolution.

The main fault splays surround the rocks exposed just below the Csókakő castle (Fig. 5a, d). These rocks are Jurassic in age, which is in sharp contrast to the footwall of Upper Triassic dolomite. There are two ways to explain the slip of the Jurassic of Csókakő from its original position; either with a large sinistral slip, or with a normal slip from the tilted Mesozoic sequence (Fig. 5b). The measured fault slip data show normal or normal-sinistral slip (Fig. 5c) (Kóta 2001). The calculated separation is around 1.25–1.5 km, much less than the other scenario, a sinistral slip of ca. 3 km (Fig. 5b).

There is an indirect constraint for the timing of this slip from landscape evolution. The tilt of the Mesozoic sequence was followed by intense denudation during the late Cretaceous, which resulted in closely sub-horizontal denudation surface, seen anywhere in the top of the Vértes Hills (Fig. 4). The fault slip should occur before this event otherwise no Jurassic would have remained for normal slip. This is the reason why one can place the motion to the Cretaceous D3 phase, between 113 and 86 Ma (Budai and Fodor 2008).

Small fragments of Jurassic are also seen in the quarry, in fault contact with the footwall Triassic dolomite (Fig. 5d,e). Along the contact a thick breccia zone developed which contain large blocks from both sides. The cemented tectonic breccia was reactivated during the Cenozoic phases, as demonstrated by varying slickenlines.

The fault at the bottom of the quarry and the castle hill was also reactivated in the Cenozoic. Fault slip data indicate a stress field of closely N-S extension and E-W compression. Outcrop-scale syn-sedimentary faults were observed close to the fault (Budai and Fodor 2008).

A composite seismic reflection profile clearly depicts the Mór Fault along its north-western strand (Fig. 6). In the hanging wall the pre-Cenozoic base can be placed along a prominent reflection at 700 ms two-way-travel time. The overlying sediment package is mostly Oligocene, it is penetrated by the Mór M-3 borehole, and it represents an 800 m or 1000 m thickness up to the datum plane (i.e. 50 m above sea level). There is also another 100–150 m package which was located above the datum line, up to the top of the hill in the footwall. In this way the total thickness of the Oligocene in the deepest part of the basin may be estimated as between 1000–1200 m. This very thick package was partly deposited dur-

ing syn-sedimentary activity of the Mór Fault, partly due to regional subsidence in compressional stress field (D7 phase).

The fault was reactivated during the syn-rift phase of the Pannonian Basin. During this phase, a dip-slip normal faulting occurred. However, no syn-rift sediments were preserved on the hanging wall block. Finally, the last movement was a dextral-normal movement, which could occur in the late Miocene or during the neotectonic phase (D12 or D13 phases).

The Mór fault was the potential source of the historic Mór earthquakes in 1810, with 5.4 on the Richter scale. The earthquake was investigated by scientists of the royal government. They published the map which showed for the first time the isoseismal lines of the earthquake (locations with the same damage) (Kitaibel and Tomcsányi, 1814). In our recent investigations Fodor et al. (2007) found several small arguments supporting the neotectonic activity of the area: diverted creeks, tectonically induced gelisolifluction structures, slump folds, fractured pebbles (data of A. Tokarski, A. Swierczewska). All these data suggests that the Mór fault is active.

Stop 3. Csákberény, Lóállás Hill: Basin-margin fault, neotectonic features

47° 20' 52.1484" N, 18° 20' 21.6096" E

A viewpoint south of Csákberény permits to study a Paleogene-Miocene fault and a neotectonically reactivated fault. The older fault bounds the Lóállási Hill to the SW and strike NW–SE. The fault has a clear morphological expression in the field, in the form of a 20–30 m high steep slope at the SW side of the Eastern Vértes Ridge.

On the SW hanging wall of this fault a Paleogene succession fills the Csákberény graben (Fig. 7). The boundary fault has been encountered by the Csákberény Csb-83 borehole. While the base of the late Miocene (Pannonian) was slightly deformed, the Oligocene shows large displacement (ca. 500 m). A smaller, parallel normal fault can be postulated along the SW margin of the trough, while E–W striking faults bound the trough in its northern end (Fig. 2).

A seismic reflection profile also crosses the graben (Fig. 7). Surface observations and boreholes are in good agreement with the interpreted

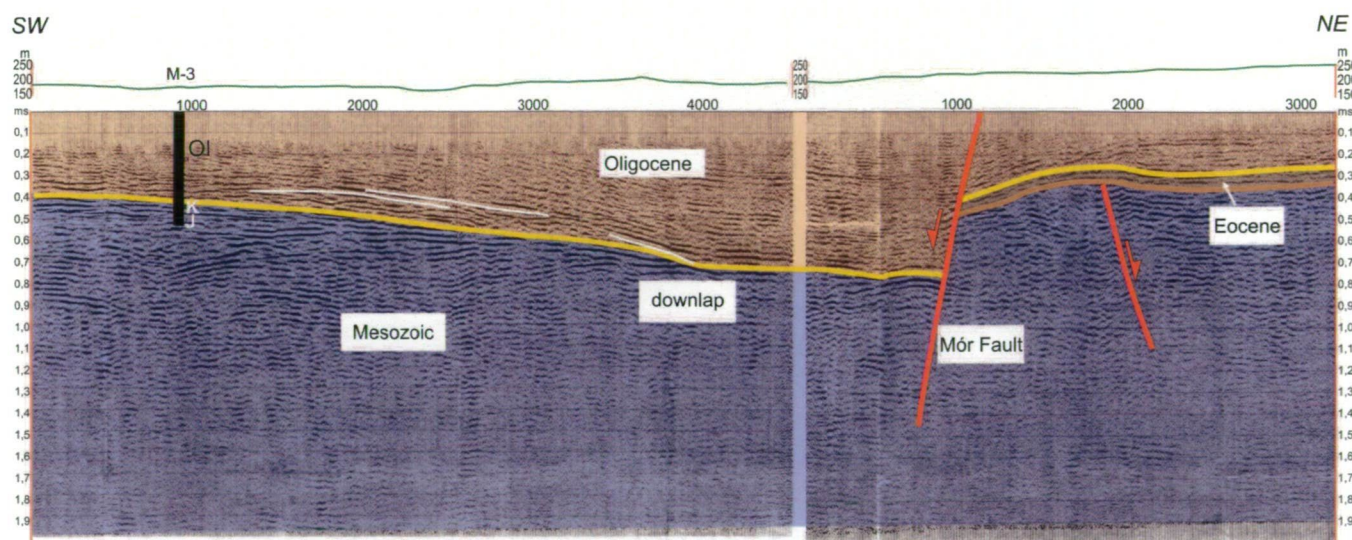


Fig. 6. Seismic reflection profile across the Mór graben boundary fault (after Fodor 2008).

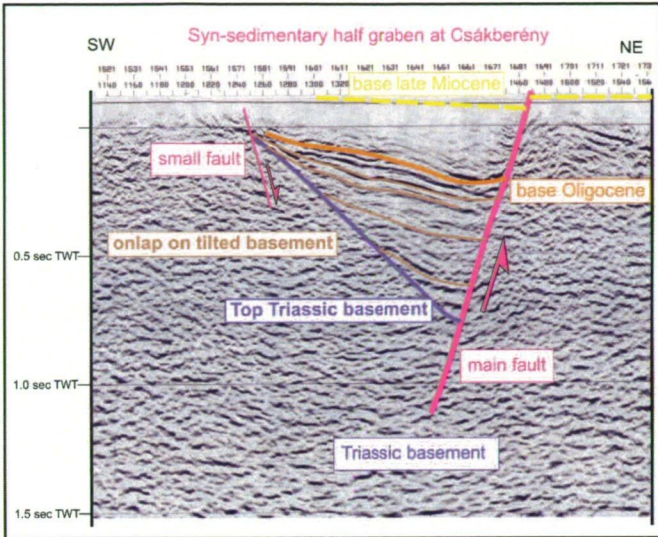


Fig. 7. Seismic profile across the Csákberény graben.

profile, which shows a major boundary fault on the NE and a very small fault on the SW side of the Csákberény graben.

This combined data set shows good agreement between surface and subsurface data and points to their strengths and complementary character. Surface data helps to characterise the fault kinematics and map view: on the basis of the stress-field data these faults could be a normal fault with a dextral oblique-slip tendency toward the northern fault termination (Fodor 2008) (Fig. 2). On the other hand, the seismic data shows more detail for the graben filling: it is asymmetric, dipping toward the main NE boundary fault, and shows wedge-shape geometry of basin filling Eocene sediments (Fig. 7). These observations suggest that fault slip started in the Eocene and reactivated after the Oligocene; a conclusion which is hard to get only from surface or point-type subsurface data (boreholes). On the other hand, borehole data suggest a small, 20m displace-

ment which affected the late Miocene basin fill; this shallow part is not imaged on seismic profile.

Demonstration of neotectonic structural element of the Pannonian Basin needs the use of both subsurface data (e.g. seismic reflection profiles, boreholes) and surface data, like morphotectonic indices, geological maps. Neotectonic analysis involves the understanding of the past landscape-forming processes, denudation events, drainage network evolution and the “pre-neotectonic” geological structure. Undoubted verification of neotectonic structural elements in the Vértes Hills is quite difficult but, in the some cases, we can suggest the existence of such structures; Stop 3 shows such an example.

North of Csákberény, near the Bucka and Lóallási Hills, borehole data and the drainage pattern help to demonstrate the neotectonic activity of the western fault of the Eastern Vértes Ridge, named here as Bucka Fault (Fig. 8). The fault displaces the pre-late Miocene denudation surface, which is exposed in the SE footwall and buried with late Miocene sediments in the NW hanging wall (Fig. 8). In the hanging wall, above the Miocene several boreholes and electric resistivity curves suggest the presence of buried Quaternary valleys with a more than 10 m-thick infilling. The bottom surface of these valley fills is lower than the bottom of the valleys exposed in the eastern footwall block. These dry valleys start right at the fault and thus it can be assumed that their former north-western upstream sections should have existed (Fig. 8b). It is presumed that the filled, buried valleys in the north-western hanging wall were the continuation of the dry valleys (wind gaps) of the footwall in the east. The valleys were disrupted into a dry south-eastern and a buried north-western segment by the neotectonic reactivation of the Bucka boundary fault. Subsidence resulted in an endorheic (closed) small depression in the hanging wall. The motion could be Quaternary and with normal kinematics, although direct data are lacking. Fractured pebbles occurring within the proluvium of a nearby valley (Horog-völgy) could be connected to this Quaternary deformation (Fodor et al. 2007).

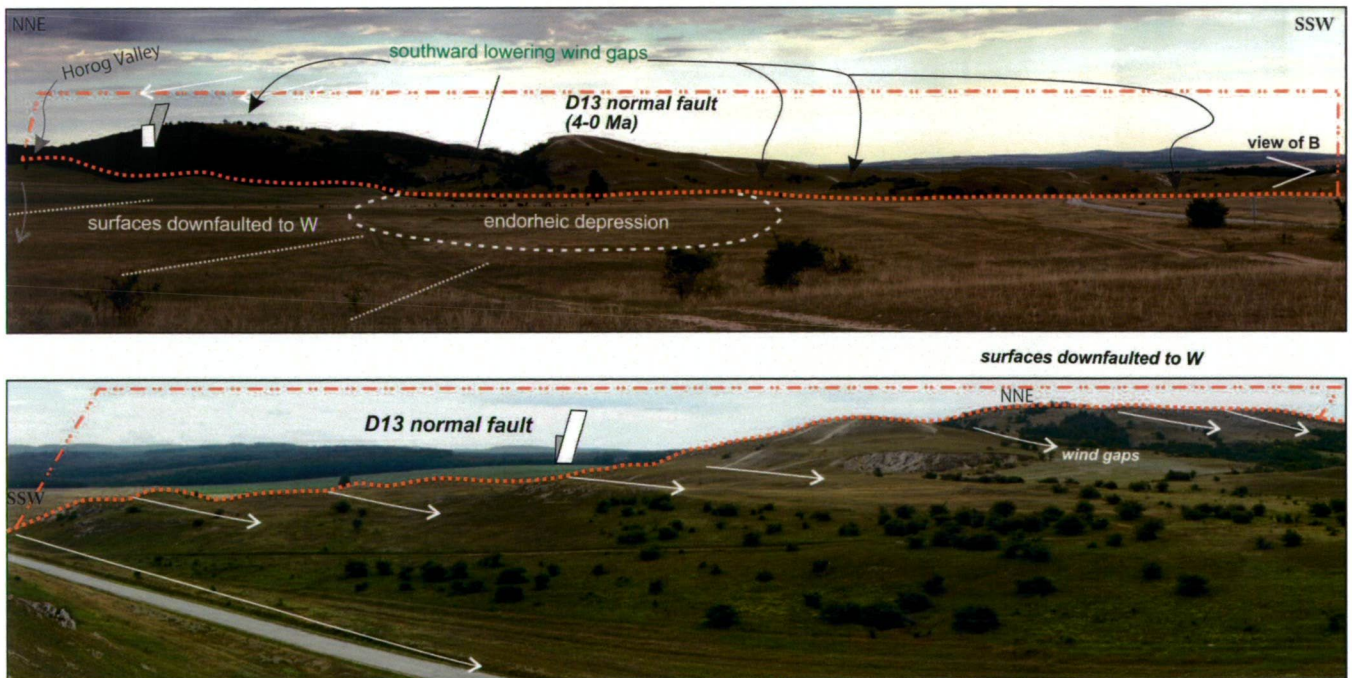


Fig. 8. Morphotectonic signs for Quaternary activity of the western boundary fault of the Eastern Vértes Ridge. A) View to SE from Stop 4 (after Budai and Fodor, 2008). B) Wind gaps (dry valleys) in the footwall of the Bucka Fault, looking to the west.

Stop 4. Gánt open pit mines: Miocene strike-slip faults, oblique-slip normal faults, relay ramps

Site A: $47^{\circ} 22' 25.5252''$ N, $18^{\circ} 23' 0.6612''$ E;

Site B: $47^{\circ} 21' 55.03''$ N, $18^{\circ} 22' 58.79''$ E

The Gánt bauxite open pit mine area is an excellent site to study fault geometry, including various types of fault segmentation. Fine details of fault planes can be seen because of excellent outcrop conditions. Part of the faults moved only in one tectonic phase, while others exhibit the signs of several fault slip events with varying kinematics. Both information are important for structural analysis and can get relatively easily in the field.

The Gánt bauxite mines are bounded by E–W and NW–SE faults (Fig. 9). The major characteristics that they are consisted of en echelon

segments. An excellent example of multiple overstepping en echelon faults is the fault array between the Harasztos and Újfeltárás mines, where the distance between the fault segments is 100m–200m (Fig. 9). Blocks between segments were tilted and form classical relay ramps in the sense of Peacock and Sanderson (1994). Connecting fault splays are not continuous between the overlapping segments which mean “soft linkage”.

The Museum Fault below the mining museum represents a small-scale en echelon fault array, where the distance between segments is only a few metres (Fig. 13). Here the relay ramp has been breached by connecting linkage faults (i.e. “hard-linkage”). As a consequence, the slips on the connected segments are not independent of each other and thus a local stress field has developed around the relay ramps

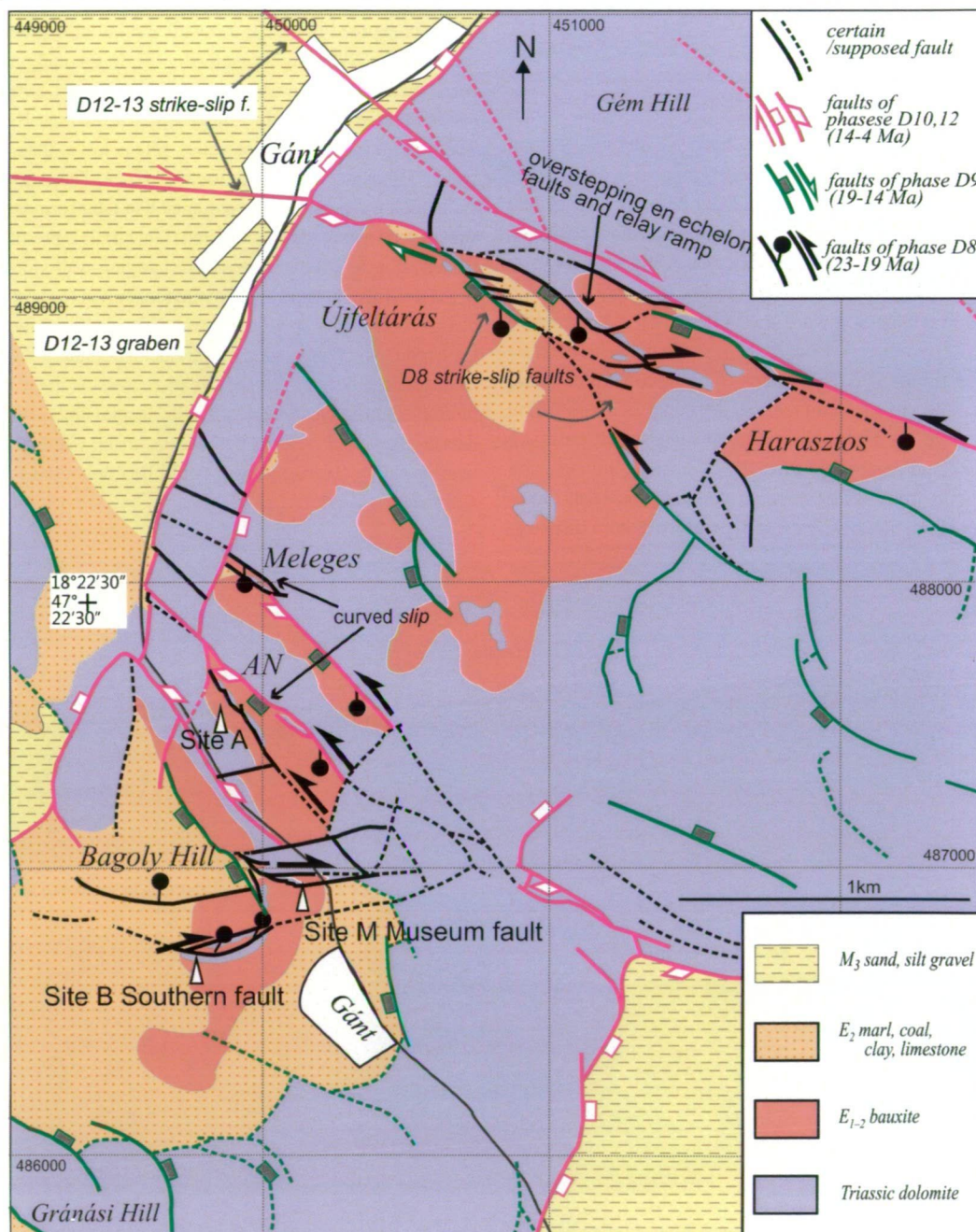


Fig. 9. Pre-Quaternary geological map of the Gánt mining area (after Fodor, 2007; Budai and Fodor, 2008)

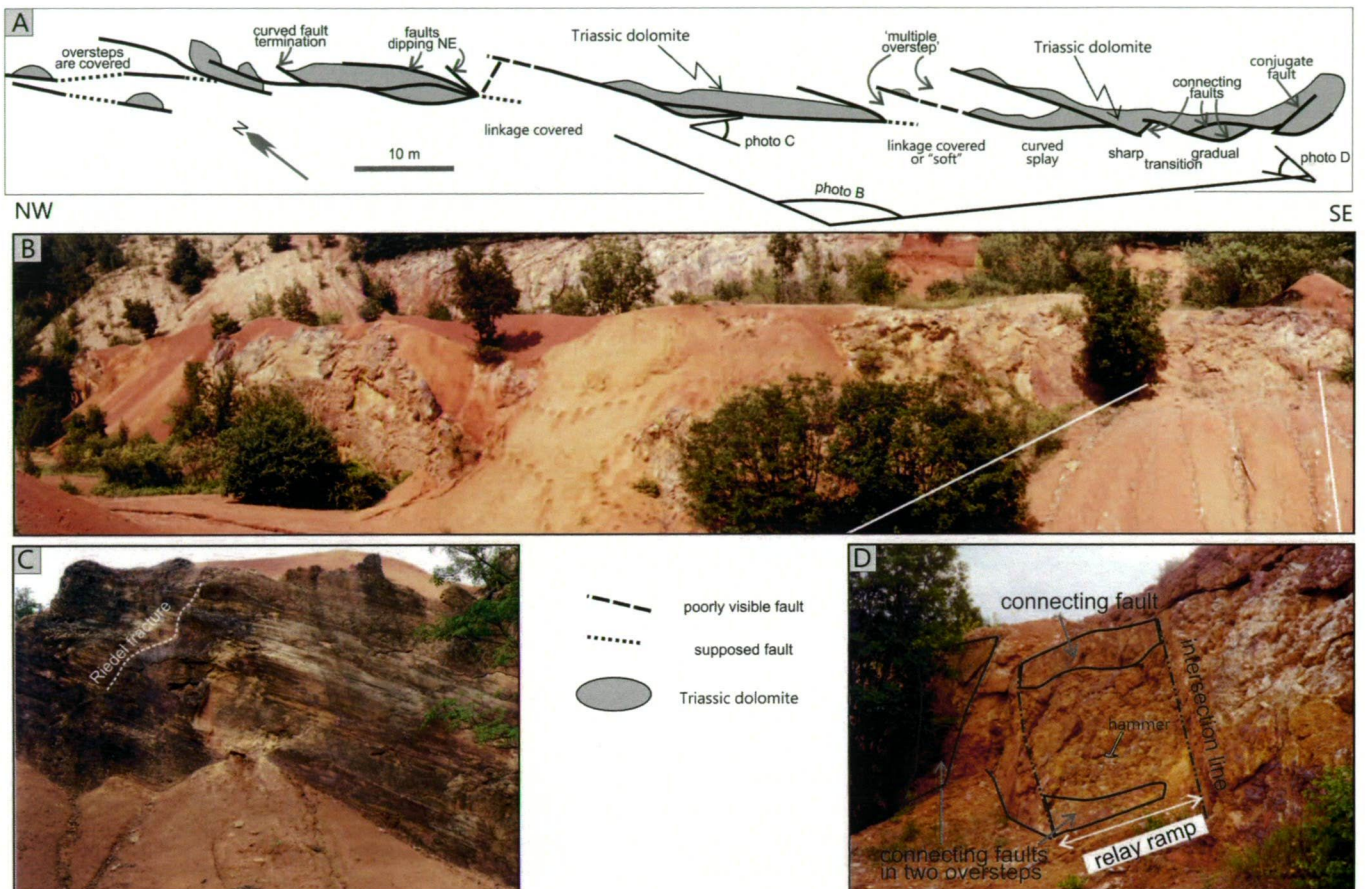


Fig. 10. Map and view of the Angerrét mine strike-slip fault

(Fodor 2007); this is difficult to fit into the regional evolution of the stress field.

In the lower level of the Anger-rét mine “hard-linked” and “soft-linked” strike-slip segments consist of a sinistral fault array. This fault preserves the regional fault geometry and was not reactivated during later phases.

Most of these faults have a normal slip component and show a transition towards an oblique-slip fault (Fig. 9).

Site A (Anger-rét open pit mine)

The fault zone of the Anger-rét open pit mine (site A) is composed of NW-trending en echelon segments. The dominant dip direction is to the SW and slickenside rake is constant, ranging from 10° to 35° to the SE. Individual segments are 10–40 m in length with spacing of 1–8 m, while the complete fault array is exposed along ~200 m (Fig. 10). Fault sense criteria like well-developed Riedel fractures (Fig. 10c), displaced fragments at the end of grooves, shaded ridges behind clasts indicate sinistral slip.

Overlap of fault segments may reach 1–10 m. In some cases more than two fault segments show oversteps, a feature that can be called ‘multiple overstep’. Part of the covered stepovers may represent soft-linked or partially breached strike-slip relay ramps. Few exposed examples of segment linkage occur in the SE end of the fault array (Fig. 10d). Connecting fault splays are curved and gradually curve into

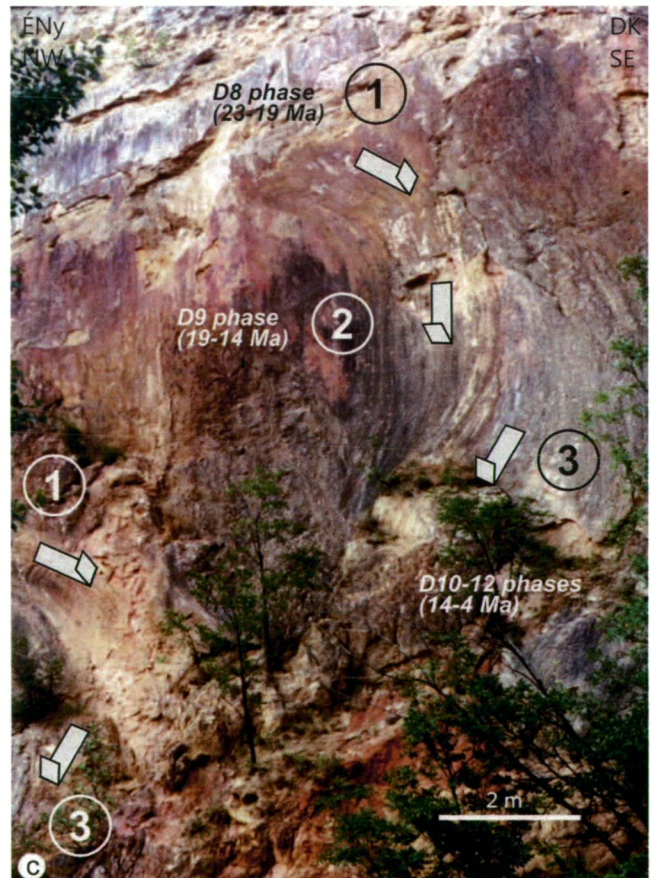


Fig. 11. Three generations of slip on the fault plane of the Meleges open pit mine (Márton and Fodor, 2003).

main fault planes, forming continuous sinuous or slightly zigzag fault geometry. Steptovers have widths of 1–3m and are dissected by several connecting faults, which resulted in brecciation (Fig. 10d). The dense network of fractures and the connecting faults resulted in the tilt of the formerly sub-horizontal basal surface of the bauxite.

The dominant strike-slip character of the faults, the tilt of a formerly horizontal reference layer would suggest the presence of a strike-slip relay ramp. To differentiate from the contractional strike-slip relay ramp of Peacock and Sanderson (1995) the structure can be termed

as transtensional relay ramp. The strike-slip segments are hard-linked and connected by an upper-ramp breach (Crider 2001).

From the footwall, the next fault plane can be seen toward the NE (Fig. 11). Here three generation of slip can be seen: a first, normal-sinistral slip, probably of Early Miocene age; a second dip-slip, which can be correlated with the rifting phase of the Pannonian Basin (19–14 Ma), then a dextral-normal slip, which can occur during the second rifting phase or during the post-rift phase (D10:14–12 or D12:11–4 Ma).

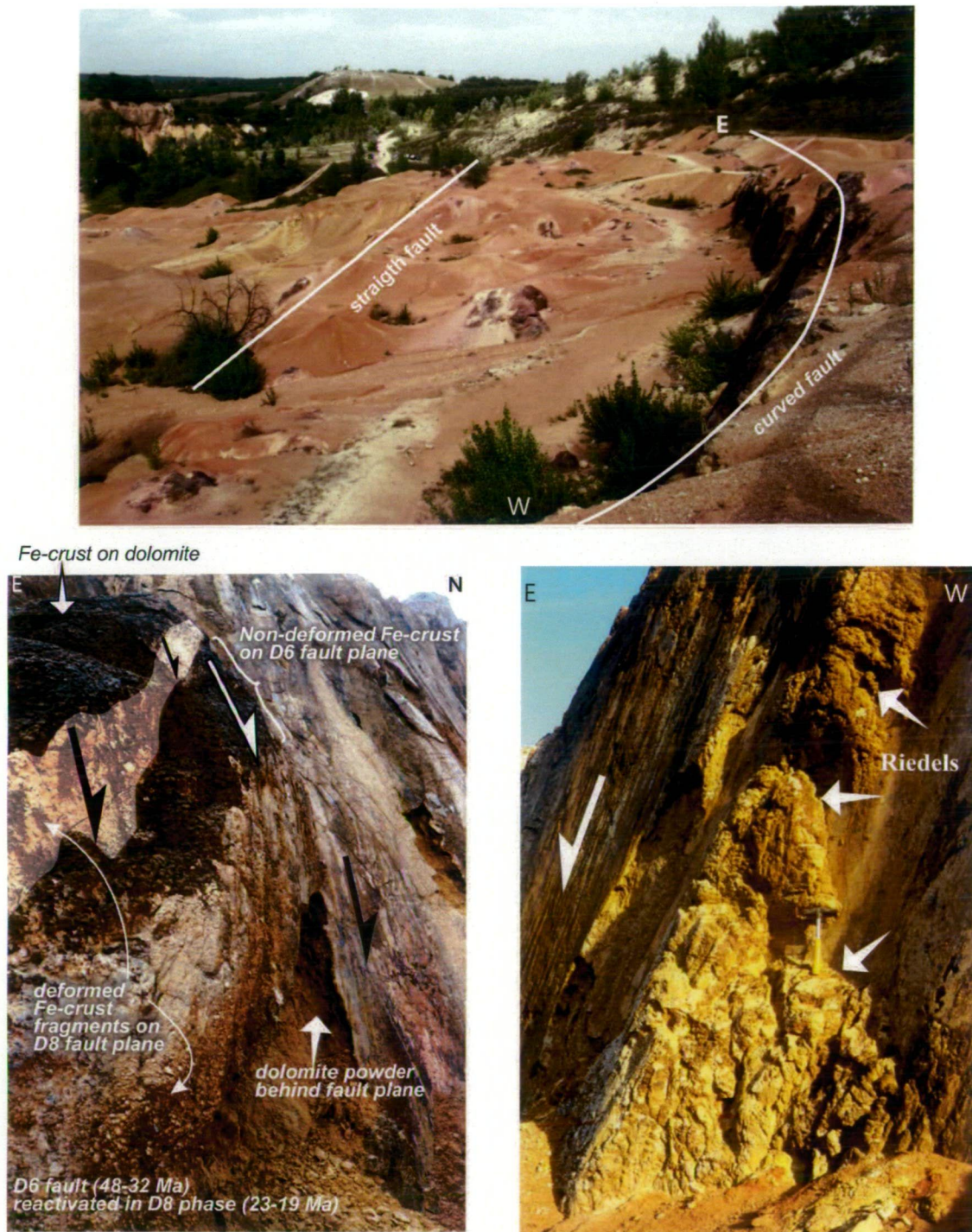


Fig. 12. Miocene and Eocene faults in the Gánt open pit bauxite mines. A) View of the southern boundary fault. B) Eocene and post-Eocene slip along the southern boundary fault of the Bagoly-hegy open pit mine. C) Riedel shears as kinematic indicators along the fault plane.

Site B (Bagoly Hill southern fault)

An E–W to ENE–WSW trending fault occurs at the southern part of the pit (Fig. 12). Here the fault plane is continuous but curved. Rakes of oblique slickensides change gradually corresponding to changing fault strike. Riedel shears, dragged clasts, large grooves with clasts at their end can be seen along the main fault plane (Fig. 12c). All features suggest dextral-normal slip. A straight fault cut across the arc of the curved fault.

A particularity of this site is the deformation of the Eocene bauxite and related ferruginous crust. The ferruginous crust between the bauxite and overlying dolomite was formed during the initial middle Eocene marine transgression, just after the deposition of the bauxite (Germán-Heins 1994) (ca. 42 Ma). This crust covers the higher parts of the southern major fault plane, which should have existed already before the encrustation (Fig. 12b). Consequently, fault activity started before the marine Eocene transgression, during or close to the deposition of the Eocene bauxite (Mindszenty and Fodor 2002). Small syn-sedimentary faults, pelitomorphic bauxite dykes are other direct evidence of faulting (Mindszenty et al. 1989). A slump fold occur just above the fault plane, which could form due to fault slip (Mindszenty 2010).

After the deposition of the Eocene sequence, possibly in the Early Miocene, the fault was reactivated: the observed slickenlines correspond to this phase of deformation. During this phase of movement, the crust itself was deformed, dragged along the fault. Fragments of crust often occur as striating objects or are part of fault breccia.

The fault offers evidence of intense fluid flow. First, the fault zone is cemented in 10–20 cm thickness. On the other hand, the footwall dolomite has been powdered just behind the cemented fault zone (Fig. 12). The two alterations (cementation and bleaching) induced a dramatic change in conductivity just within 1 m around the fault zone.

Site M (Museum fault)

The E–W striking Museum Fault array is exposed along 150 m below the mining museum. It was first described in an unpublished MSc thesis (Almási 1993) then more in detail in Fodor (2007) and Fodor (2008). The fault array is composed of overlapping fault segments. Individual fault segments are 15–100 m long, quite linear (Fig. 13). Faults are subvertical to steeply south-dipping, although local undulations with northerly dip exist.

The main faults have slickenlines with rakes of 20° and 30°. Kinematic indicators demonstrate normal-dextral sense of slip (Almási 1993). Considerable dip-slip component of displacement resulted in staircase lowering positions of the basal Cenozoic discordance surface. Several overstepping faults occur in the hanging wall of the northern fault segment. The particularity of the site is the connection of some segments near the quarry level, which are overstepping with overlaps of 4–8 m (Fig. 13) and are completely exposed.

The main subvertical faults bound 3–6 m wide transtensional relay ramps, which are strongly deformed (Fig. 13c). Relay ramps are cut through by one major connecting fault splay, which forms hard linkage between fault segments (Almási 1993). Other connecting faults have strikes of 30–70° (up to 90°) clockwise from the main strike-slip segments. Dip degree varies from 60–40°, but locally can be 30°. Dip and strike vary systematically with respect to main faults; larger the strike deviations shallower the dip angle.

Connecting faults have oblique dextral-normal or pure normal kinematics. The ratio of dip-slip and strike-slip components varies with connecting fault strike, with larger strike deviation associates with smaller rake. Intersection lines of the main fault with individual connecting splays are close to the orientations of striations on secondary faults. However, a small angular difference (up to 15°) can be observed between fault intersection line and striae of main faults (Fig. 13d).

Observations permitted to suggest a simple geometrical model for transtensional relay ramps (Fodor 2007). Assuming rigid footwall and hanging wall blocks, an ideal single connecting fault would intersect the main fault parallel to its striae (slip direction) (Fig. 14b, c). Slip on the combined zigzag shaped fault prevents further propagation of the main fault, thus the further increase of the overlap; the structure resembles to a double-bended fault more than to a true relay ramp. The steepness of connecting faults will depend on the rake of the main fault and on the strike difference between the main and connecting faults; the larger this strike difference, the lower dip angle has the connecting fault (Fig. 14c). The rake of slickenlines on the connecting faults will change similarly; the lowest angle fault has pure dip-slip striae, and this fault will deviate in strike the most from the main fault.

A more complex model incorporates several connecting faults. In this case, the connecting faults show a smaller total horizontal component of slip with respect to an ideal single connecting fault, meaning a 'deficit in extension' across the relay ramp. The necessary additional extensional deformation can be accommodated by brecciation and veins (Fig. 14d).

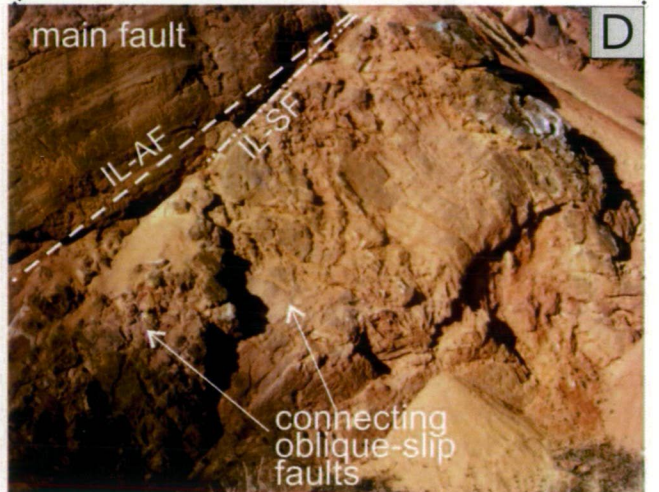
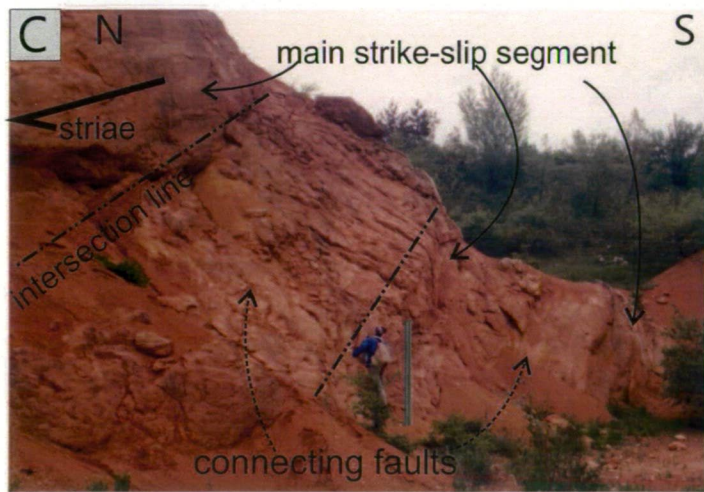
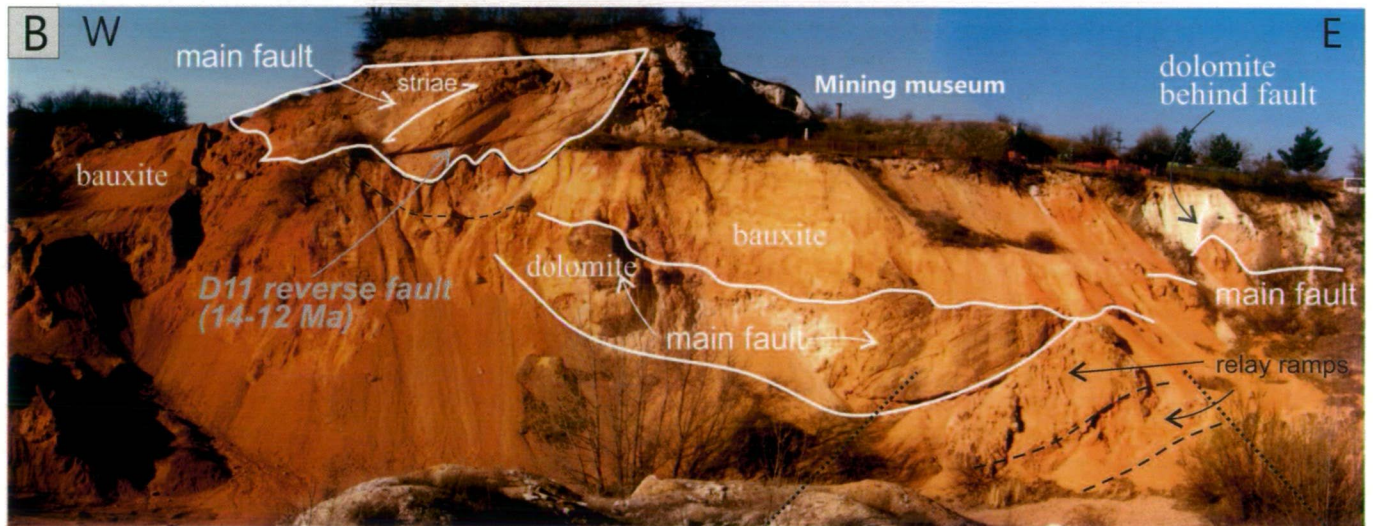
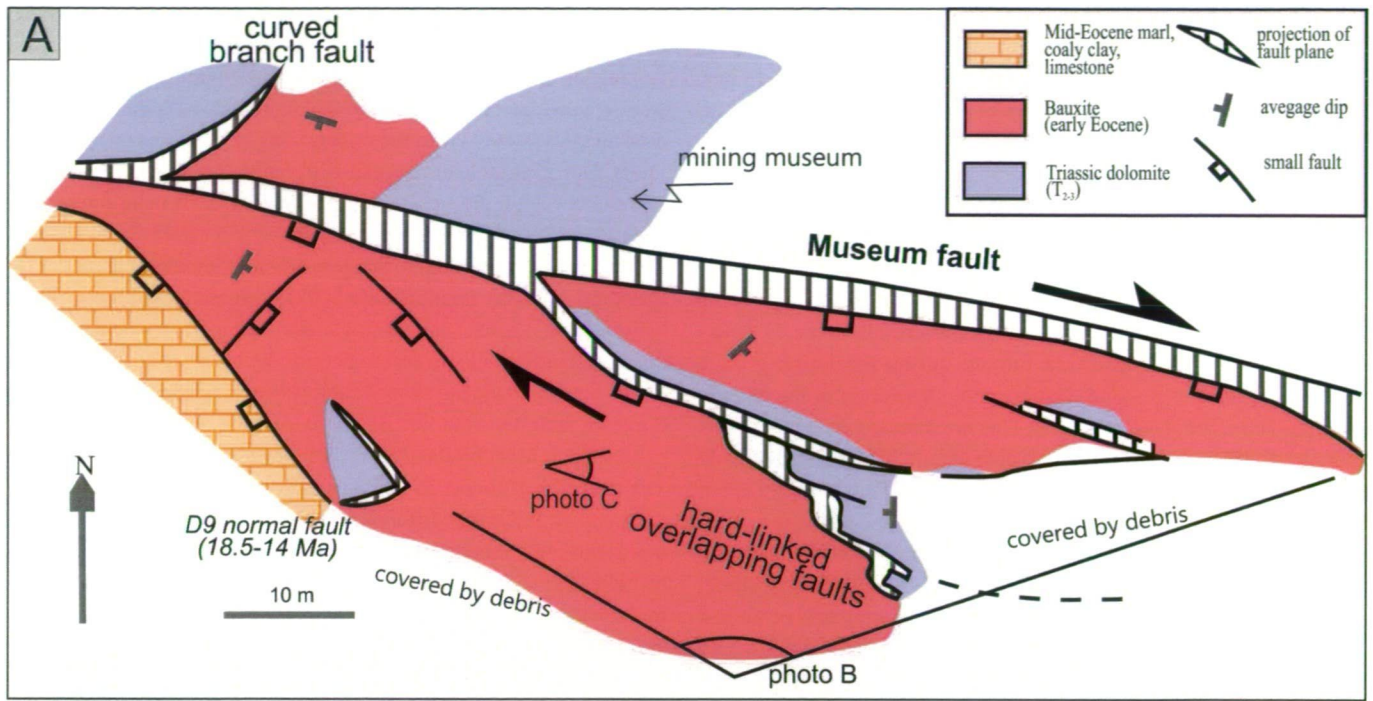


Fig. 13. View and schematic map of the Museum Fault, northern boundary fault of the Bagoly-hegy open pit mine (after Fodor, 2007; Budai and Fodor, 2008).

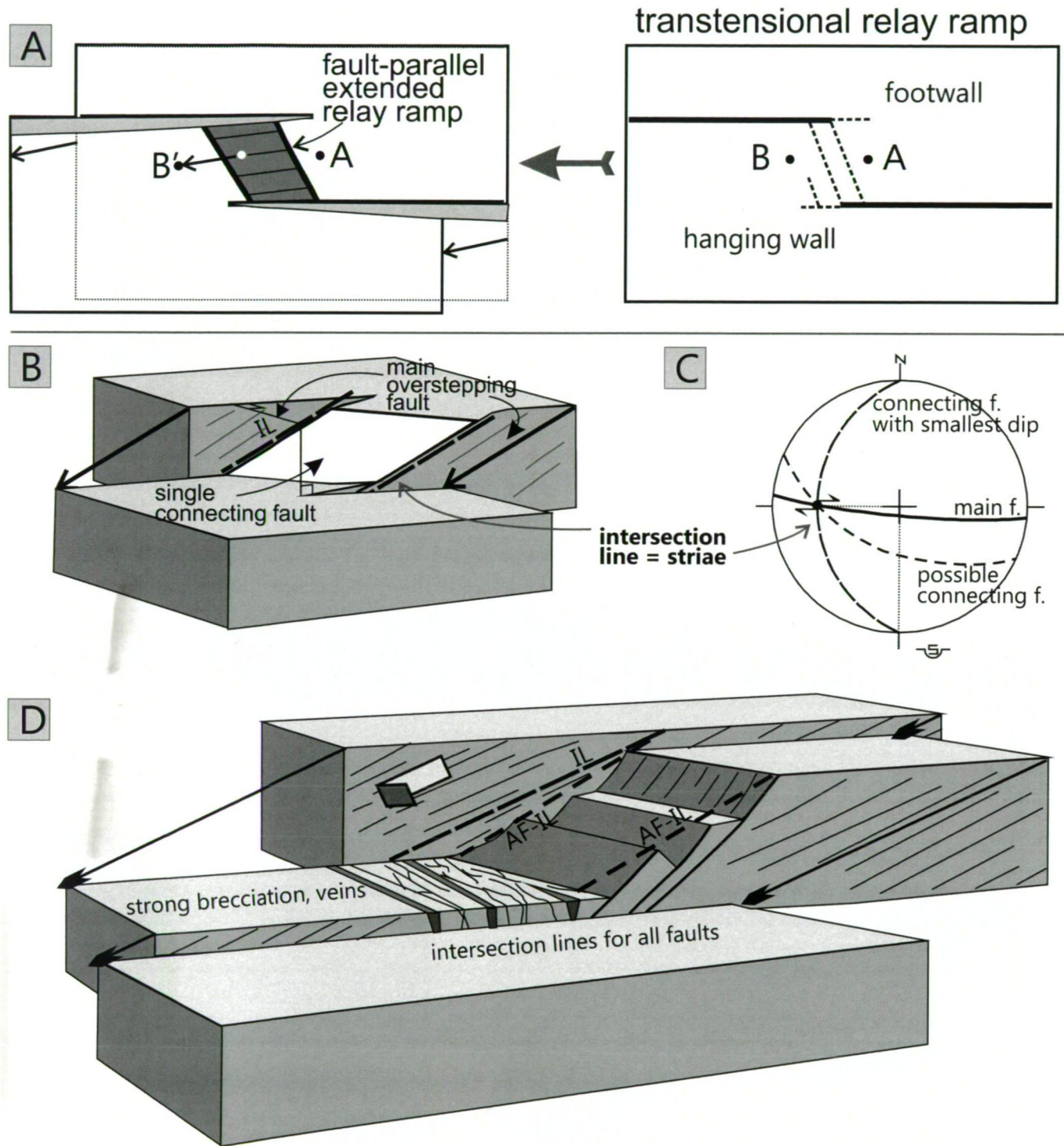


Fig. 14. Model for fault system in strike-slip relay ramps (Fodor, 2007, modified). A) Transtensional relay ramp in map view. B) Relay ramp model with one connecting fault. C) Stereogram of main and possible connecting faults. D) Relay ramp model with several connecting faults.

Stop 5. Csákvár, Kőlik-völgy (Kőlik Valley)

47° 23' 45.3984" N, 18° 26' 39.1416" E

The eastern margin of the Vértes Hills represents one of the most spectacular morphological scarps of the Transdanubian Range. The mountain range scarp is consisted of N-S, NNE-SSW and NW-SE to WNW-ESE trending segments (Fodor et al. 2008). All morphological

scarps correspond to eroded Miocene or younger faults (Csillag et al. 2002, Budai and Fodor 2008) (Fig. 2). The maximal vertical displacement could be 400–600m. The Eastern Vértes Fault zone bounds the Eastern Vértes Ridge, consisted of Triassic dolomite and Eocene cover. On the western side of this ridge, another fault zone bounds the Gánt Depression (Fig. 2). On the other hand, the Eastern Vértes Fault Zone and the Felcsút Ridge bound the Csákvár-Zámoly Basin. This

rhomboidal basin can have transtensional origin, as suggested by its geometry and the stress field data (Budai and Fodor 2008). Fault kinematics can be estimated using some outcrop-scale fault-slip data suggesting E-W tension and locally N-S compression (normal and strike-slip type deformation, respectively).

The relative chronology of the four fault sets is not clear. Cross-cutting relationships suggest that they are coeval. The faults segments are overlapping and show variable displacement, as can be seen near Csákvár (Fig. 2, 15). The fault deformed and tilted a pre-Late Miocene denudation surface in the footwall block. Due to this footwall deformation, the morphological slope has variable height: this correspond the displacement of the fault underlying the slope. The Csákvár segment of the Eastern Vértes Boundary Fault is important because it makes possible to verify the syn-sedimentary nature of the fault. After faulting increments, the fault plane changed to an eroded fault scarp. Finally, the fault scarps were covered by late Miocene abrasional conglomerate and breccia (Fig. 15b,c). While the gravels, conglomerates occur at the mid-slope, breccias occupy the higher part of the slope. Maximum lake level possibly reached this transitional zone. The

eroded and covered fault scarp indicates late Miocene formation of the boundary fault system. The evidence for syn-sedimentary motions is also supported by the presence of fissure fillings and sedimentary dykes filled with sandstone and dolomite silt (Csillag et al. 2002) (Fig. 15c).

Cross-sections and seismic sections clearly indicate that certain segments were active during the late Middle and Late Miocene sedimentation. The sediment thickness of the Late Miocene claymarl changes considerably between boreholes Csv-22 and Csá-1, Csv-23a (Fig. 16). This fault has had no effect on the youngest formation and it was active before the late Miocene. On the other hand, the fault segment between the boreholes Csv-22 and -21 deform the youngest formation and thus it was still active at least in the early(?) Pliocene. The basin margin fault equally has late Miocene synsedimentary activity, as revealed by the eroded and covered scarp. Finally, the oldest motion occurred in the late Middle Miocene, when a clastic wedge was deposited along the fault between the boreholes Csv-22 and Csá-1, Csv-23a (Fig. 16). The section suggests that fault activity was more

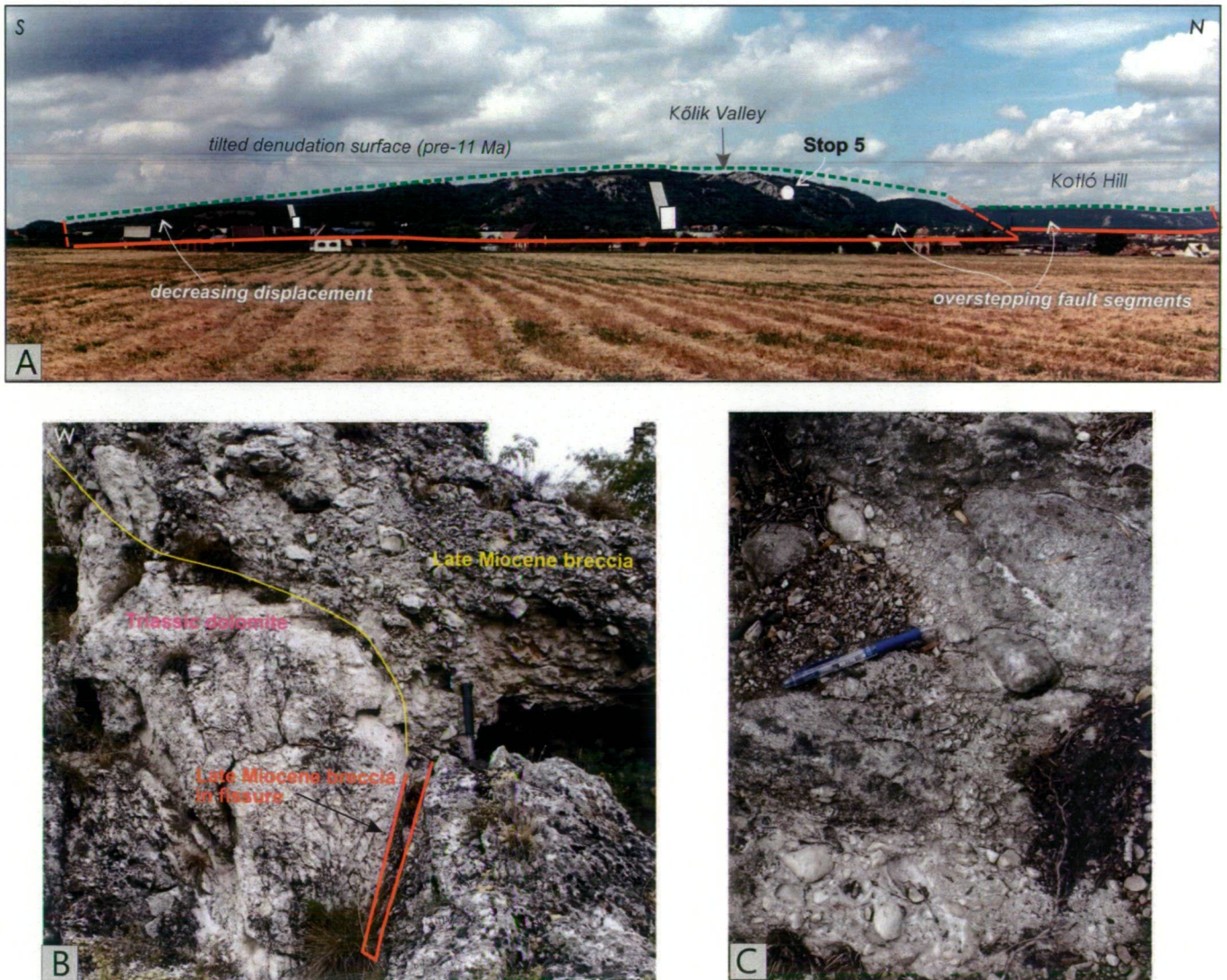


Fig. 15. Late Miocene structures and sediments along the western margin of the Zámoly Basin. A) View of the Eastern Vértes Fault scarp. B) Abrasional conglomerate and breccia of late Miocene age covering the eroded fault scarp. C) Late Miocene clastics fill tectonic fissures indicating active deformation during sedimentation.

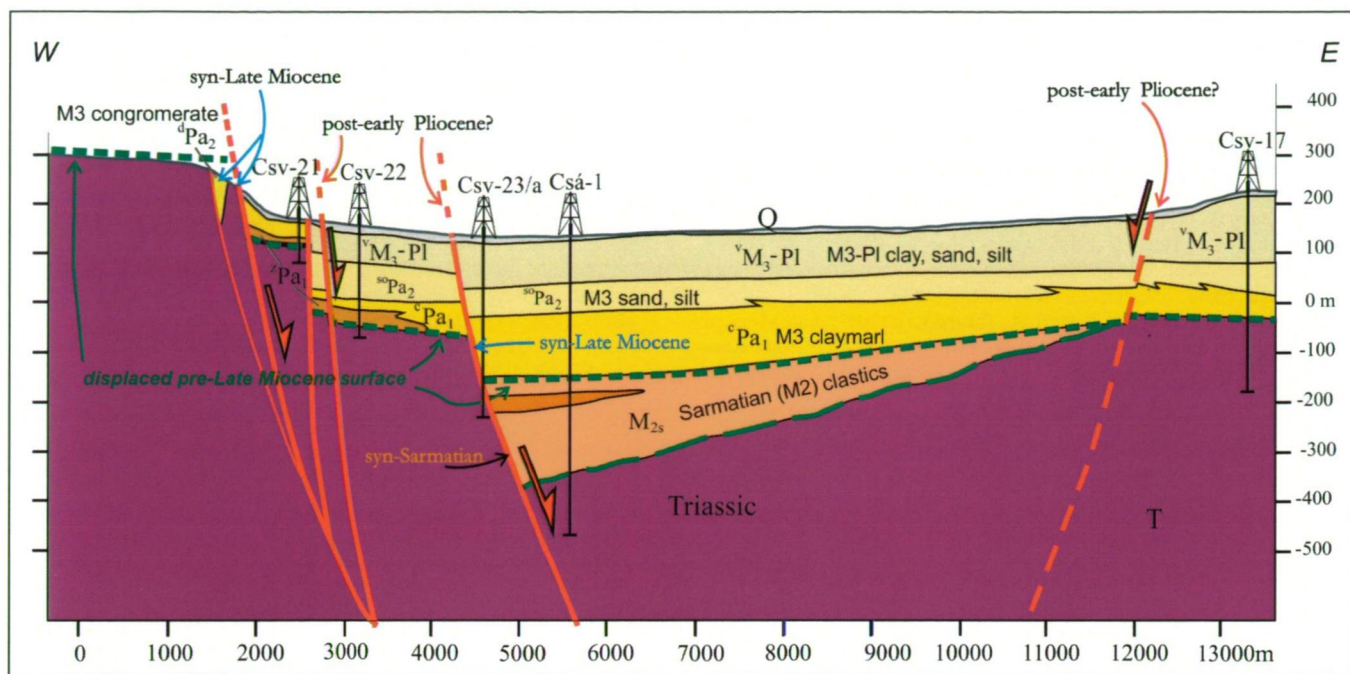


Fig. 16. Cross section of the Csákvár-Zámoly Basin demonstrating fault activity at different time periods.

or less continuous from late Middle Miocene up to the Pliocene (from 14 Ma to 4 Ma) but location of fault slip varied in space.

This conclusion is supported by surface, borehole and seismic reflection data sets. Surface data contribute in fault kinematics, and the characterisation of sediments covering the eroded fault scarp.

The origin of this Late Miocene basin is not clear. In the classical conception (Royden and Horváth, 1988) the late Miocene should be characterised by post-rift thermal subsidence, which is rather uniform and does not really associated with faulting. One possible explanation is that the faulting and basin subsidence was still coeval with the final thrusting along the East Carpathian thrust front and could be due to ongoing roll back of the subducting lithosphere. Although the triggering process was quite far from the central TR, but new data support early Late Miocene faulting in different parts of the eastern Pannonian Basin (Maženco et al. 2012). In this case, the late Miocene faulting could represent a renewed rifting activity in a back-arc position.

The other scenario could be local differential faulting, between the uplifting TR and subsidence of deep parts of the Pannonian Basin. However, the uplift of the Vértes Hills during the Late Miocene is not demonstrated, and the area was covered by at least a shallow lake during most of the Late Miocene evolution. On the other hand, the Vértes is not located at the margin of deep basin part which underwent large subsidence during the late Miocene. The understanding of this Late Miocene faulting and basin formation needs more works and consideration of deep lithospheric processes.

References

- Almási, I. (1993): Structural geological research of the Gánt bauxite mining area. MSc. Work, Eötvös University, Dept. Applied and Environmental Geology (in Hungarian).
- Bada, G., Horváth, F., Fejes, I., Gerner, P. (1999): Review of the present day geodynamics of the Pannonian basin: progress and problems. *Journal of Geodynamics*, 27, 501–527.
- Bergerat, F. (1989): From pull-apart to the rifting process: the formation of the Pannonian Basin. *Tectonophysics*, 157, 271–280.
- Budai T., Császár G., Csillag G., Fodor L., Gál N., Kercksmár Zs., Kordos L., Pálfalvi S., Selmecezi I. (2008): Geology of the Vértes Hills. Explanatory book to the Geological Map of the Vértes Hills 1:50000. Magyar Állami Földtani Intézet, Budapest, 368 p.
- Crider, J. G. (2001): Oblique slip and the geometry of normal-fault linkage: mechanics and a case study from the Basin and Range in Oregon. *Journal of Structural Geology*, 23, 1997–2009.
- Csillag, G., Fodor, L., Peregi, Zs., Roth, L., Selmecezi, I. (2002): Pliocene-Quaternary landscape evolution and deformation in the eastern Vértes Hills, (Hungary): the heritage and reactivation of Miocene fault pattern. *Geologica Carpathica*, 53, spec. issue, 206–208.
- Csillag, G., Kordos, L., Lantos, Z., Magyar, I. (2008): Late Miocene. In: Budai, T., Fodor, L. (eds.): Geology of the Vértes Hills. Explanatory book to the Geological Map of the Vértes Hills 1:50000. Geological Institute of Hungary, Budapest, 93–105.
- Csontos, L. (1995): Tertiary tectonic evolution of the Intra-Carpathian area: a review. *Acta Vulcanologica*, 7, 1–13.
- Csontos, L., Nagymarosy, A. (1998): The Mid-Hungarian line: a zone of repeated tectonic inversion. *Tectonophysics*, 297, 51–72.
- Csontos, L., Tari, G., Bergerat, F., Fodor, L. (1991): Structural evolution of the Carpatho-Pannonian area during the Neogene. *Tectonophysics*, 199, 73–91.
- Fodor, L. I. (2007): Segment linkage and stress field in transtensional strike-slip fault array: Field examples from the Pannonian Basin. In: Cunningham, D., Mann, P. (eds): *Tectonics of Strike-slip Restraining and Releasing Bends*. Geological Society, London, Special Publications 290, 417–431.

- Fodor L. (2008): Structural geology. In: Budai T., Fodor L. (eds.): *Geology of the Vértes Hills. Explanatory book to the Geological Map of the Vértes Hills 1:50000. Magyar Állami Földtani Intézet*, 145–202, 282–300.
- Fodor L., Csontos, L., Bada, G., Györfi, I. & Benkócs, L. (1999): Tertiary tectonic evolution of the Pannonian basin system and neighbouring orogens: a new synthesis of paleostress data. – In: Durand, B., Jolivet, L., Horváth, F., Séranne, M. (eds): *The Mediterranean Basins: Tertiary extension within the Alpine Orogen*. Geological Society, London, Special Publications 156, 295–334.
- Fodor L., Bada, G., Csillag, G., Horváth, E., Ruzsiczay-Rüdiger, Zs. Palotás, K., Sikhegyi, F., Timár, G., Cloetingh, S., Horváth, F. (2005): An outline of neotectonic structures and morphotectonics of the western and central Pannonian basin. *Tectonophysics*, 410, 15–41.
- Fodor L., Csillag G., Lantos Z., Kiszely M., Tokarsky, A. (2007): Late Miocene to Quaternary deformation and landscape evolution in the Vértes and forelands: inferences from geological mapping. Abstracts of the Annual Meeting of the Hungarian Geological Society, HUNTEK Workshop, Sopron, Hungary, 20–22/09/2007, 37–38.
- Fodor L., Csillag G., Lantos Z., Budai T., Kercksmár Zs., Selmeczi I. (2008): Geological Map of the Vértes Hills, 1:50000. Geological Institute of Hungary, Budapest.
- Germán-Heins, J. (1994): Iron-rich encrustation on the footwall of the Gánt bauxite (Vértes Hills, Hungary) – evidence for preservation of organic matter under exceptional conditions? *Sedimentary Geology*, 94, 73–83.
- Gyalog, L. (1992): Data from structural geology of Várgesztes. Ann. Report of the Geological Institute of Hungary from 1990, 69–74.
- Horváth, F. (1995): Phases of compression during the evolution of the Pannonian Basin and its bearing on hydrocarbon exploration. *Marine and Petroleum Geology*, 12, 837–844.
- Horváth, F., Royden, L. (1981): Mechanism for the Formation of the Intra-Carpathian Basins: a Review. *Earth Evolution Sci.* 3, 307–316.
- Horváth, F., Bada, G., Szafián, P., Tari, G., Ádám, A., Cloetingh, S. (2006): Formation and deformation of the Pannonian Basin: constraints from observational data. In: Gee, D., Stephenson, R. (eds.), *European lithosphere dynamics, EUROPROBE*. Geol. Soc. London, Spec. Publ.
- Jámbor, Á. (1989): Review of the geology of the s.l. Pannonian formations of Hungary. *Acta Geologica Hungarica*, 32, 269–324.
- Juhász, Gy. (1991): Lithostratigraphical and sedimentological framework of the Pannonian (s.l.) sedimentary sequence in the Hungarian Plain (Alföld, eastern Hungary). *Acta Geologica Hungarica*, 34, 53–72.
- Kitaibel, P., Tomcsányi, Á. (1814): *Dissertatio de terrae motu in genere ac in seie Mórensi anno 1810*. Budae (faximile 1960).
- Kóta, E. 2001. A Vértes-hegység DNy-i előterének szerkezetföldtani újraértékelése, a térinformatika alkalmazásával. MSc. Work, Eötvös University, Dept. Applied and Environmental Geology, 70 p.
- Magyar, I., Radivojević D., Sztanó, O., Synak, R., Ujszászi, K., Pócsik, M. (2012): Progradation of the paleo-Danube shelf margin across the Pannonian Basin during the Late Miocene and Early Pliocene. *Global and Planetary Change*, 103, 168–173.
- Márton, E., Fodor, L. (2003): Tertiary paleomagnetic results and structural analysis from the Transdanubian Range (Hungary); sign for rotational disintegration of the Alcapa unit. *Tectonophysics*, 363, 201–224.
- Maţenco, L., Bertotti, G. (2000): Tertiary tectonic evolution of the external East Carpathians (Romania). *Tectonophysics* 316, 255–286.
- Maţenco, L., Radivojević, D. (2012): On the formation and evolution of the Pannonian Basin: Constraints derived from the structure of the junction area between the Carpathians and Dinarides. *Tectonics*, 31, TC6007, DOI: 10.1029/2012TC003206
- Mindszenty A. (2010): Bauxite deposits of Gánt (Vértes Hills, Hungary). *Acta Mineralogica-Petrographica Field Guide Series*, 11, 11p.
- Mindszenty A., Fodor L. (2002): A Gánti Bauxit felhalmozódásának tektonozedi-mentológiai értelmezése. Abstract volume, Geological Society of Hungary, Annual Meeting at Bodajk, p. 23.
- Mindszenty A., Szóts A., Horváth A. (1989): Excursion A3: Karstbauxites in the Transdanubian Midmountains. In: Császár, G. (ed): *Excursion Guidebook IAS 10th Regional Meeting*, Budapest. Budapest, 11–48.
- Peacock, D.C.P., Sanderson, D.J. (1994): Geometry and development of relay ramps in normal fault systems. *American Association of Petroleum Geologists Bulletin*, 78, 147–165.
- Peacock, D.C.P., Sanderson, D.J. (1995): Strike-slip relay ramps. *Journal of Structural Geology* 17, 10, 1351–1360.
- Royden, L. H., Horváth, F. (1988): The Pannonian basin. *A Study in Basin Evolution*. AAPG Memoir 45.
- Royden, L.H., Horváth, F., Nagymarosy, A., Stegena, F. (1983): Evolution of the Pannonian Basin System. 2. Subsidence and thermal history. *Tectonics* 2, 91–137.
- Taeger H. (1909): A Vérteshegység földtani viszonyai. *Annals of the Geological Institute of Hungary*, 17, 1–256.
- Tari, G., (1994): Alpine Tectonics of the Pannonian basin. PhD. Thesis, Rice University, Texas, USA, 501 p.
- Tari, G., Horváth, F., Rumpler, J., (1992): Styles of extension in the Pannonian Basin. *Tectonophysics*, 208, 203–219.
- Tari, G., Báldi T., Báldi-Beke, M. (1993): Paleogene retroarc flexural basin beneath the Neogene Pannonian Basin: a geodynamic model. *Tectonophysics*, 226, 433–455.
- Vakarc, G., Vail, P., Tari, G., Pogácsás, Gy., Mattick, R., Szabó, A. (1994): Third-order Middle Miocene–Pliocene depositional sequences in the prograding delta complex of the Pannonian Basin. *Tectonophysics*, 240, 81–106.



X 175794



ACTA MINERALOGICA-PETROGRAPHICA FIELD GUIDE SERIES

VOLUME 31 2013
HU ISSN 0324-6523
HU ISSN 2061-9766

established in 1922

